

# CHALMERS



## Definition of structural attenuation from engine block using loudspeaker tests and acoustic camera

Master's Thesis in the Master's programme in Sound and Vibration

**ANDERS SÖDERBERG**

Department of Civil and Environmental Engineering  
*Division of Applied Acoustics*  
*Vibroacoustics Group*  
CHALMERS UNIVERSITY OF TECHNOLOGY  
Göteborg, Sweden 2013  
Master's Thesis 2013:19

MASTER'S THESIS 2013:19

# Definition of structural attenuation from engine block using loudspeaker tests and acoustic camera

Anders Söderberg

Department of Civil and Environmental Engineering  
*Division of Applied Acoustics*  
*Vibroacoustics Group*  
CHALMERS UNIVERSITY OF TECHNOLOGY  
Göteborg, Sweden 2013

**Definition of structural attenuation from engine block using loudspeaker tests and acoustic camera**

© Anders Söderberg, 2013  
Göteborg, Sweden 2013

Master's Thesis 2013:19

Department of Civil and Environmental Engineering  
Division of Applied Acoustics  
Vibroacoustics Group  
Chalmers University of Technology  
SE-41296 Göteborg  
Sweden

Phone: +46-(0)31-772 2200  
Fax: +46-(0)31-772 2212

# Definition of structural attenuation from engine block using loudspeaker tests and acoustic camera

Anders Söderberg

**Chalmers University of Technology**  
Department of Civil and Environmental Engineering  
Vibroacoustics Group  
Division of Applied Acoustics

## Abstract

Due to increasing demands on CO<sub>2</sub> emissions, the combustion excitation increases due to more efficient combustion. There are great needs of increasing the engine block structural attenuation to take care of the combustion noise near the source. The purpose of this thesis is to develop a new method for measuring the structural attenuation of an engine block by using an acoustic camera and a loudspeaker placed inside the combustion chamber. This new method is based upon the current method for measuring the structural attenuation introduced by the Lucas Industries Noise Centre in the 1980s.

Two different assembly designs are used to demonstrate that the new proposed method works. For both designs the new method, Lucas Near-Field function, is validated against the current method based upon the Lucas filter function. The new method measures the sound pressure 3 cm away from the engine block while the current method measures it 1 m away. The outcome when comparing the new method, the Lucas Near-Field function, and the current method, Lucas filter function, is that they have the same pattern but a level difference. This level difference is discussed.

The structural attenuation is studied by comparing two different assembly designs; for this a matlab-software was developed. The discussion regarding the validation of the proposed method is done by comparing the outcome from the matlab-software with the figures obtained from the commercial software Array Acoustic.

From these two validations the outcome is that the new proposed method for measuring the structural attenuation is a good complement to the method used today.

**Keywords:** Combustion excitation, Structural attenuation, Lucas filter, Acoustic camera



# Contents

<b>Abstract</b>	<b>iii</b>
<b>Contents</b>	<b>iv</b>
<b>Acknowledgements</b>	<b>ix</b>
<b>Notations</b>	<b>x</b>
<b>1. Introduction</b>	<b>1</b>
1.1. Background . . . . .	1
1.2. Purpose . . . . .	1
1.3. Aim and objective . . . . .	1
1.4. Thesis structure . . . . .	2
<b>2. Theory</b>	<b>3</b>
2.1. The Diesel engine . . . . .	3
2.1.1. The history of the Diesel engine . . . . .	3
2.1.2. Combustion . . . . .	4
2.1.3. Noise emission . . . . .	5
2.2. FRF - Frequency Response Function . . . . .	6
2.3. FFT - Fast Fourier Transform . . . . .	6
2.4. Acoustical Holography . . . . .	7
2.4.1. Statistically Optimal Near-Field Acoustical Holography (SONAH) . . . . .	9
2.5. Principal Components Analysis (PCA) . . . . .	12
2.6. Lucas filter . . . . .	13
2.6.1. Banger Rig . . . . .	13
2.6.2. Regression methods . . . . .	14
<b>3. Implementation</b>	<b>16</b>
3.1. Measurements . . . . .	16
3.1.1. Gearbox NVH test cell . . . . .	16
3.1.2. Loudspeaker element . . . . .	16
3.1.3. Distance to Top Dead Center . . . . .	18
3.1.4. Measurement setup . . . . .	21

3.2. Post-processing . . . . .	25
<b>4. Results</b>	<b>28</b>
4.1. Lucas Near-Field function vs. Lucas function . . . . .	29
4.2. Array Acoustic: estimated sound pressure level . . . . .	30
4.2.1. "Open" assembly design . . . . .	31
4.2.2. "Closed" assembly design . . . . .	35
4.3. Lucas Near-Field function . . . . .	39
4.3.1. "Open" assembly design . . . . .	39
4.3.2. "Closed" assembly design . . . . .	41
<b>5. Discussion</b>	<b>44</b>
5.1. Lucas Near-Field function vs. Lucas function . . . . .	44
5.2. Lucas Near-Field function . . . . .	45
<b>6. Conclusion</b>	<b>47</b>
6.1. Lucas Near-Field function vs. Lucas function . . . . .	47
6.2. Lucas Near-Field function . . . . .	47
<b>7. Future work</b>	<b>48</b>
7.1. Sound power level and the Lucas near-field function . . . . .	49
<b>References</b>	<b>51</b>
<b>Appendix A. Loudspeaker elements</b>	
A.1. Gradient: TPC80NV/4 . . . . .	I
A.1.1. Measurement on TPC80NV/4 . . . . .	II
A.2. Visaton: FRS 8-4ohm . . . . .	III
<b>Appendix B. Layout: Piston</b>	<b>V</b>
<b>Appendix C. Structural attenuation measurements</b>	<b>VI</b>
C.1. Instrumentation . . . . .	VI
C.2. Measurement areas . . . . .	VII
C.3. Post-Processing . . . . .	VII
C.3.1. Setup in Array Acoustic . . . . .	VII
<b>Appendix D. Measurements conducted on the other sides</b>	<b>VIII</b>
D.1. Gearbox side . . . . .	VIII
D.1.1. Lucas Near-Field function vs. Lucas function . . . . .	VIII
D.1.2. Array Acoustic . . . . .	X
D.1.3. Lucas near-field function . . . . .	XIV

D.2. Exhaust side . . . . .	XVIII
D.2.1. Lucas Near-Field function vs. Lucas function . . . . .	XVIII
D.2.2. Array Acoustic . . . . .	XX
D.2.3. Lucas Near-Field function . . . . .	XXIV
D.3. Front side . . . . .	XXVIII
D.3.1. Lucas Near-Field function vs. Lucas function . . . . .	XXVIII
D.3.2. Array Acoustic . . . . .	XXX
D.3.3. Lucas Near-Field function . . . . .	XXXIV
D.4. Top side . . . . .	XXXVIII
D.4.1. Lucas Near-Field function vs. Lucas function . . . . .	XXXVIII
D.4.2. Array Acoustic . . . . .	XL
D.4.3. Lucas Near-Field function . . . . .	XLIV
D.5. Bottom side . . . . .	XLVII
D.5.1. Lucas Near-Field function vs. Lucas function . . . . .	XLVII
D.5.2. Array Acoustic . . . . .	XLVIII
D.5.3. Lucas Near-Field function . . . . .	LII



# Acknowledgements

This master of science thesis was written during the spring of 2013 as a part of the Master's programme in Sound and Vibration at the Division of Applied Acoustics at Chalmers University of Technology.

This master thesis topic was proposed by the Powertrain NVH division at Volvo Car Corporation situated in Gothenburg, Sweden.

First and foremost, I would like to thank my supervisors at Powertrain NVH, Henrik Hedberg and Frédéric Wullens, their technical expertise, experience and guidance has been invaluable for the completion of this thesis. I would also like to thank my supervisor at Applied Acoustics, Patrik Andersson, for his help and support.

I would also like to thank all my colleagues and all the staff for the informative lectures, labs, exercises and projects. I have never had so much fun while studying as I have had at the master's programme. These two years have gone by too fast.

Once again, Thank you all!

Anders Söderberg  
Gothenburg, June 2013

## Notations and abbreviations

$CO_2$	Carbon dioxide
$NVH$	Noise, Vibration & Harshness
$FRF$	Frequency Response Function
$DFT$	Discrete Fourier Transform
$FFT$	Fast Fourier Transform
$SONAH$	Statistically Optimal Near-Field Acoustical Holography
$NAH$	Near-Field Acoustical Holography
$PCA$	Principal Components Analysis
$TDC$	Top Dead Center
$H(\omega)$	Frequency Response Function
$Y(\omega)$	Output signal
$X(\omega)$	Input signal
$k, i$	indexes
$N$	Number of samples
$\Phi_m(r)$	Elementary waves
$k$	Wave number
$p(r)$	Sound pressure as column vector
$T$	Transpose
$c(r)$	Transfer vector
$A, B$	Matrices
$H$	Hermitian transpose
$I$	Total number of measurement positions
$\tilde{u}_\chi(r)$	Particle velocity
$\chi$	Particle velocity in a direction
$S$	Covariance matrix
$\lambda$	Eigenvalues
$x_{ij}$	Measurement of i:th variable
$\bar{x}_i$	Sample mean of a variable

$SP$	Engine sound power level
$SP_m$	Mechanical sound power
$CP$	Cylinder pressure sound power
$G$	Transfer coefficient
$L$	Square of the engine torque
$HT$	Height of piston
$S$	Stroke
$c$	Rod
$a$	Crank angle in radians
$r$	Half of stroke

# 1. Introduction

## 1.1. Background

With increasing demands on  $CO_2$  emissions the combustion excitation increases due to more efficient combustion. There are great needs of increasing the engine block structural attenuation to take care of the combustion noise near the source.

The current method today when measuring the structural attenuation is based upon the Lucas filter function introduced by the Lucas Industries Noise Centre in the 1980s. This method measures the radiated noise one metre away from the engine structure at four different positions around the engine, and at the same time it measures the combustion excitation. From this a transfer function analysis is calculated and the result is a graph depicting the structural attenuation for that particular side in 1/3 octave band. However, this method is not that accurate that the engineer can point out the weak areas.

## 1.2. Purpose

The purpose of this thesis is to develop a new method for measuring the structural attenuation based upon the current Lucas filter function. This new method named Lucas Near-Field function will make use of an acoustic camera to define weak areas and as an excitation source a loudspeaker element will be placed in one of the cylinder chambers on a 4-cylinder prototype diesel engine. By using an acoustic camera the structural attenuation are visualized on the engine block so that the engineer can define which countermeasures to take.

## 1.3. Aim and objective

The aim of this thesis is to present a new method, the Lucas Near-Field function, for measuring and visualizing the structural attenuation of an engine block.

The method is based on that the engineer first could look at the current method, the Lucas filter function, to look after a certain frequency or frequency range for which the structural attenuation is worst and then by using the new method the engineer could go further into where this weakness is situated on the engine block until the weakness has been identified, so that the engineer can apply proper countermeasures to solve the problem.

## 1.4. Thesis structure

The structure of this thesis is as follows:

- *Chapter Two:* Contains theory about the diesel engine, the theory behind Frequency Response Function, theory about the Acoustical Holography system and how it is used and an introduction to what kind of methods that is used today for measuring the structural attenuation of an engine block.
- *Chapter Three:* Presents the implementation details regarding the new method Lucas Near-Field function.
- *Chapter Four:* Covers the results from the measurements done for two different assembly designs, in order to verify the new method. It covers both results using the current method Lucas filter function and results for the new method, Lucas Near-Field function.
- *Chapter Five:* Discusses the validity between the new method, Lucas Near-Field function, and the current method in use, Lucas filter function. It covers also the discussion and conclusion regarding the demonstration that the new method works by comparing two different assembly designs of the engine.
- *Chapter Six:* Covers what can be done to improve the new method.

## 2. Theory

### 2.1. The Diesel engine

#### 2.1.1. The history of the Diesel engine

The history of the diesel engine starts on February 27, 1892 when a German engineer named Rudolf Diesel filed a patent with the Imperial Patent Office in Berlin for a "new rational heat engine". Almost a year later February 23, 1893, he was granted the patent DRP 67207 for the working method and design for combustion engines dated February 28, 1892. This was the first step toward the Diesel engine [1].

At the Polytechnikum München, Diesel realized during lectures on the theory of caloric machines that the steam engine (the dominant heat engine of the day), wasted a tremendous amount of energy when it was compared to the ideal energy conversion cycle formulated by Carnot in 1824 [1].

From his time at the Polytechnikum left lecture notes shows that Diesel already considered to implement the Carnot cycle as a student, if possible by directly utilizing the energy contained in coal without steam as an intermediate medium. He ambitiously pursued the idea of a rational engine while working at Lindes Eismaschinen, and ultimately filed and was granted the aforementioned patent. Diesel claimed also a patent protection of multi-stage compression and expansion and for that Diesel proposed a three cylinder compound engine, but be able to implement the Carnot cycle, he reverted to the four-stroke cycle considered "state-of-the-art" since Nikolaus Otto's day (famous for the Otto engine, spark ignition engine) [1].

In order to win over the industry and also to propagate his ideas, Diesel wrote a treatise of the "Theory and design of a Rational Heat Engine" and sent it to professors and industrialists. After a year of efforts and planning, he finally signed a contract in early 1893 with the renowned Maschinenfabrik Augsburg AG, which was a leading manufacturer of steam engines, and the construction of the first uncooled test engine begun in the early summer of 1893. This engine was later provided with water cooling and other modifications, the fuel could no longer be injected directly, it could only be injected, atomized and combusted with the help of compressed air. From these modifications

the engine idle for the first time on February 17, 1894, and it became autonomous directly. A third test engine was made and acceptance test was conducted on it (February 17, 1897) and the results from these test was presented June 16, 1897, at a meeting of the Association of German Engineers. This engine was the first heat engine with an efficiency of 26.6 % this was a sensational result in those days [1].

Rudolf Diesel died September 29, 1913, and left behind is his life's work. The high pressure engine that evolved from the theory of heat engines, which bears his name and, 100 years later, is still what its ingenious creator intended. The most rational heat engine of his and even our day [1].

### 2.1.2. Combustion

A diesel engine is either 2-stroke or 4-stroke, which means that the cycle of combustion occurs either at 2 or 4 piston strokes. In cars the most common cycle is the 4-stroke engine, which can be seen in figure 2.1.

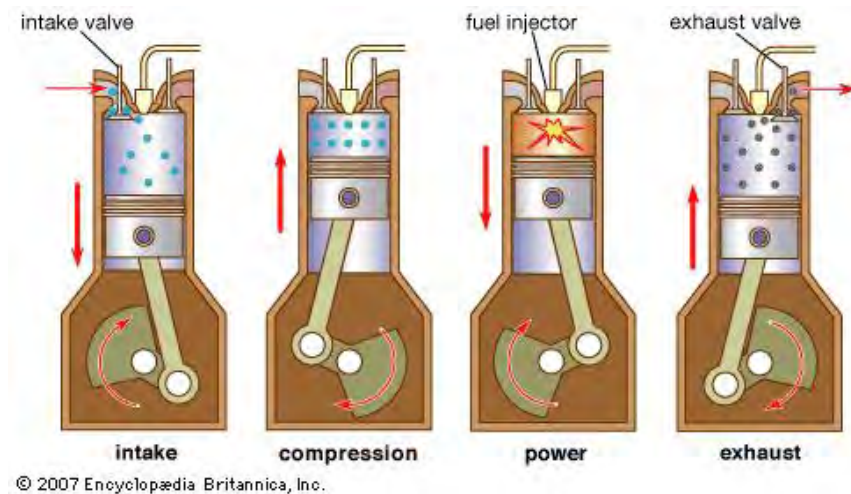


Figure 2.1.: The 4-stroke diesel engine cycle [2]

Figure 2.1 illustrates the combustion cycle in a 4-stroke engine. For the first stroke "intake stroke", the valves opens and in the same time piston moves down. This allows the intake air to flow through the open intake valve and into the combustion chamber. In the second stroke "compression", the valves closes and the piston moves up and the air inside the chamber becomes compressed. For the third stroke "power", the fuel is injected into the chamber. The mixture of highly compressed air and fuel becomes very warm and the outcome is that the mixture self-ignites and forces the piston down again. In the last stroke "exhaust", the piston moves up and forces the burned fuel-air

mixture through the open exhaust valves [1].

In the third stroke the fuel got mixed together with the highly compressed air inside the chamber "internal mixture formation", this can be compared against the gasoline engine where the fuel-air mixture forms during the intake and compression cycle, which makes the gasoline engine to have a "external mixture formation". The same comparison can be made between the two different systems for the power stroke. In a diesel engine the mixture becomes very warm and the mixture self-ignites because of the high temperature, the diesel engine is said to have "auto-ignition". While a gasoline engines air-fuel mixture gets ignited by a spark plug [1].

### **2.1.3. Noise emission**

To be able to reduce the emitted noise from the engine certain knowledge about the noise sources of the engine is of interest. Engines excite noise by [1]:

- Structure-borne noise (engine surface noise/vibrations).
- Pressure pulsations (aerodynamic noise) generated by intake, exhaust and cooling system(s).
- Transmission of vibrations by the engine mount to the chassis or foundation.

#### **Structure-borne noise**

The structure-borne noise can be divided into three sections; Mechanical noise, Combustion noise and Primary drive noise. In the case of combustion noise it can be divided into two sections; Direct combustion noise and Indirect combustion noise.

The different excitation mechanisms are [1]:

- Direct combustion noise is a result from excitation of the combustion walls by the gas force (the combustion pressure force) and this cover typically the frequency range of 500 – 3000 Hz.
- Indirect combustion noise is a result from relative movements influenced by the gas force (crank mechanism and spur gear transmission) or influenced by load-dependent forces (injection pump), e.g. piston noise; impact process between pistons and cylinders.
- Mechanical noise results from relative movements influenced by inertial force (crank mechanism and valve gear), e.g. impact process when the valves closes.

- Primary drive noise is noise that can neither be classified as indirect combustion noise nor as mechanical noise, e.g. pump gear teeth movement relatively to each other excites the engine structure through the gear bearings.

## 2.2. FRF - Frequency Response Function

The frequency response function is defined as the ratio between an output signal  $Y(\omega)$  from a linear system expressed as the function of the angular frequency  $\omega$  and the corresponding input signal  $X(\omega)$  [3].

$$H(\omega) = \frac{Y(\omega)}{X(\omega)} \quad (2.1)$$

Equation (2.1), can be interpreted as the constant of proportionality in the linear relation between the input and output signal complex amplitudes.

The FRF is one of the most important quantities when analyses are done on sound and vibration problems. A common method used to characterize the vibration behaviour of an arbitrary structure is to excite the structure with a known input force and measure its response. For example, this can be applied to a ventilation duct; when the sound pressure at one point is known then the sound pressure at the outlet can be calculated.

## 2.3. FFT - Fast Fourier Transform

The fast Fourier transform is a highly optimized implementation of the DFT (Discrete Fourier Transform) and both gives identical result except that the FFT do it faster [4].

To understand the FFT certain knowledge of the DFT is of importance. A DFT is simply a transform between two domains; the time domain and the frequency domain. It takes a sequence of sampled data and computes the frequency content of that sampled data sequence. This gives the representation of the signal in the frequency domain, as opposed to the time domain representation. Conceptually, the DFT takes a complex signal and break it up into a sum of many cosine and sine waves of different frequencies. The DFT equation is defined as follows [4]:

$$DFT (time \rightarrow frequency) : X_k = H \left( \frac{2\pi k}{N} \right) = \sum_{i=0}^{N-1} X_i e^{-j2\pi ki/N} \quad (2.2)$$

where:  $X$  is the signal represented in the frequency domain,  $k$  and  $i$  are both indexes run from 0 to  $N-1$ ,  $H$  is the frequency response and  $N$  is number of samples.

This equation requires that every single sample in the frequency domain has a contribution from each and every one of the time domain samples. To be able to compute a single sample requires  $N$  complex multiplications and addition operations and in order to calculate the entire transform requires computing  $N$  samples, for a total of  $N^2$  multiplication and addition operations. This can become a computational problem when  $N$  grows large and this is why the DFT is slow and unpractical to use in applications [4].

This is the reason why the FFT got invented, to calculate the DFT in a more efficient way. Rather than requiring  $N^2$  complex multiplies and additions, the FFT requires  $N \times \log_2(N)$  complex multiplication and addition operations. For example, when having an FFT algorithm with a sample of 1024, the computational requirements are reduced to less than 1% of what the DFT algorithm would require [4].

Each time the FFT doubles in size ( $N$  increases by 2), only an additional summation has to be applied, e.g. for  $N = 4$  there is two summations and for  $N = 8$  there are three summations. The number of computations required for each summation is proportional to  $N$ . The required number of summations is equal to  $\log_2(N)$ , and therefore the FFT computational load increases by  $N \times \log_2(N)$  while the DFT computational load increases with  $N^2$ .

The true advantage with FFT compared to DFT is that the FFT algorithm reuses partial products in multiple calculations. For example, if  $X_0$  and  $X_1$  also are present in  $X_2$  and  $X_3$  there are no need to recompute those terms during the calculations of  $X_2$  and  $X_3$ .

## 2.4. Acoustical Holography

Acoustical Holography consists of three components [5];

- Measurement (which means measuring of the sound pressure on the hologram plane).
- Prediction of the acoustic variables (including the velocity distribution on the plane of interest).
- Analysis of the holographic reconstruction

At the NVH department at Volvo Cars the acoustical holography system in use consists of a microphone array with  $120 \frac{1}{4}$ "-microphones placed in a rectangular array with the dimension of  $0.27 \times 0.33$  m and the microphones has a spacing of 3 cm, figure 2.2.



Figure 2.2.: The microphone array with 3 cm spacing.

The microphone grid spacing follows a "rule of thumb" and that is that the spacing is based on the half wavelength criterion; the microphone spacing in cm times the upper frequency in kHz is approximately 15, table 2.1. Together with this "rule of thumb" it is important to keep in mind the requirement of the source distance not being smaller than the microphone grid spacing [6].

Upper frequency (kHz)	×	Microphone grid spacing (cm)	≈ 15
1.0		15	
1.5		10	
2.0		7.5	
3.0		5	
5.0		3	

Table 2.1.: The "rule of thumb" for deciding the upper frequency.

In this case with an array with a microphone grid spacing of 3 cm the upper frequency will be 5 kHz.

As mentioned above, the requirement of the source distance not being smaller than the microphone grid spacing is a result that the resolution (the ability of the system

to distinguish closely spaced sound radiating regions on the source surface) is defined as the smallest separation  $R$  between two point sources such that the system still can separate two distinct maxima in a contour plot of the sound field at the source surface. The low-frequency source resolution is approximately equal to the distance between the measurement plane and the source [6].

In this case with a separation of 3 cm ( $d = 3$  cm) the closest distance to measure is 3 cm ( $a = 3$  cm) away from the source/surface and thus the source resolution cannot be better than approximately 3 cm. This means that two distinct radiating regions on the source surface less than 3 cm ( $R < 3$  cm) apart will appear as one radiating region [6], figure 2.3.

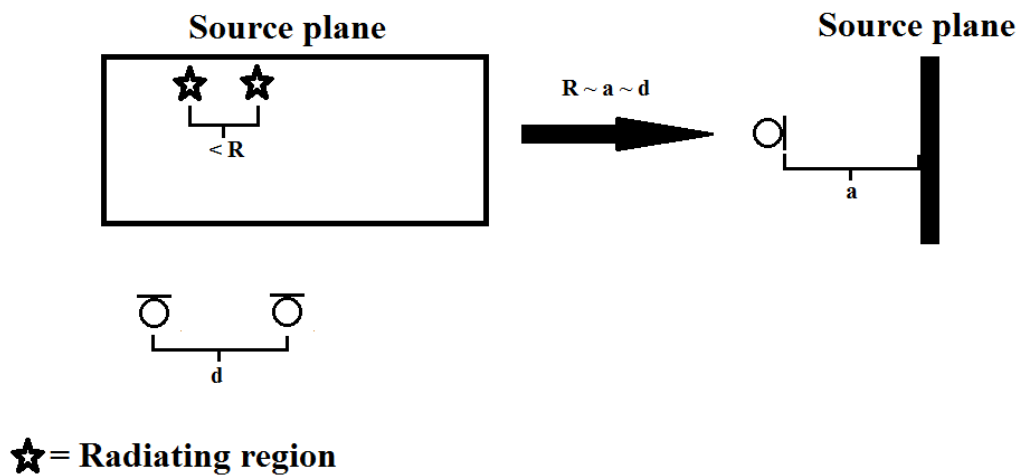


Figure 2.3.: Two distinct radiating regions on the source surface less 3 cm apart appear as one radiating region [6].

What an acoustical holography does is to make an approximate value of e.g. the sound pressure at a specified area. This area could either be in front of the measurement array or behind it, so the user never sees the true value at the actual measurement area but instead an approximated value at the chosen distance.

#### 2.4.1. Statistically Optimal Near-Field Acoustical Holography (SONAH)

The microphone array in use is much smaller than the object under study, hence the use of the Statistically Optimal Near-Field Acoustical Holography, SONAH, method intro-

duced by Brüel & Kjær. This method permits the use of measurement array's much smaller than the object under test [7], and overcomes the limitations of the Near-Field Acoustical Holography, NAH, calculation method [8]. Traditionally it is the NAH calculation method that is used in acoustical holography systems such as Spatial Transformation of Sound Fields, STSF, and Non-stationary STSF, NS-STSF. The SONAH method can operate with irregular arrays without severe spatial windowing effects [9]. Another advantage of the SONAH method compared to the NAH method is that it avoids spatial transforms and thus it avoids truncation effects i.e. leakage in the wave number domain. This is why the measurement array can be smaller than the source [10].

The term statistically optimal near-field acoustical holography is a result of that all the elementary waves (plane and evanescent waves) have an amplitude of unity in the source plane, equation (2.3), from which it follows that the transfer vector  $c(r)$ , equation (2.6), is optimized for a "white" wave number spectrum, i.e. a flat-line spectrum, in the source plane, figure 2.4, [10] and [11].

$$\Phi_m(r) = e^{-j(k_{x,m}x + k_{y,m}y + k_{z,m}z)} \quad (2.3)$$

$$m = 1, 2, \dots, M, M \rightarrow \infty$$

$$k_{z,m} \equiv \begin{cases} \sqrt{k^2 - k_{x,m}^2 - k_{y,m}^2} \text{ for } \sqrt{k_{x,m}^2 + k_{y,m}^2} \leq k \\ -j\sqrt{k_{x,m}^2 + k_{y,m}^2 - k^2} \text{ for } \sqrt{k_{x,m}^2 + k_{y,m}^2} \geq k \end{cases} \quad (2.4)$$

where:  $k$  is the wave-number in the source plane,  $k_{x,m}^2$  is the wave-number for an arbitrary position above the source,  $k_{y,m}^2$  is the wave-number for an arbitrary position above the source,  $z$  is the virtual source plane and  $\Phi_m(r)$  are the elementary waves.

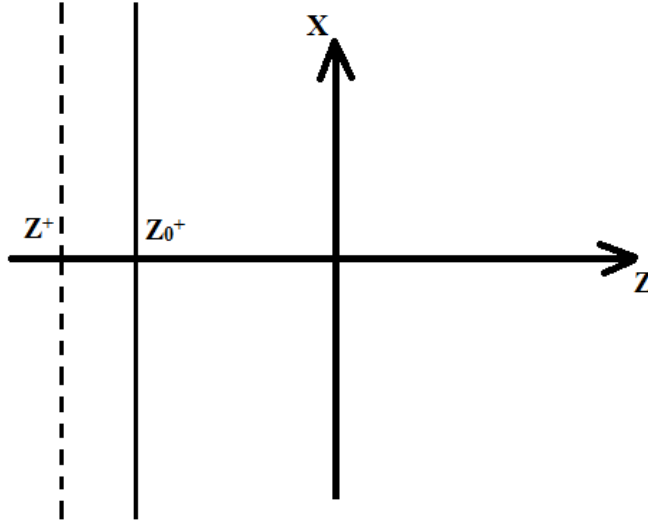


Figure 2.4.: The geometry over a free-field measurement, with only one source plane (vertical line) and one virtual source plane (dashed vertical line), ( $z = z - z^+$ ), [11].

For the sound pressure measurement the SONAH method uses a transfer matrix that works directly on the measured data; therefore the sound pressure at an arbitrary position above the source,  $r = (x, y, z)$  (where  $z > 0$ ), is expressed as a weighted sum of the sound pressures measured at  $N$  positions ( $r_{h,n}$ ) in the hologram plane ( $z = z_h$ ) [10],[11].

$$p(r) \cong \sum_{n=1}^N c_n(r) p(r_{h,n}) = p^T(r_h) \mathbf{c}(r) \quad (2.5)$$

where: T is transpose,  $p(r)$  is the sound pressure as a column vector and  $\mathbf{c}(r)$  is a transfer vector expressed in terms of the least-squares formula.

$$\mathbf{c}(r) = (\mathbf{A}^H \mathbf{A} + \epsilon \mathbf{I})^{-1} \mathbf{A}^H \alpha(r) \quad (2.6)$$

$$\alpha(r) = \mathbf{B}^T \mathbf{c}(r) \quad (2.7)$$

where: matrix  $\mathbf{A}$  is the transpose of  $\mathbf{B}$ ,  $\mathbf{B}$  is a matrix of wave function values at the measurement position,  $H$  is representing Hermitian transpose and  $\mathbf{I}$  is the total number or measurement positions [11].

$\mathbf{c}(r)$  are not dependent on the sound field but only on positions and it is determined by requiring that an infinite set of propagating and evanescent elementary waves of

the form of equation (2.3), are projected from the measurement plane to the prediction plane with optimal accuracy [10].

The SONAH method is also capable to calculate the sound intensity. To get the sound intensity the SONAH method obtains the particle velocity estimates by applying Euler's equation, equation (2.8), to the SONAH pressure estimate given by equation (2.5) and equation (2.6), [11].

$$\tilde{u}_\chi(r) = \frac{-1}{j\omega\rho_0} \frac{\delta\tilde{p}(r)}{\delta\chi} \quad (2.8)$$

where:  $\chi$  is the particle velocity in a direction,  $\omega$  is the angular frequency and  $\rho_0$  is the density of the medium.

$$\tilde{u}_\chi(r) = \frac{-1}{j\omega\rho_0} \frac{\delta\tilde{p}(r)}{\delta\chi} = \frac{1}{\rho_0 c} \mathbf{p}^T (\mathbf{A}^H \mathbf{A} + \epsilon \mathbf{I})^{-1} \mathbf{A}^H \beta_\chi(r) \quad (2.9)$$

where:

$$A^H \beta_\chi(r) \equiv \frac{-1}{jk} \frac{\delta \{ \mathbf{A}^H \alpha(\mathbf{r}) \}}{\delta\chi} \quad (2.10)$$

Then the sound intensity is calculated as [6]

$$I(t) = p(t) \cdot u(t) \quad (2.11)$$

From the sound intensity the radiated sound power can be obtained

$$P = I \cdot A \quad (2.12)$$

where:  $A$  is the area of the measurement plane.

## 2.5. Principal Components Analysis (PCA)

Principal Component Analysis, PCA, is multivariate statistical tool which purpose is to simplify and condense data into a smaller and more manageable set of measurements. The main objective with PCA is data reduction and interpretation [12]. What PCA do is to realign the measurement axes of a set of data such that they coincide with the variability in the data; which gives a more manageable and more comprehensive set of measurement data which is to be analysed. These new axes are linear combinations of the original measurements; this can give useful insights into the relative importance of and interactions between the measurement variables otherwise these effects would have not been readily apparent.

The principal component axes are created by applying the principal axes theorem to the covariance matrix  $\mathbf{S}$ , equation (2.13), the off-diagonal elements of the resulting

matrix are all zero and the diagonal elements are the eigenvalues,  $\lambda$ , of  $\mathbf{S}$  and these represent the variance in each of the resulting principal component directions [13].

$$\mathbf{S} = \begin{pmatrix} S_{11} & \cdots & S_{1p} \\ \vdots & \ddots & \vdots \\ S_{p1} & \cdots & S_{pp} \end{pmatrix} \quad (2.13)$$

$$S_{jk} = \frac{1}{n-1} \sum_{i=1}^n (x_{ij} - \bar{x}_i) (x_{kj} - \bar{x}_k) \quad (2.14)$$

where:  $S_{jk}$  is the sample covariance,  $x_{ij}$  is the measurement of the  $i$ :th variable and  $\bar{x}_i$  is the sample mean of a variable.

Sum up the two main objectives of PCA are (1) data reduction and (2) data interpretation. The data reduction is accomplished by using a set of principal components  $k$  which is smaller than the original set of measurements  $p$ . The selection of these components and how many there should be used is based on an examination of the eigenvalues  $\lambda$ . The data interpretation is accomplished through an examination of the eigenvectors; which means to examine the linear combinations of the original variables which were used to compute the resulting principal components [13].

## 2.6. Lucas filter

The common method today when measuring the structural attenuation is to use the combustion noise meter, more common known as Lucas filter, which was introduced by Lucas Industries Noise Centre in the 1980s. This instrument uses the signal from a cylinder pressure transducer to calculate and display the combustion noise level of the engine. The displayed value shows what the noise level measured one meter from the engine would be if only the combustion noise were included [14].

What Lucas Industries did was to measure the structural response to combustion excitation on several diesel engines and then where the structural responses of all the engines averaged together to form a response curve, the Lucas filter. This filter is then used as a weighting function on the signal from the cylinder pressure transducer, and then the signal is A-weighted [14]. There is no influence from either the mechanical or ambient noise in this method.

### 2.6.1. Banger Rig

One of the methods used at Volvo Cars today when measuring the structural attenuation of a diesel engine is to use a banger rig. What this banger rig does is to excite a

non-running engine with realistic combustion forces, which allows studies on only the combustion induced noise in absence of mechanical noise [15].

The set-up of this method is that the engine is set at top-dead centre (the firing stroke) on the cylinder under investigation. The injector is replaced by a banger unit and the combustion chamber is filled with a pre-determined mixture of propane, oxygen and air; via the banger unit. This mixture is then ignited by the spark plug. This method is then repeated with 3 seconds intervals [15].

The cylinder pressure is measured by an in-cylinder piezoelectric pressure transducer and the sound pressure outside the cylinder is measured at 4 standard, 1 metre, microphone positions [15]; from this the structural attenuation is obtained.

The structural attenuation, equation (2.15), is defined as the attenuation in the process whereby the combustion pressure vibration in the cylinder is transmitted from the combustion chamber wall surface through the engine structure to eventually become external surface vibrations and finally radiated as combustion noise [16].

$$\text{Structural attenuation} = \frac{\text{Cylinder pressure}}{\text{Combustion noise}} \quad (2.15)$$

A low noise attenuation means that the structural attenuation is large.

### 2.6.2. Regression methods

There are other methods for determining the structural attenuation which is based on regression and is carried out on running engines.

One of these methods is the combustion/mechanical (C/M) noise breakdown calculation method. This method is calculated from load sweep from minimum to maximum engine torque at an array of constant speeds throughout the engine speed range. Then multiple regression techniques are employed to determine the percentage split of each noise type [17].

To obtain the structural attenuation the equation of the engine sound power is used, equation (2.16).

$$SP = SP_m + H \times CP + G \times L \quad (2.16)$$

where: SP is the engine sound power level,  $SP_m$  is the mechanical sound power, CP is the cylinder pressure sound power, H is the transfer coefficient between the cylinder pressure sound power and combustion noise sound power, L is the square of the engine

torque and  $G$  is the transfer coefficient between torque and load dependent noise.

By solving  $H$  from equation (2.16), the structural attenuation of the engine is known [17].

## 3. Implementation

This chapter covers how the proposed method for measuring the structural attenuation of an engine block was developed. It covers two major areas; measurements on a diesel engine with the acoustic camera and the development of a matlab-software for post-processing.

This proposed method, Lucas Near-Field function, was then validated against the current method for measuring the structural attenuation, the Lucas filter function described in section 2.6.

All measurements were conducted in the gearbox NVH test cell at Volvo Car Corporation's NVH department situated in Göteborg, Sweden, between April and May 2013.

All measurements were conducted on a 4-cylinder prototype diesel engine.

### 3.1. Measurements

#### 3.1.1. Gearbox NVH test cell

The gearbox test cell is an anechoic chamber in which measurements on gearboxes are conducted. Anechoic chambers are used to mimic free-field conditions, i.e. conditions where only the direct sound field is present.

The dimensions of the test cell is  $7 \times 3.5 \times 3.5$  m and the usable floor area is  $24.5$  m<sup>2</sup>; the floor and the roof in the test cell are separated from the rest of the building. The test cell complies with ISO 3745 down to 250 Hz and upwards it has an absorption coefficient greater than 0.95 ( $\alpha \geq 0.95$ ).

#### 3.1.2. Loudspeaker element

Two loudspeaker elements were used; TPC80NV/4 manufactured by Gradient and FRS 8 - 4 ohm manufactured by Visaton, see appendix A for the product sheets. The reason why two loudspeaker elements were used was that after the first measurements the TPC80NV/4's voice coil had almost melted and it had to be replaced.

These two elements were chosen because they had the right dimensions to fit in the chamber, 3.3". Unfortunately, there was no sufficient amount of data regarding the loudspeaker element TPC80NV/4, so a measurement regarding its frequency response was conducted at Chalmers in the Department of Applied Acoustic's anechoic chamber, see appendix A.1.1

For the measurements the loudspeaker elements were excited with white noise with an overall level of  $\sim 150dB$  inside the combustion chamber; this level was chosen to get sufficient Signal to Noise Ratio on the outside of the engine. Fortunately, with this high overall level it did not create any resonance in the frequency range of interest (500 - 3000 Hz) as can be seen in figure 3.1.

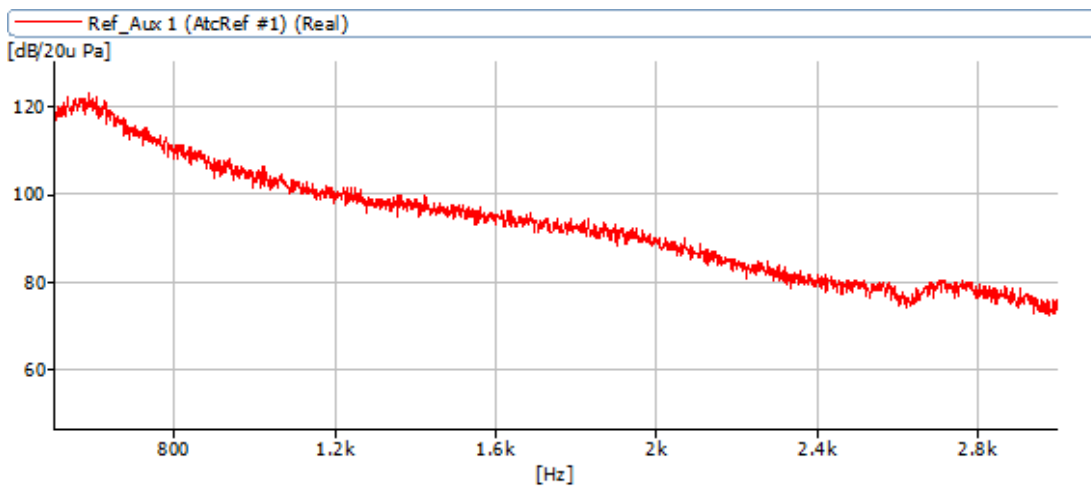


Figure 3.1.: No resonances in the frequency range of interest. Y-axis depicts the Sound Pressure Level in dB and X-axis depicts Frequency in Hz.

To be able to place the loudspeaker element in one of the cylinder chambers, a model of a piston, figure 3.2, was constructed out of the plastic material polyoxymethylene (common known by the sales name Delrin), which is a thermoplastic used for precision parts which requires high stiffness, low friction and excellent dimensional stability. The layout for this piston can be viewed in appendix B and the complete configuration can be viewed in figure 3.3.



Figure 3.2.: The model of a piston made out of Delrin.



Figure 3.3.: The configuration with the loudspeaker element placed in the piston model.

### 3.1.3. Distance to Top Dead Center

To know at which distance inside the cylinder chamber the loudspeaker piston had to be placed to resemble the distance from top dead center, TDC, the real piston has when the pressure inside the chamber has it maximum; the data from a crank angle measurement were used. This measurement, figure 3.4, indicates at which crankshaft angle the piston has when pressure maximum occurs inside the chamber.

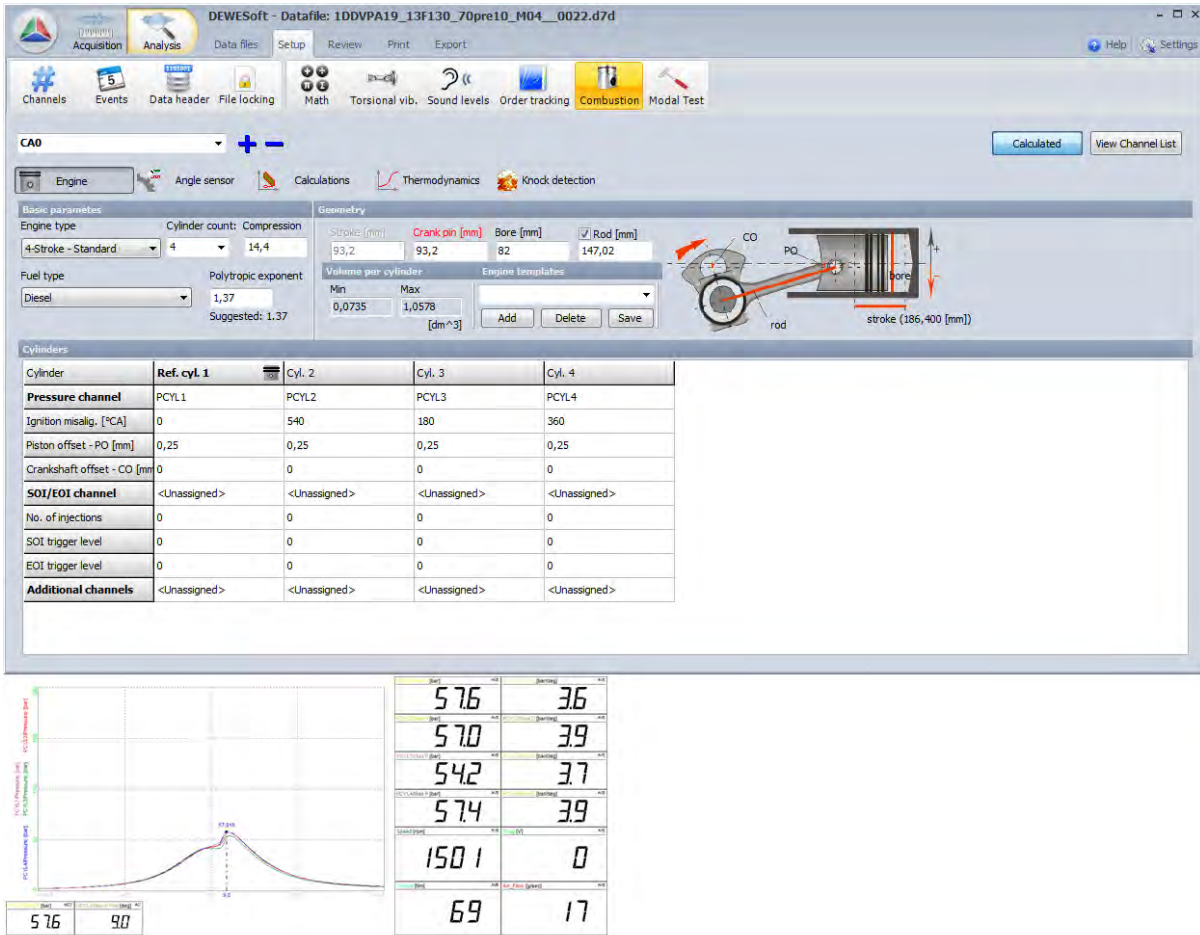


Figure 3.4.: The crank angle measurement; pressure maximum at 9 deg.

To get the distance the piston has travelled from TDC before pressure maximum occurs, a commonly used equation was used, equation (3.1) [18].

$$HT = (r + c) - (r \times \cos(a)) - \sqrt{c^2 - (r \times \sin(a))^2} \quad (3.1)$$

where: HT is the height of piston, S is the stroke, c is the rod length, a is the crank angle in radian and r is half of stroke.

The necessary numbers for this calculation were taken from figure 3.4.

From equation (3.1) the height of the piston became 0.76 mm, and to verify that this equation was correct another approach based on trigonometry was also used, figure 3.5.

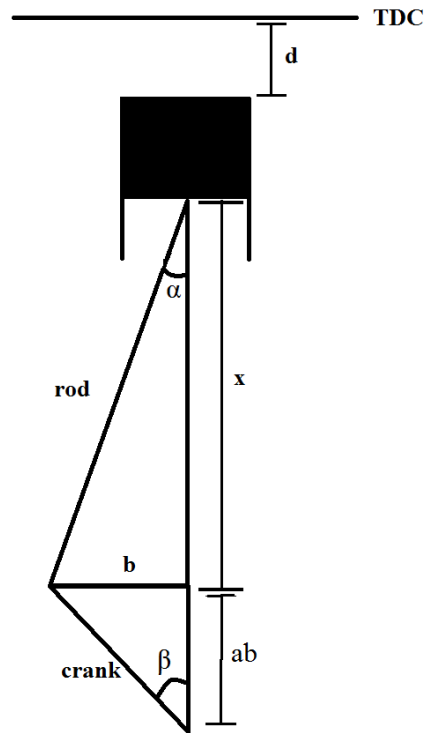


Figure 3.5.: The piston distance calculate with trigonometry.

$$crank = \frac{93.2}{2} = 46.6 \quad (3.2)$$

$$b = \sin(\beta) \times crank \quad (3.3)$$

$$ab = \cos(\beta) \times crank \quad (3.4)$$

$$rod = 147.02 \quad (3.5)$$

$$\alpha = \sin^{-1}\left(\frac{b}{rod}\right) \quad (3.6)$$

$$x = \cos(\alpha) \times rod \quad (3.7)$$

$$d = rod + crank - ab - x \quad (3.8)$$

where:  $\beta$  is the crank angle when pressure maximum occurs.

Also in this calculation all the numbers are from the crank angle measurement figure 3.4.

This approach gave a distance,  $d$ , of 0.7546 mm which means that the first approach used were correct. This means that the distance that the piston has travelled when pressure maximum occurs is 0.75 mm. But, due to practicable reasons this distance could not be used. Instead a distance of 10 mm was used, figure 3.6.



Figure 3.6.: The placement of the loudspeaker element inside the combustion chamber.

#### 3.1.4. Measurement setup

All measurements were conducted on a computer with Windows 7; Enterprise 64-bit, Intel core i7, CPU @ 2.60 GHz and 8 GB RAM. The software used for the measurements was developed by Brüel & Kjær and is called Pulse LabShop. The computer was connected to a front-end configuration, to which also the loudspeaker, the holography system and two reference microphones were connected to, figure 3.7 shows the complete configuration and appendix C shows the list of instrumentation used.

One of the reference microphones, ref.1 in figure 3.7, was placed TDC inside the cylinder chamber at the position where normally the injection nozzle is placed, figure 3.8. This microphone was placed there because the pressure inside the chamber was of importance to know in order to be able to create an FRF, section 2.2.

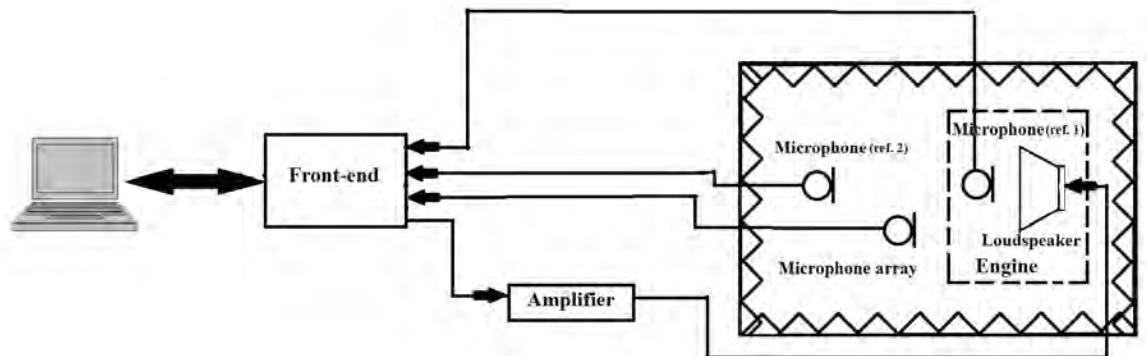


Figure 3.7.: The measurement configuration used.



Figure 3.8.: The reference microphone placed at the injection nozzle position.

The other reference microphone, ref.2 in figure 3.7, was placed outside the engine one metre away at five different positions around the engine. From this microphone the Lucas function, section 2.6, were calculated for each side in order to be able to validate the

new method.

The 4-cylinder prototype diesel engine under test was completely stripped of accessories. The only parts attached to it were: the cylinder head and oil pan (the oil pan was drained of oil) on the outside and on the inside was only the crankshaft attached without any pistons attached to it and only the cylinder at which the loudspeaker was placed in had its cylinder valves closed.

Two different assembly designs were used for this engine; one when all the openings to the engine were open, "Open" assembly design, and one were they had been closed with rubber plugs, "Closed" assembly design, figure 3.9 shows the two assembly designs. These two assembly designs were used to demonstrate that the technique worked on different designs. The engine itself was hanged from a steel frame, figure 3.10.

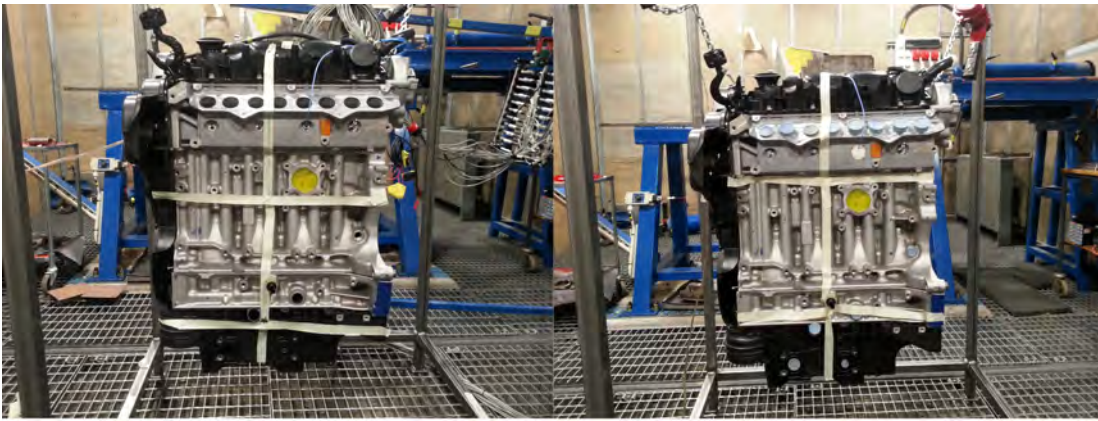


Figure 3.9.: The picture to the left is "Open" assembly design and the picture to the right is "Closed" assembly design.



Figure 3.10.: The steel frame that the engine was hanged from during the measurements.

### **Microphone array**

The microphone array used by the holography system is an array consisting of 120  $\frac{1}{4}$ "-microphones, placed with 3 cm spacing between each other and the dimension of the array is  $0.27 \times 0.33$  m. This array is a complete solution from Brüel & Kjær and belongs to their Acoustical Holography system, section 2.4. The array was placed 3 cm away from the engine, see section 2.4 for the theory behind this, and each side of the engine was divided into a certain number of measurement areas, appendix C.2, in order to be able to cover each side completely. With a distance of 3 cm mean that the array is placed in the near-field; hence the name SONAH, see theory section 2.4.1. These areas were then configured in LabShop to correspond to a certain measurement area by using a global coordinate system and then each area was connected to separate measurements.

## 3.2. Post-processing

The post-processing was done with two different software's developed by Brüel & Kjær; Array Acoustic and Pulse Reflex.

In Array Acoustic the data from LabShop were processed and the outcome was sound pressure and/or sound intensity in the frequency range of 400 - 4000 Hz with 1 Hz frequency resolution, see appendix C.3 for specifications. This range was chosen because the frequency range of interest is 500 - 3000 Hz, and when the conversion into 1/3-octave band was performed sufficient amount of data in the lower and upper frequencies were available. The frequency range of 500 - 3000 Hz was chosen because it is in this range that the combustion noise is most prominent.

To get the sound pressure and/or sound intensity level from the holography system, Array Acoustic first converts the time data into frequency domain, then it applies the theory of principal component analysis, theory section 2.5, to the data; PCA is applied to all the measurement channels in order to separate the coherent components in the sound field so that it would be able to project the sound field from the grid plane into a plane in front of the grid as close as possible to the surface of the structure. The last step is that it is performing holography calculations; which creates an estimate of the sound pressure level at the chosen calculation plane.

To get the sound pressure level for the two different reference microphones another post-processing program was used, Pulse Reflex. This program converts the time data for each signal into frequency domain using ordinary FFT, theory section 2.3, on the signals.

Also a new post-processing program was developed in Matlab; this program imports the processed data from both Array Acoustic and Pulse Reflex in order to calculate the Lucas function and the new function, the Lucas Near-Field function. For the new function it takes the sound pressure from Array Acoustic which corresponds to the sound pressure measured by the array and divides it with the sound pressure from Pulse Reflex which is the data for the reference microphone placed inside the cylinder chamber; this method is also known as a frequency response function, theory section 2.2. The division occurs for each signal in the array (120 signals) and also with an average over all the measurement areas on each side and every microphone signal. After this the data is transformed into sound pressure level and then an A-weighting filter is applied to the data; this is because it still follows the definition of the Lucas function, theory section 2.6.

The new program then displays the average value both in narrowband and in 1/3-octave band. The program can also display weakness of a complete side of engine by selecting a frequency in the narrowband. The program can show a complete side of the engine because it puts together every measurement area into one complete area. Figure 3.11 and 3.12 shows how the matlab program looks like and works.

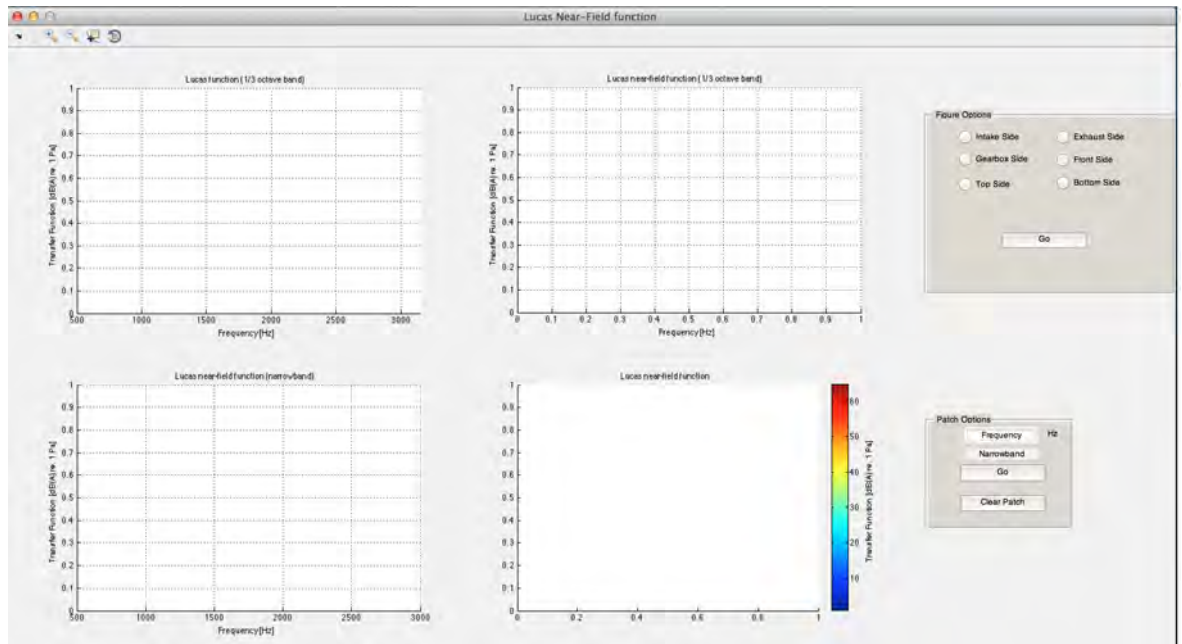


Figure 3.11.: The matlab program developed for the Lucas near-field function.

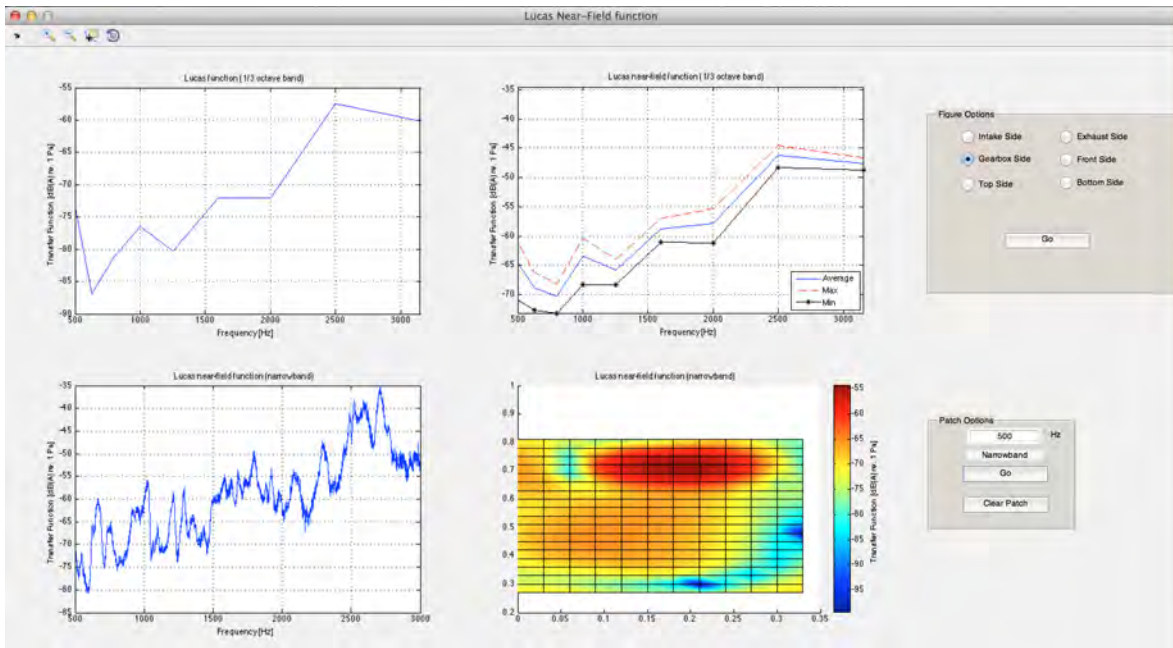


Figure 3.12.: The matlab program analysing the gearbox side.

## 4. Results

From the measurements carried out on the 4-cylinder prototype diesel engine, only the measurements on the intake side will be presented in this chapter. This is because all sides displays the same behaviour with certain areas having a higher radiating sound pressure then other areas.

In appendix D the measurements carried out on the other sides can be viewed.

There will be a comparison between two different assembly design's of the engine; "Open" and "Closed". The difference between these two designs is that with "Open" it means e.g. that the intake holes are open while with "Closed" it means that e.g. that the intake holes are closed with rubber plugs, as can be viewed in figure 3.9. This comparison is conducted to demonstrate that the technique works on different assembly designs.

## 4.1. Lucas Near-Field function vs. Lucas function

Figure 4.1 shows the Lucas Near-Field function (averaged over the intake surface six measurement areas) compared against the Lucas function while having the "Open" assembly design.

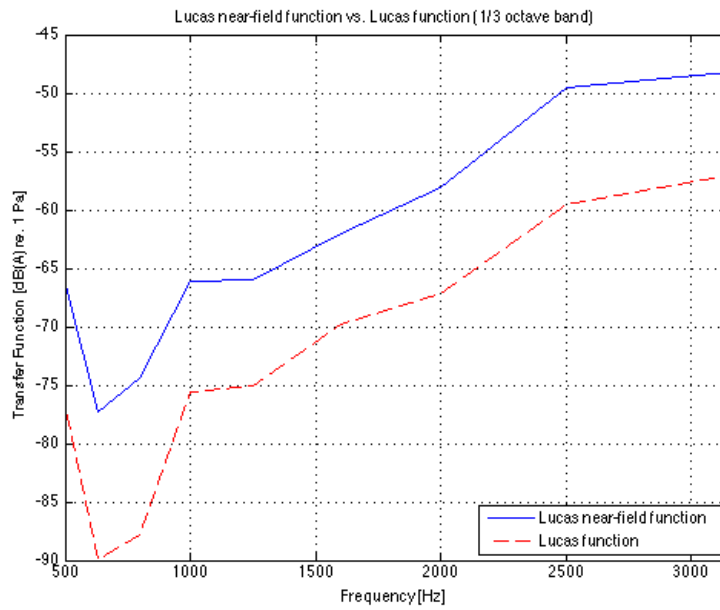


Figure 4.1.: The Lucas Near-Field function vs. the Lucas function with "Open" assembly design.

Figure 4.2 shows the Lucas Near-Field function (averaged over the intake surface six measurement areas) compared against the Lucas function while having the "Closed" assembly design.

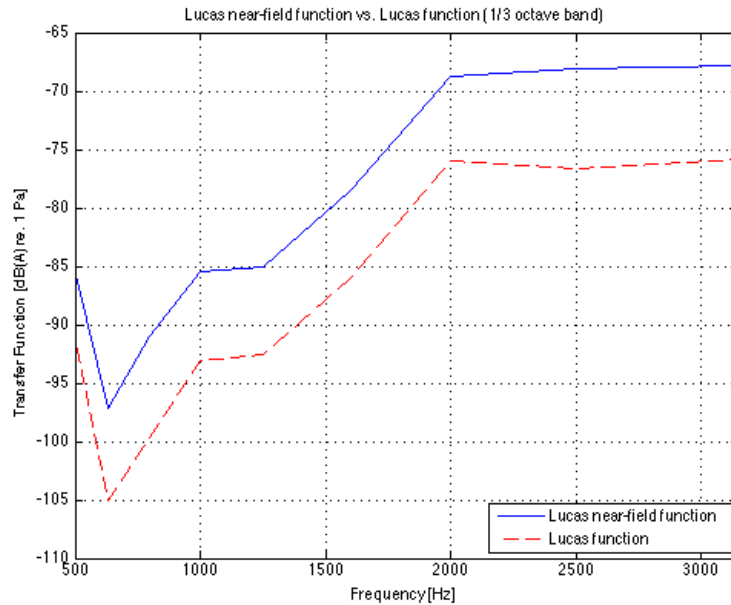


Figure 4.2.: The Lucas Near-Field function vs. the Lucas function with "Closed" assembly design.

## 4.2. Array Acoustic: estimated sound pressure level

For the intake side four different frequencies were chosen to see the difference between "Open" and "Closed" assembly design. These frequencies were: 500, 1029, 1290 and 2720 Hz. They were chosen because at those frequencies there were distinct peaks in the total radiated sound pressure plot from the software Array Acoustic. As mentioned in theory section 2.4, these values are only the estimated sound pressure level on the engine surface. In figure 4.3 - 4.10 the sound pressure level on the intake side for the four different frequencies are presented.

### 4.2.1. "Open" assembly design

At 500 Hz, figure 4.3, there are two main areas that have the highest radiating sound pressure level; the oil pan and the cylinder head.

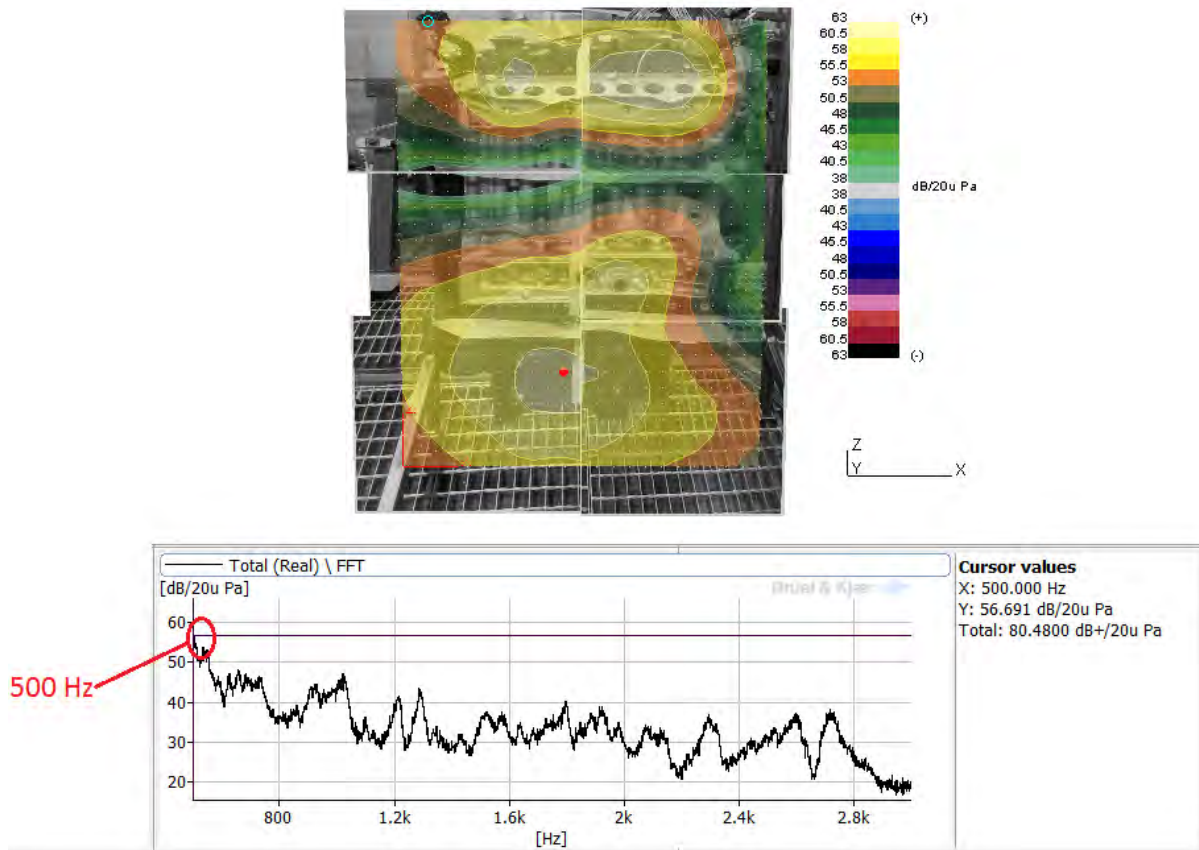


Figure 4.3.: The estimated radiated sound pressure level at 500 Hz.

At 1029 Hz, figure 4.4, the area that has the highest radiating sound pressure level is the cylinder head, but now it is possible to recognize two distinct sound sources i.e. cylinder 1 and cylinder 3 (counting from the right side).

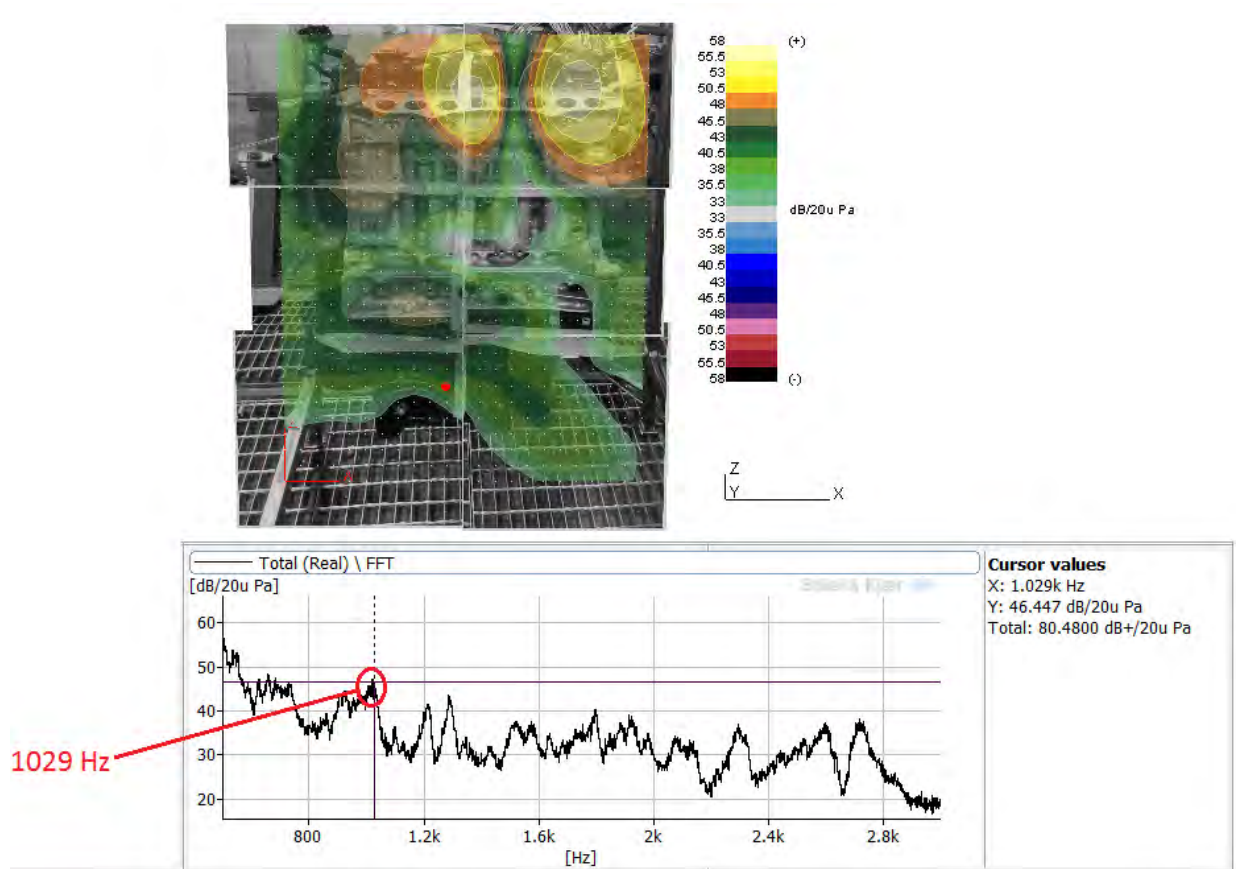


Figure 4.4.: The estimated radiated sound pressure level at 1029 Hz.

At 1290 Hz, figure 4.5, there are three main areas that has the highest radiating sound pressure level. These areas are covering three openings in the oil pan, i.e. oil cooler, oil pipe and oil temperature sensor. Also there are two distinct areas still at the cylinder head i.e. cylinder 2 and cylinder 4.

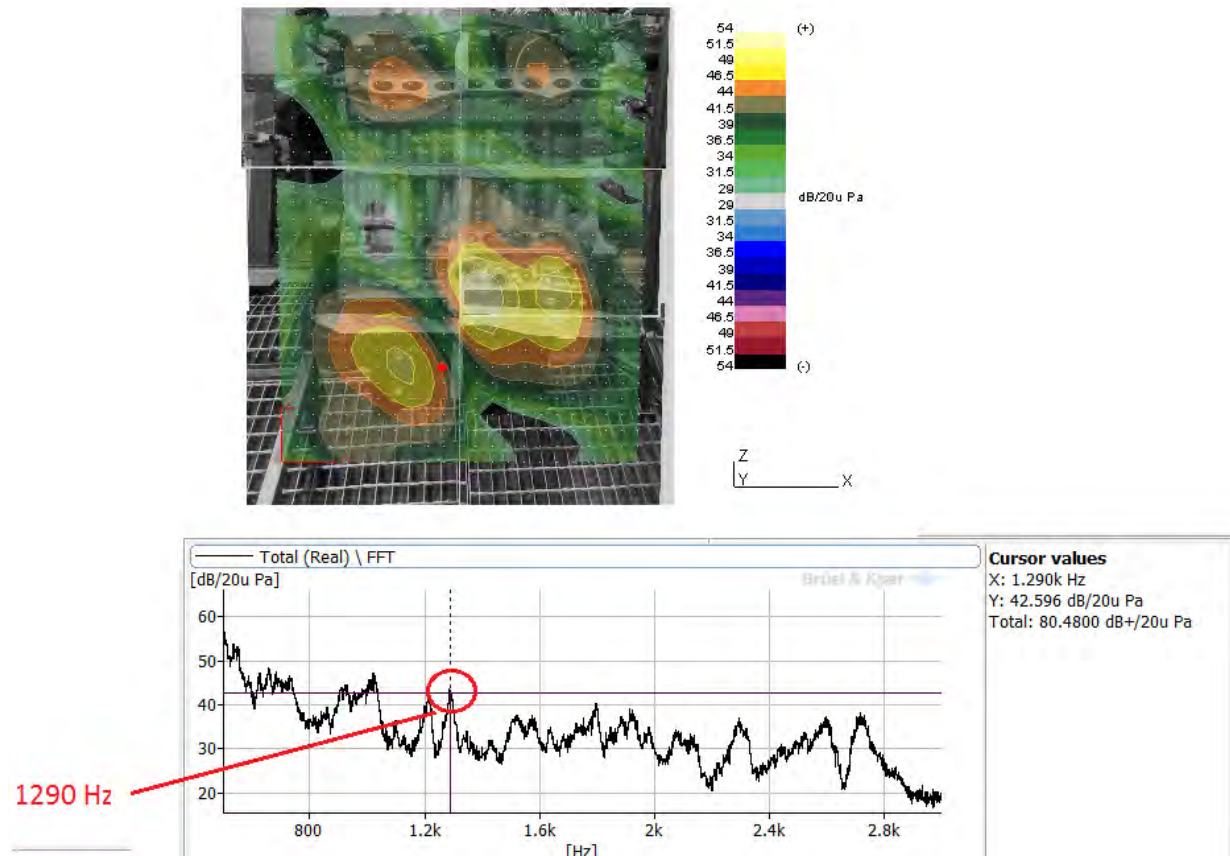


Figure 4.5.: The estimated radiated sound pressure level at 1290 Hz.

At 2720 Hz, figure 4.6, there are four areas that has the highest radiating sound pressure level. Three of these areas are on the cylinder head approximately around cylinder 1, 2 and 4. The fourth area is at the oil suction pipe.

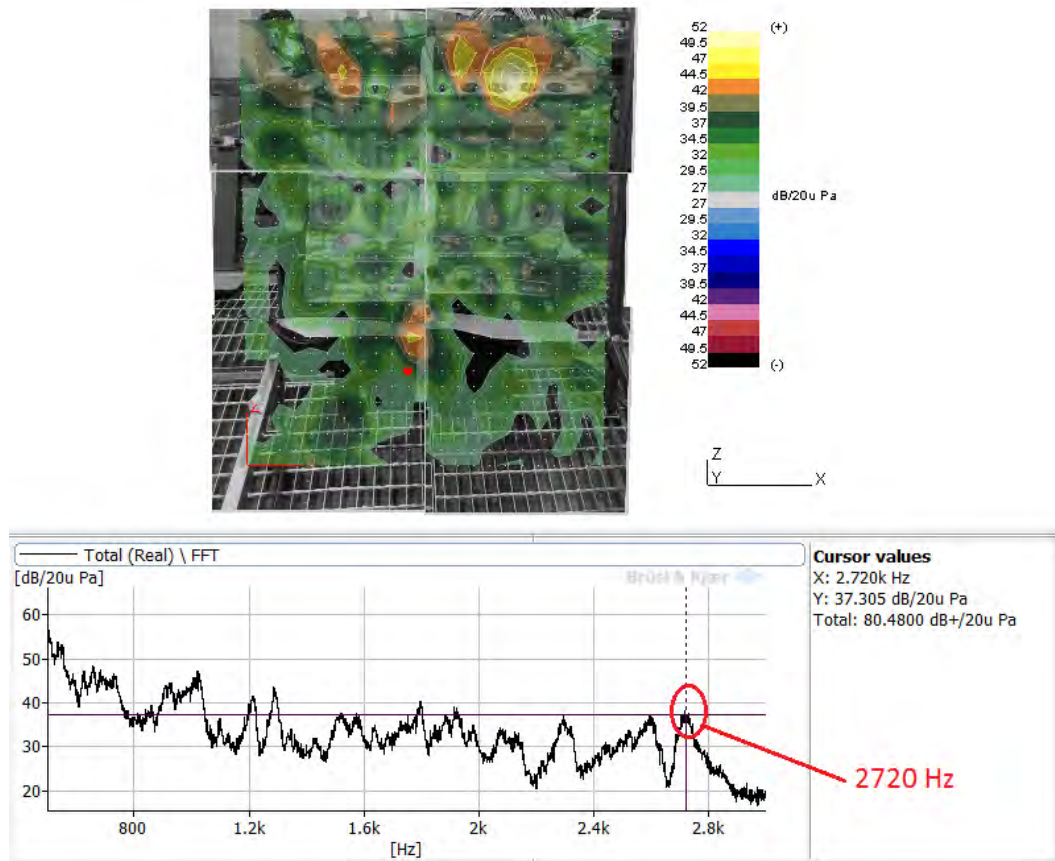


Figure 4.6.: The estimated radiated sound pressure level at 2720 Hz.

### 4.2.2. "Closed" assembly design

As mentioned "Closed" assembly design refers to when intake and exhaust holes has been closed with rubber plugs.

At 500 Hz, figure 4.7, the main area of radiating sound is still the oil pan as in the case with "Open" engine assembly. However, there are no longer any radiating sound from the cylinder head, instead the area radiating sound now is located at the fourth cylinders glow-plug. The area to the upper right position in the figure are a result from that the array was position a bit outside the surface of the intake side and hence picked up some sound from the gearbox side. One interesting result in this figure is the area that cut straight through the figure and separates the two sides from each other, because this resembles a node from a vibrating surface.

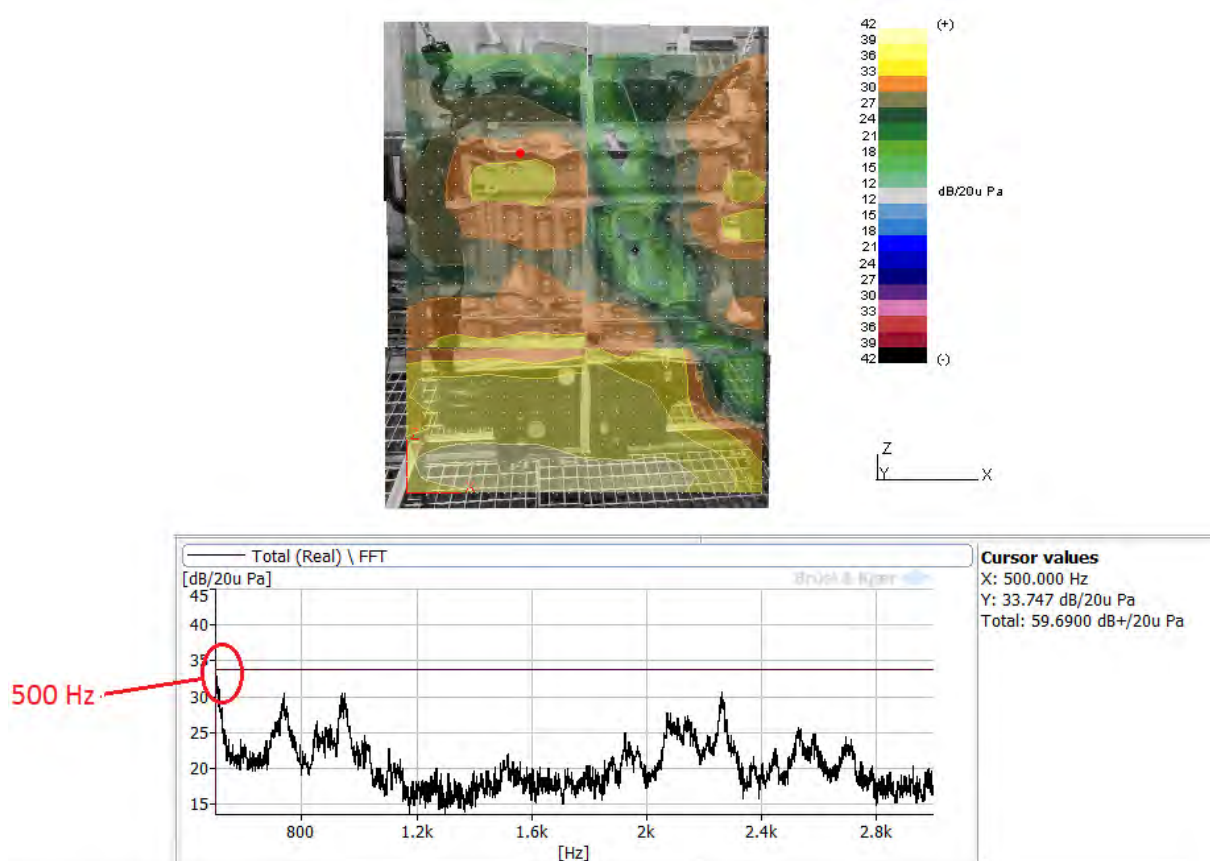


Figure 4.7.: The estimated radiated sound pressure level at 500 Hz.

At 1029 Hz, figure 4.8, the estimated sound pressure level on the intake side has a complex appearance compared to the "Open" assembly design. The main radiating area is the oil pan.

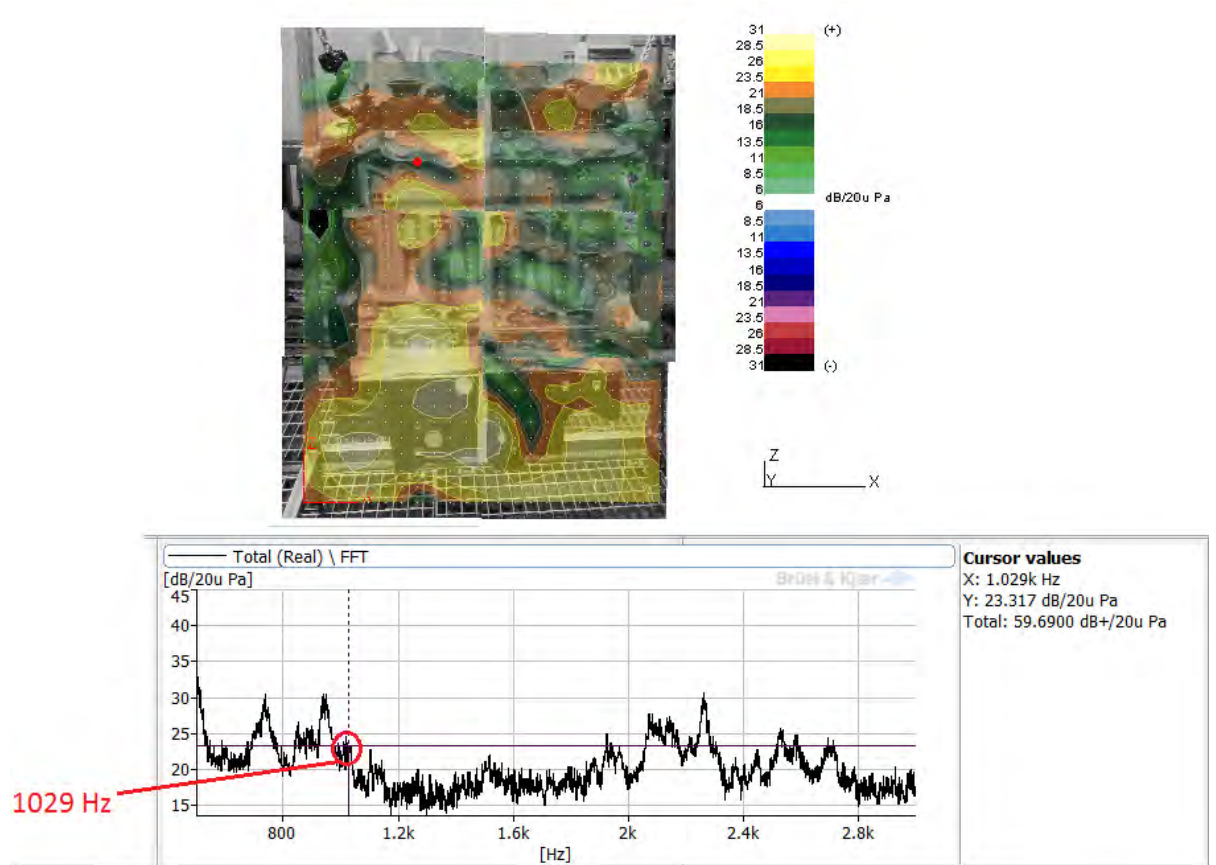


Figure 4.8.: The estimated radiated sound pressure level at 1029 Hz.

At 1290 Hz, figure 4.9, there are not any dominating area on the intake side that dominates the radiated sound. Instead there are a number of small areas scattered around the intake side, with a concentration around the middle of the engine.

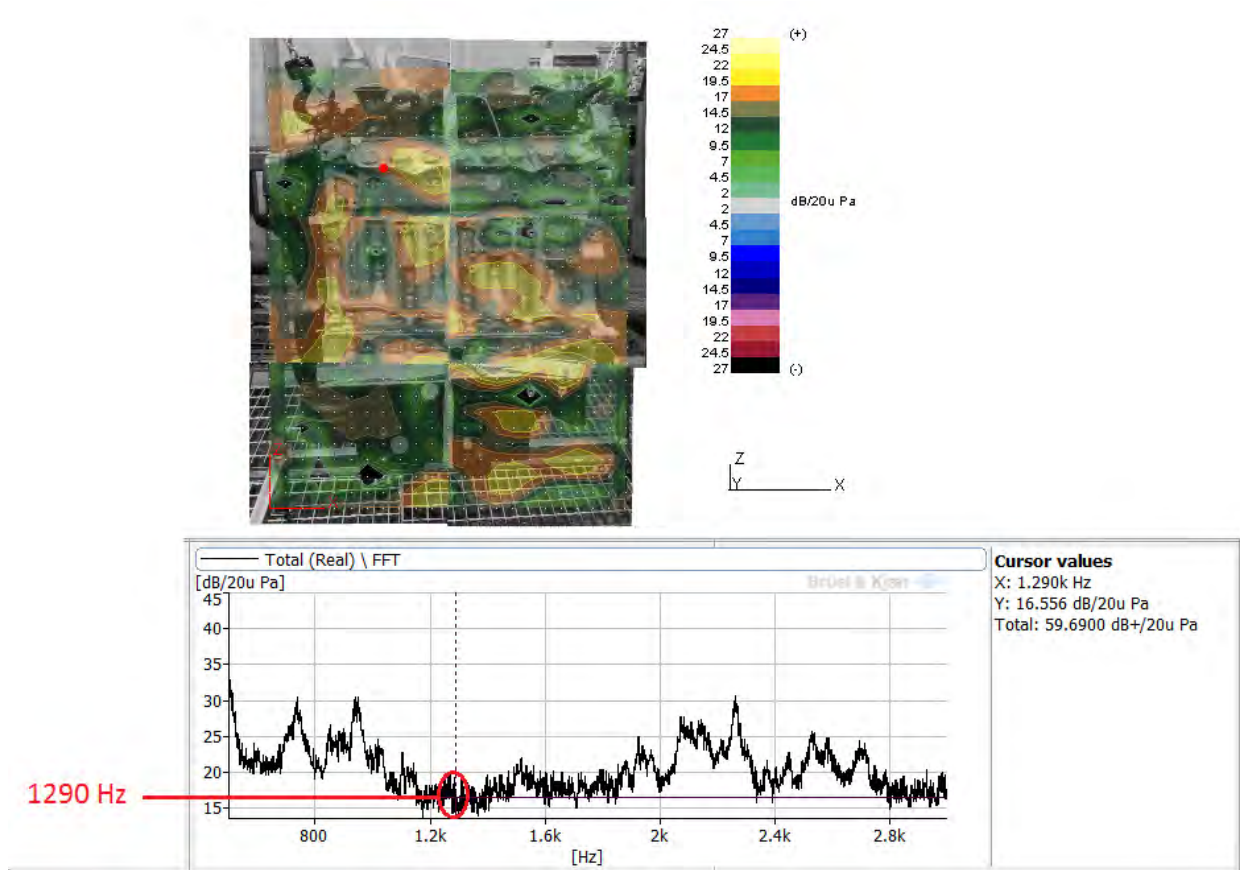


Figure 4.9.: The estimated radiated sound pressure level at 1290 Hz.

At 2720 Hz, figure 4.10, the main radiating area is once again concentrated around the oil pan.

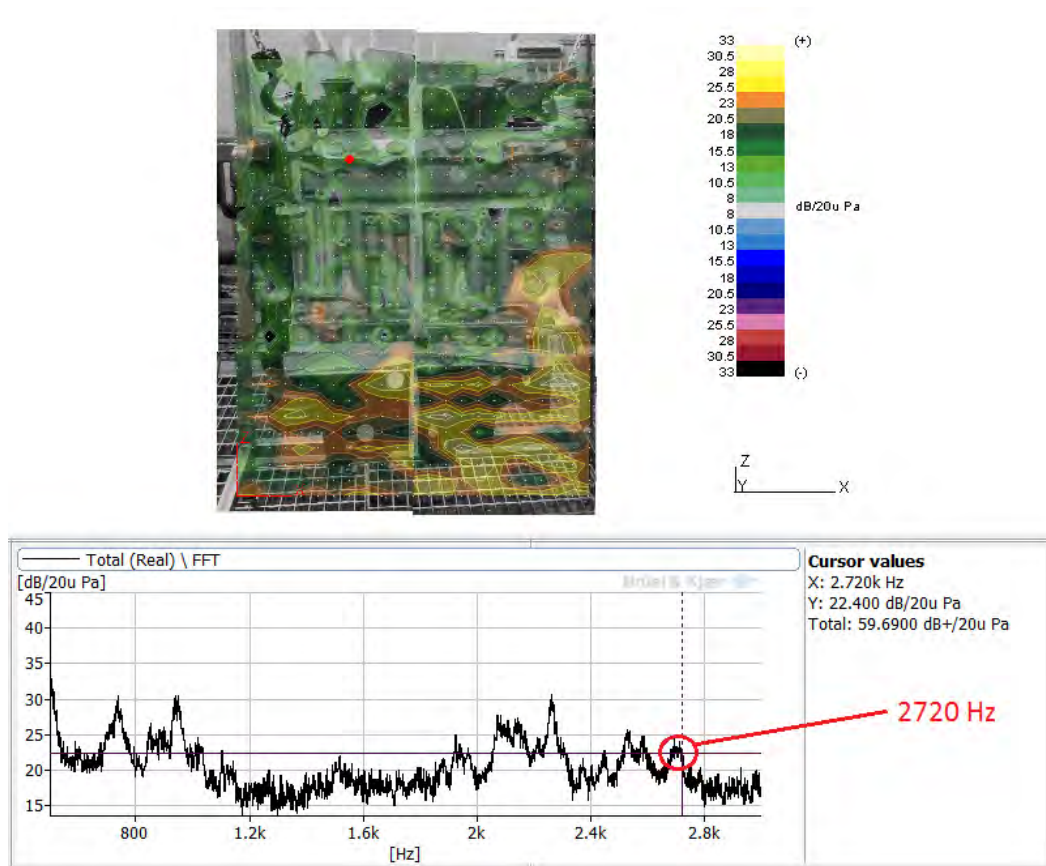


Figure 4.10.: The estimated radiated sound pressure level at 2720 Hz.

### 4.3. Lucas Near-Field function

For the Lucas Near-Field function the same frequencies as used for the Array Acoustic calculations were used for the two assembly designs: 500, 1029, 1290 and 2720 Hz.

The following figures, in the two subsections, shows the transfer function as patch objects, where each node refers to a microphone in the microphone array. These figures are made to be a complement to the figures obtained from the software Array Acoustic and the current method, the Lucas function.

#### 4.3.1. "Open" assembly design

In this section the transfer function of the "Open" assembly design are presented. They do not have exactly the same dB range as the figures obtained from the software Array Acoustic, this is because these figures show the transfer function while the figures from Array Acoustic only show the estimated sound pressure level on the outside of the engine. The figures show the wanted resemblance with the figures in the "Open" assembly design section" from section 4.2.

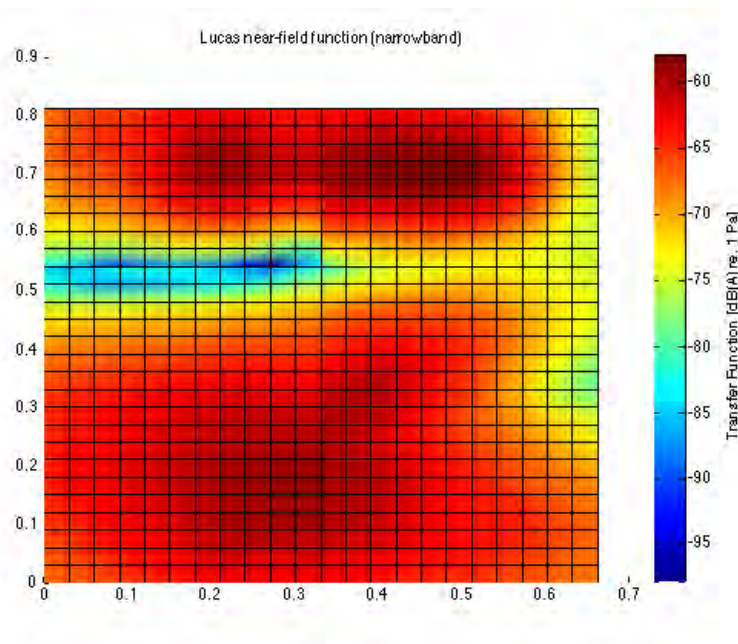


Figure 4.11.: The transfer function over the intake side at 500 Hz.

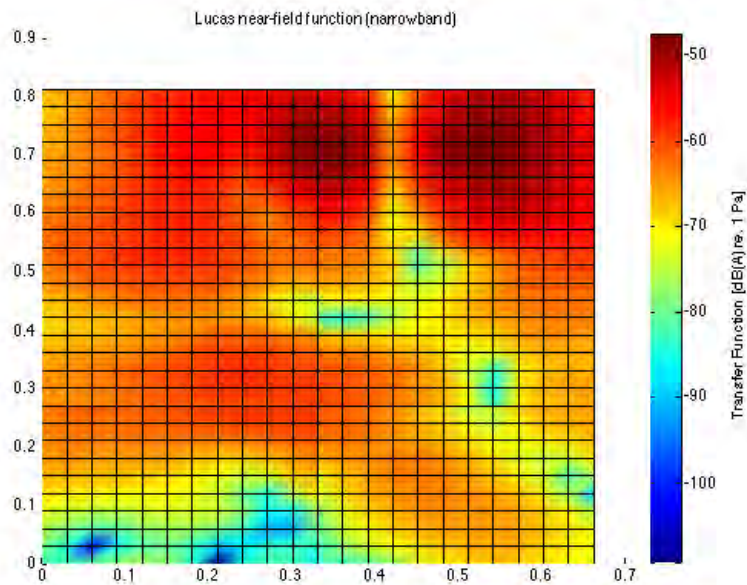


Figure 4.12.: The transfer function over the intake side at 1029 Hz.

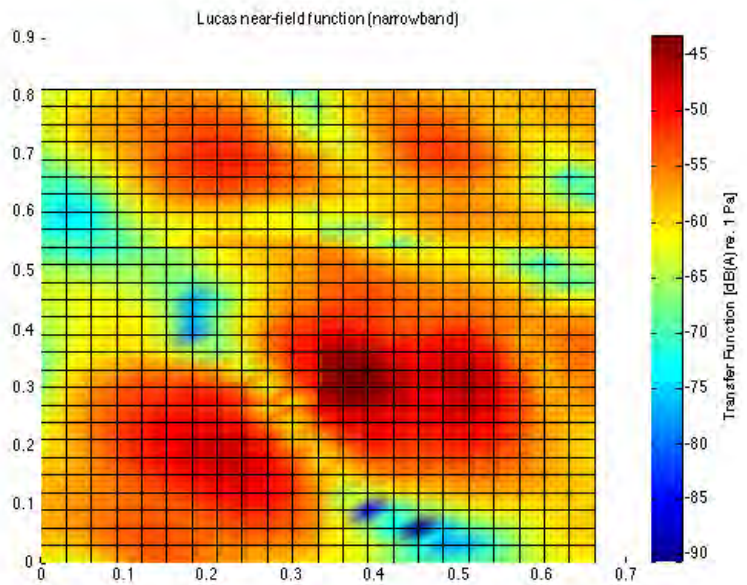


Figure 4.13.: The transfer function over the intake side at 1290 Hz.

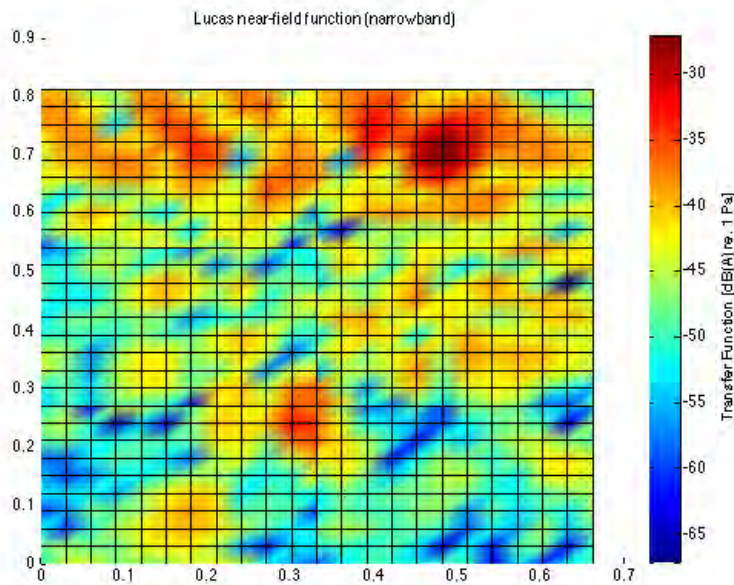


Figure 4.14.: The transfer function over the intake side at 2720 Hz.

#### 4.3.2. "Closed" assembly design

In this section the transfer function of the "Closed" assembly design are presented. They do not have exactly the same dB range as the figures obtained from the software Array Acoustic. The figures shows the wanted resemblance with the figures in the ""Closed" assembly design section" from section 4.2.

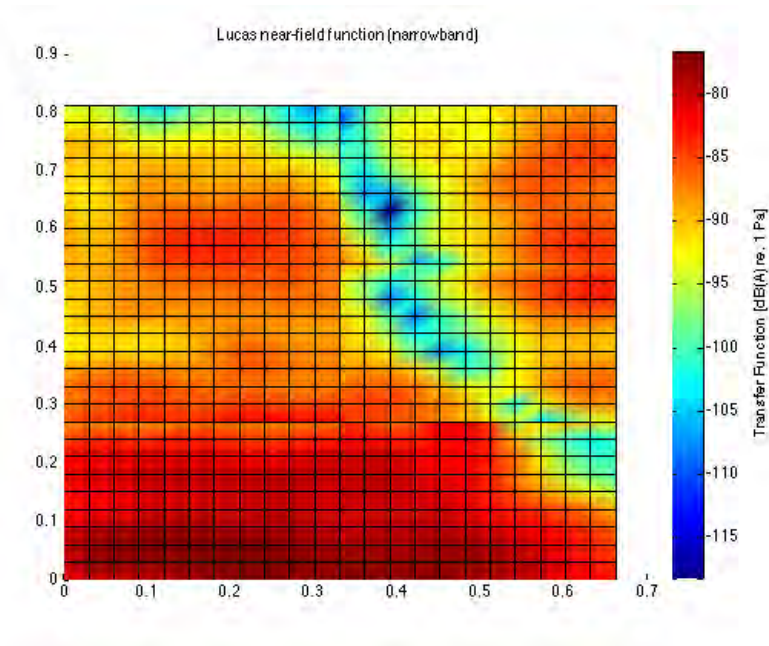


Figure 4.15.: The transfer function over the intake side at 500 Hz.

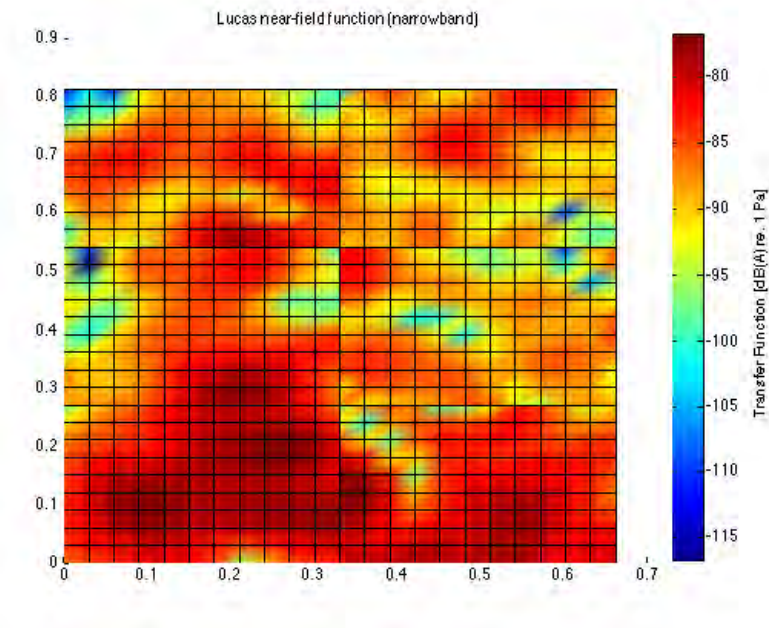


Figure 4.16.: The transfer function over the intake side at 1029 Hz.

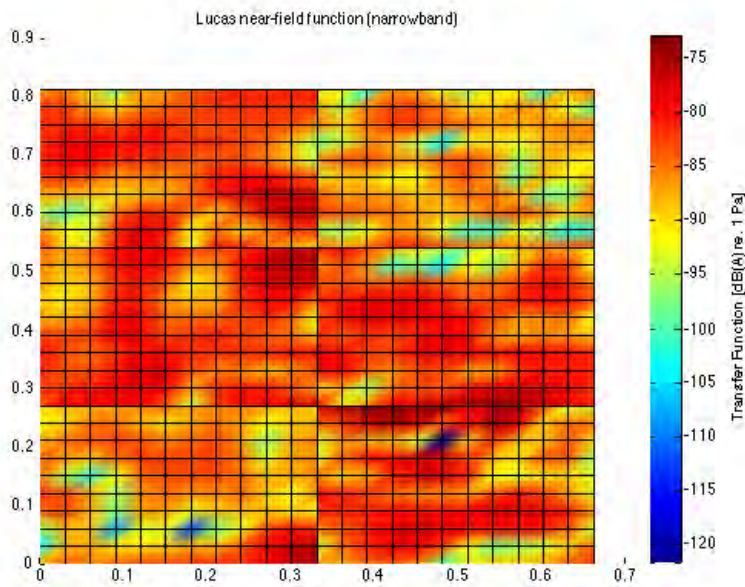


Figure 4.17.: The transfer function over the intake side at 1290 Hz.

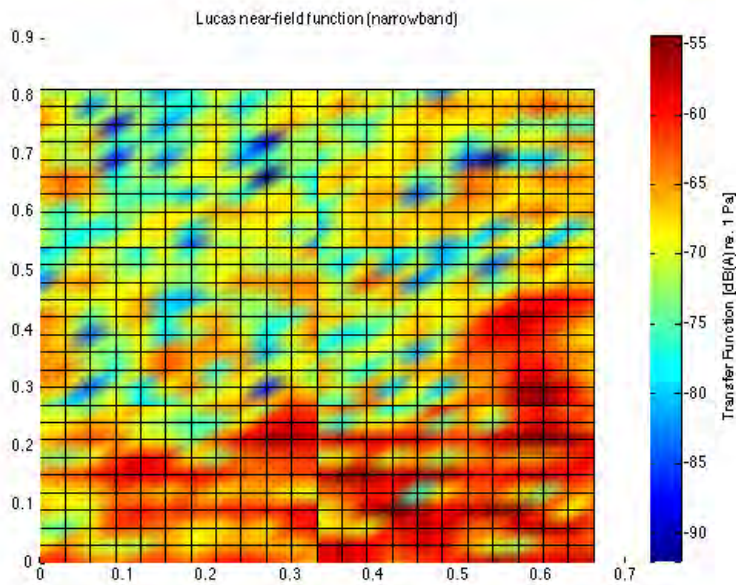


Figure 4.18.: The transfer function over the intake side at 2720 Hz.

## 5. Discussion

### 5.1. Lucas Near-Field function vs. Lucas function

By comparing the current method of today when measuring the structural attenuation of an engine, the Lucas function, with the proposed method for measuring the structural attenuation of an engine using an acoustic camera, the Lucas Near-Field function, it is possible to see in both cases "Open" assembly design and "Closed" assembly design, figure 4.1 and 4.2, that the two different functions have the same pattern. The only difference between the method used today and the proposed method is the level difference.

This level difference is a result from that the proposed method, Lucas Near-Field function, is placed in the near-field which as mentioned in the theory section 2.4.1 contains both plane waves and evanescent waves. These evanescent waves exhibits an exponential decay with the distance from the boundary were they were formed. This explains the level difference between Lucas Near-Field function and the current method the Lucas function which is measured one metre away. However, the exponential decay is steeper at higher frequencies ( $> 1500$  Hz) and this means that the effect should be smaller at these frequencies, which in this case can not be seen. The distance law does also have an significant impact on the result of the microphone placed one metre away. If this is the case then that is the explanation to the level difference, but the level difference between them are not as big as one should expect from the distance law (it should in that case be in the range of 30 dB). Now the difference is only 10 dB and this have something to do with that when doing calculations with the distance law one expect that the source is a monopole, but in this case the engine is not a monopole and this explains somewhat the level difference. Another significant impact to the level difference is that closer to the source there is one dimensional plane waves and farther away from the source these waves becomes spherical which has an decay of -6 dB per distance doubling.

The reason why the engine attenuates noise more effectively at lower frequencies which creates a curve which propagates upwards in frequency is due to that the engine is stiff at the area of the combustion chamber which makes the radiation efficiency very low at the lower frequencies ( $< 1500$  Hz) which leads to that the block structure

reduces the combustion noise effectively in this frequency range. When the radiation efficiency increases together with the frequencies the structural attenuation decreases. The sudden rise after 630 Hz could be due to structural modes of the block e.g. bending and torsion modes.

## 5.2. Lucas Near-Field function

When comparing the figures from the software Array Acoustic in section 4.2, which displays the estimated sound pressure level on the intake side, with the transfer function figures in section 4.3 it shows a striking similarity between them. In those areas in the figures from Array Acoustic that has the highest sound pressure level, the same areas in the transfer function figures shows up as having the worst transfer function value. From this the conclusion is that the matlab-code developed to calculate and display the transfer functions are correct. Together they complement each other in a positive way.

In section 4.3 two different assembly designs are presented, this is to give a demonstration that this technique works. By first studying figures 4.11 - 4.14, under the "Open" assembly design" - section it is clear that there is always two areas that are almost always present for each frequency under investigation i.e. the cylinder head and the oil pan. This is because that in those areas the biggest openings are present i.e. the intake openings, oil cooler openings, oil suction pipe openings, oil pipe openings and oil temperature sensor. In the case of the cylinder head it is especially cylinder 1 and 3 (counting from the right side of the intake side) that radiates the most, this is because they are closest to the cylinder where the loudspeaker element is placed i.e. cylinder 2.

This leads to that it is at these openings that the transfer function value has its highest value which means that the structural attenuation in these areas are worst due to a direct path into the engine and the loudspeaker placement.

Then by studying figures 4.15 - 4.18, under the "Closed" assembly design" - section it is clear that the areas that exhibit the lowest value of the transfer function when having the "Open" assembly design are gone, e.g. the cylinder head openings. Instead, it is clear that when studying the structural attenuation for frequencies 500, 1029 and 2720 Hz that the oil pan now is the area that exhibits the worst structural attenuation i.e. highest value of the transfer function. For the frequency 1290 Hz it is harder to specify a certain area as the main concern, but it still shows that the Lucas Near-Field function works because the area of main concern from the "Open" assembly design are gone. A fun thing to add is that the pattern that occurs for the frequency 1290 Hz,

resembles a vibrational pattern because when measuring pressure this close (and also even closer) to the structure the vibrational pattern of the side is measured.

As mentioned above, the oil pan is the area that exhibits the highest value of transfer function when the engine has "Closed" assembly design. This would maybe not occur in normal cases when there is oil inside the oil pan which would have acted as an absorptive liquid and then maybe another area would have been the area of concern.

The overall value of the structural attenuation has decreased significantly when having the "Closed" assembly design compared to when having the "Open" assembly design.

## **6. Conclusion**

### **6.1. Lucas Near-Field function vs. Lucas function**

The conclusion from the comparison between the current method, Lucas function, and the new proposed method, Lucas Near-Field method, is that they resemble each other in shape but has a level difference due to reason mentioned above. From this it is possible to say that the proposed method is validated against the current method and that the new proposed method works.

### **6.2. Lucas Near-Field function**

As an conclusion, it is possible to say that the new proposed method for measuring the structural attenuation works. This is validate by comparing the "Open" assembly design against the "Closed" assembly design, because it shows that the areas of main concern when the engine has the "Open" assembly design e.g. the cylinder head are gone when having the "Closed" assembly design. Instead, new areas has risen as concerns but these areas does not have the same value of the transfer function as they did with the "Open" assembly design. Together with the figures from the software Array Acoustic it is possible to specify exactly what on the engine structure that exhibits the worst structural attenuation, so the Lucas Near-Field function is a good compliment to the software Array Acoustic and the current method Lucas function.

## 7. Future work

As mentioned in the Discussion and Conclusion chapter 5, the proposed method for measuring the structural attenuation works for the two different assembly designs, but the method could be refined further. This is what this chapter will be about.

First thing to look further into is what will happen with the SNR when adding more parts to the engine. This is an area to study further because there was some minor problems at certain frequencies for the SNR when working with the "Closed" assembly design. To solve this and still have the same input power to the loudspeaker throughout every measurement one should either look into other loudspeakers which could generate a higher value of sound pressure level i.e. manage a higher input power. Or, by adding a bandpass filter in the frequency range of interest.

The second thing to look further into is to validate this method against an engine with normal conditions e.g. having all the pistons attached to it and having oil inside the oil pan. This is to see in the case with the oil how much it absorbs the sound and also how much impact the rest of the engine parts has to the structural attenuation of the engine. A problem here is that one can not run the engine with e.g. the banger rig because the SONAH method can not handle transient sounds.

The third area to look into is that one could make an FEM model of the engine and see if the weak areas that shows up at the measurements also shows up in the FEM model. This is also a way to validate this method.

The fourth area to look into is to develop this method so it can work with swept sine instead of white noise. The advantage of swept sine is that there is more energy in individual frequencies than in the case of white noise.

The fifth is to develop this method so it can work with sound power, for this the sound power level inside the cylinder chamber has to be known and this is a current problem because it is a complex room that the loudspeaker is placed in. This is what the next section 7.1 will be about.

## 7.1. Sound power level and the Lucas near-field function

As mentioned above it would be of interest to develop this method so it also can work with sound power. The interesting fact is that the SONAH method already has the possibility to work with sound intensity as mentioned in the theory section 2.4.1 and also demonstrated with figure 7.1 - 7.2, and these sound intensity measurements can be calculated into sound power by the software Array Acoustic. This is (as also is the case for the sound pressure) only the estimated sound intensity on the surface, but still the possibility for further development of this proposed method are already there if one can come up with an idea for how one can measure the sound power inside the cylinder chamber. One way to do this is to place an accelerometer on the loudspeaker membrane and measure the displacement. If the sound power could be determined inside the chamber then a complete transfer function between different systems of the engine could be visualized e.g. from cylinder chamber to the end of the exhaust and then be able to measure the radiated sound pressure/power from the exhaust.

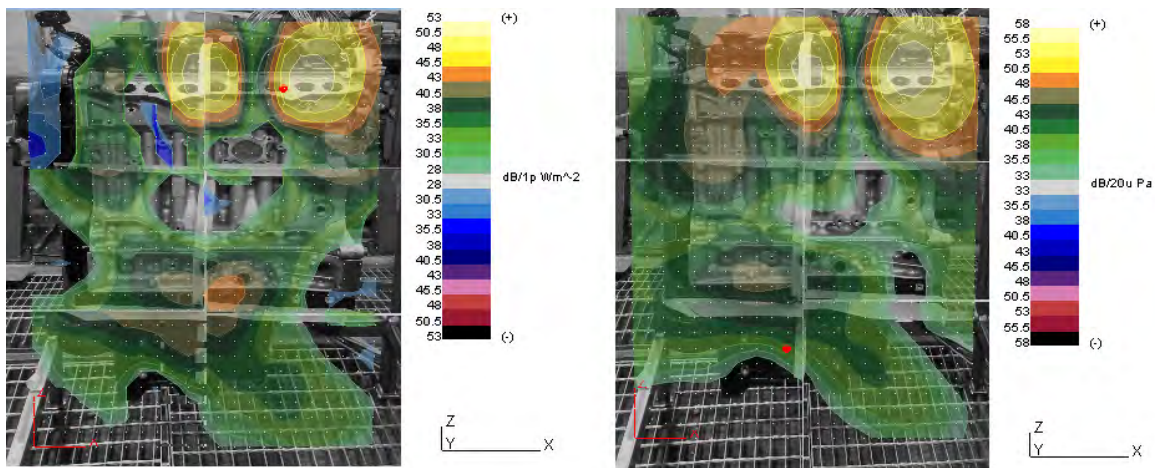


Figure 7.1.: The sound intensity (left) vs. the sound pressure (right) with "Open" assembly design at 1029 Hz.

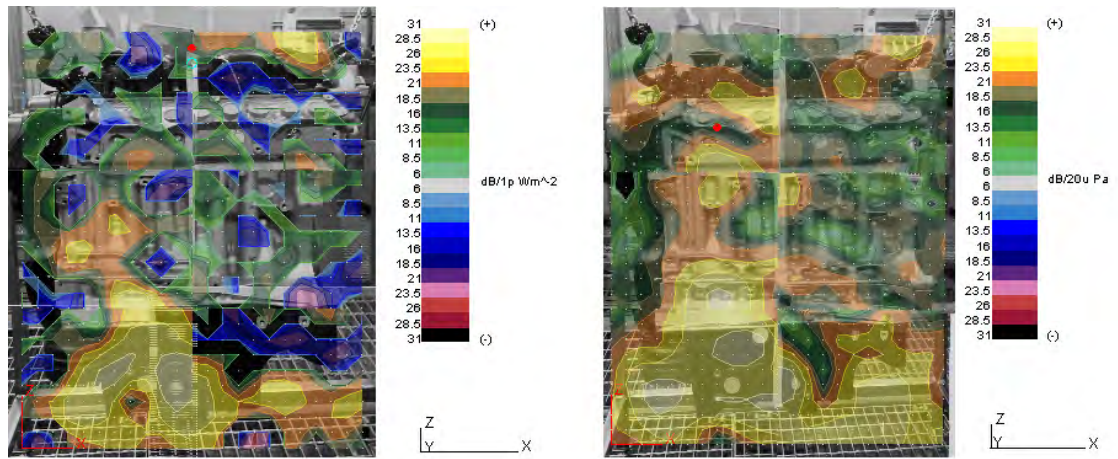


Figure 7.2.: The sound intensity (left) vs. the sound pressure (right) with "Closed" assembly design at 1029 Hz.

## References

- [1] Mollenhaur, K., Tschke, H., et.al.: *Handbook of Diesel Engines*, Springer-Verlag, Berlin Heidelberg, 2010, ISBN 9783540890836
- [2] <http://global.britannica.com/EBchecked/topic/162716/diesel-engine/45706/Two-stroke-and-four-stroke-engines> \#\$ref914736, May 2013
- [3] Boden, H., Glav, R., Wallin, H. P., Åbom, M.: *Ljud och Vibrationer*, Marcus Wallenberg Laboratoriet för Ljud- och Vibrationsforskning. Inst. för Farkostteknik, KTH, 2001. ISBN 91-7170-434-5
- [4] Parker, M.: *Digital Signal Processing 101: Everything you need to know to get started*, Newnes, USA, 2010, ISBN 9781856179218
- [5] Rossing, D. T., et.al.: *Springer Handbook of Acoustics*, Springer, New York, 2007, ISBN 978-0-387-30446-5
- [6] Brüel & Kjær: *Non-stationary STSF*, Lecture Notes, Brüel & Kjær Sound and Vibration Measurement A/S, 2000
- [7] Brüel & Kjær: *Pulse: Labshop version 17.1.0*, Introduction Notes, Brüel & Kjær Sound and Vibration Measurement A/S, 1996
- [8] Crocker, J. M., et.al.: *Handbook of noise and vibration control*, John Wiley & Sons Inc, New Jersey, 2007, ISBN 9780471395997
- [9] Brüel & Kjær: <http://www.e-pages.dk/brue1/4/>, The international Sound and Vibration Magazine from Brüel & Kjær, No. 2, 2007
- [10] Jacobsen, F. and Jaud, V.: *Statistically optimized near field acoustic holography using an array of pressure-velocity probes*, The Journal of Acoustical Society of America, 2007, ISSN 0001-4966
- [11] Hald, J.: *Basic theory and properties of statistically optimized near-field acoustical holography*, The Journal of Acoustical Society of America, 2009, ISSN 0001-4966

- [12] Johnson, A. R. and Wichern, D. W.: *Applied multivariate statistical analysis, Fifth edition*, Prentice Hall, New Jersey, 2002, ISBN 0-13-092553-5
- [13] Fernholz, M. C.: *Multivariate Statistical Methods for the Analysis of NVH Data*, SAE Technical Paper 2005-01-2518, 2005, doi:10.4271/2005-01-2518.
- [14] Reinhart, E. T.: *An Evaluation of the Lucas Combustion Noise Meter on Cummins B Series Engines*, SAE Technical Paper 870952, 1987, doi:10.4271/870952.
- [15] Dixon, J.: *Banger Rig Evaluation of a Volvo 5 Cylinder HSDI Engine*, Institute of Sound and Vibration Research Automotive Design Advisory Unit, 2005, Consultancy Report No. 1348/05.
- [16] Nakashima, K., Yajima, Y. and Yamamoto, M.: *Measurement of Structural Attenuation of a Diesel Engine*, SAE Technical Paper 912710, 1991, doi:10.4271/912710.
- [17] RICARDO: *Appendix 8: Details of CMB3 Method for Combustion/Mechanical Noise Breakdown Calculation*, RD. 08/234501.1.
- [18] [http://www.engineersedge.com/engine\\_formula\\_automotive.htm](http://www.engineersedge.com/engine_formula_automotive.htm), Equation: Piston travel vs. Crank Rotation, visited: February 2013
- [19] [https://www.intertechnik.de/Shop/Lautsprecher/Gradient-Select/\\_70027\\_H121-TPC80NV-4\\_1768,de,36,52243?no=intro&app=Shop/Lautsprecher/Gradient-Select/&dummy=&navid=1768&lang=de&basis=36&detail=52243&extra1=&extra2=](https://www.intertechnik.de/Shop/Lautsprecher/Gradient-Select/_70027_H121-TPC80NV-4_1768,de,36,52243?no=intro&app=Shop/Lautsprecher/Gradient-Select/&dummy=&navid=1768&lang=de&basis=36&detail=52243&extra1=&extra2=), Intertechnik, visited: February 2013
- [20] [http://www.visaton.de/en/chassis\\_zubehoer/breitband/frs8\\_4.html](http://www.visaton.de/en/chassis_zubehoer/breitband/frs8_4.html), Intertechnik, visited: May 2013



# A. Loudspeaker elements

## A.1. Gradient: TPC80NV/4



### TPC80NV/4

TPC 80 NV Der Nachfolger des legendären Breitbandlautsprechers TPC 80  
8 cm Miniatur-Tiefonlautsprecher mit Kunststoffkorb. Dämpfend beschichtete Papiermembran. 19 mm hochbelastbare Schwingspule. Wenn auch klein, aber sehr hochwertiger Lautsprecher für den Einsatz in 2-Wege Kombinationen.

Empfohlener Übertragungsbereich bis 5000 Hz. Gehäuse Reflex: 1,5 - 2,0 Liter.  
Gehäuse geschlossen: 1,0 - 1,5 Liter.  
Passendes Schutzgitter erhältlich.

### Merkmale

Typ	Breitband
Korbmaß (Zoll)	3
Imp. (Zn/ohm)	4
Freq.(Hz)	80 - 8000
Music (W)	60
Nominal (W)	80
SPL (1W/1M)	83,00
VC (d)	19
VC (h)	5,3
Re (Ohm)	3,3
fs	93
Mms(g)	2,5
Sd (cm <sup>2</sup> )	35
VAS	1,9
QMS	2,63
QES	,38
QTS	,33
Membranmaterial	Papier
Sicke Material	Polypropylen
Korb Material	Kunststoff
Magnetmaterial	Ferrite
Außendurchmesser (mm)	80,00
Einbaulochmaß (mm)	72
Einbautiefe (mm)	45
Hersteller / Marke	Gradient

Figure A.1.: Product sheet over the loudspeaker element TPC80NV/4 [19].

### A.1.1. Measurement on TPC80NV/4

The measurements conducted on this loudspeaker element followed the methods and setup mentioned in the Audio Technology and Acoustics lab: Anechoic Chamber edition 2012.

#### Instrumentation:

- Sound Card: E-MU 0404 USB, serial no.: Re 34
- Amplifier NAD stereo integrated amp. 310, serial no.: M783102951
- Brüel & Kjær type 4190  $\frac{1}{2}$ " microphone, serial no.: Mi34
- G.R.A.S power module type 12AA, serial no.: PR18
- Brüel & Kjær microphone calibrator type 4231, serial no.: CA1
- Baffle (according to standard)
- Voltmeter
- Software: Room-Capture
- Software: Matlab R2012b

#### Room-Capture setup:

Stimulus and analyser settings			
Stimulus	Properties	No. average	Start Hz
LSS: Log Sine Sweep (chirp)	3.2s per octave	5	30

**Result:**

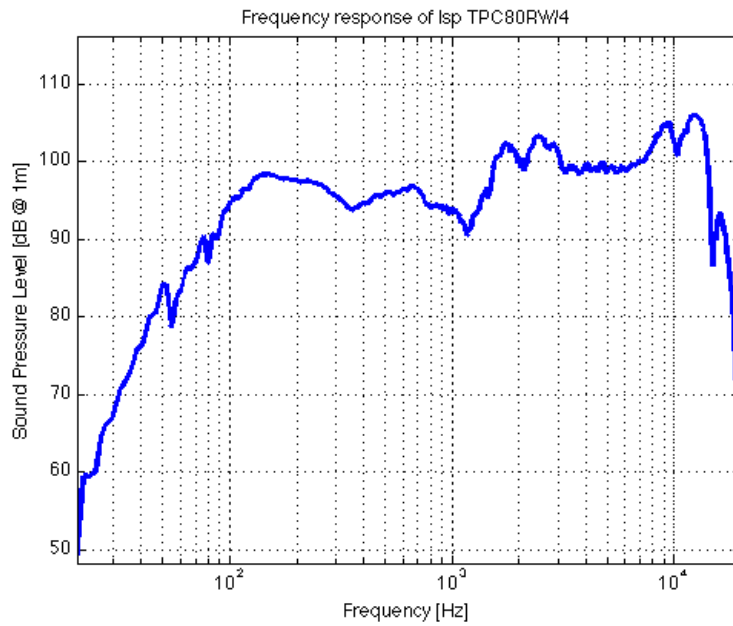


Figure A.2.: The frequency response of the loudspeaker element TPC80NV/4.

**A.2. Visaton: FRS 8-4ohm**

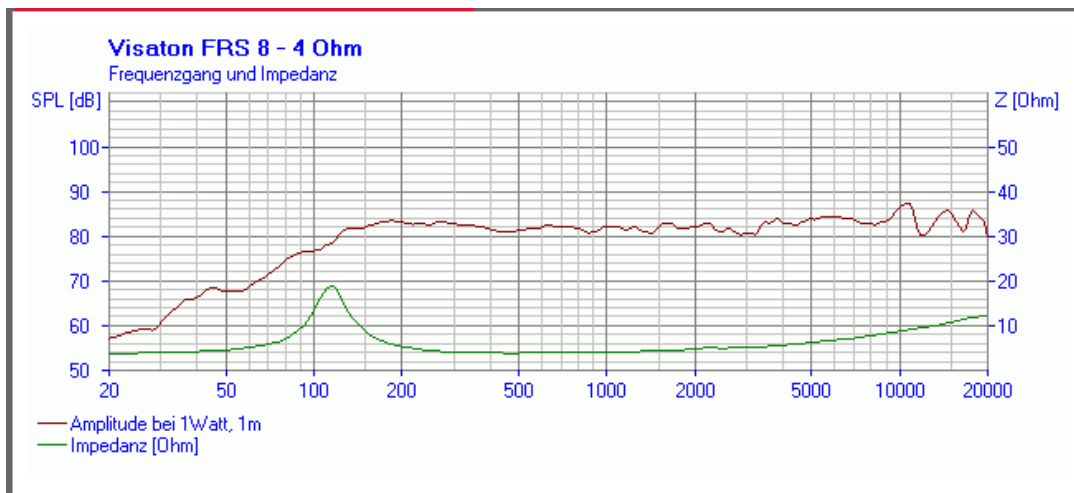


Figure A.3.: The frequency response of the loudspeaker element FRS 8-4ohm [20].

## FRS 8 - 4 Ohm



Technical Data	
Rated power	30 W
Maximum power	50 W
Nominal impedance Z	4 Ohm
Frequency response	100–20000 Hz
Mean sound pressure level	82 dB (1 W/1 m)
Opening angle (-6 dB)	180°/4000 Hz
Excursion limit	+/-2,5 mm
Resonance frequency fs	120 Hz
Magnetic induction	0,8 T
Magnetic flux	200 μWb
Height of front pole-plate	4 mm
Voice coil diameter	20 mm
Height of winding	4,5 mm
Cutout diameter	73 mm
Net weight	0,28 kg
D.C. resistance Rdc	3,5 Ohm
Mechanical Q factor Qms	3,61
Electrical Q factor Qes	0,85
Total Q factor Qts	0,69
Equivalent volume Vas	1 l
Effective piston area Sd	31 cm²
Dynamically moved mass Mms	2,5 g
Force factor Bxl	2,2 T m
Inductance of the voice coil L	0,4 mH
Temperature range	-25 ... 70 °C

Figure A.4.: Product sheet over the loudspeaker element FRS 8-4ohm [20].

## B. Layout: Piston

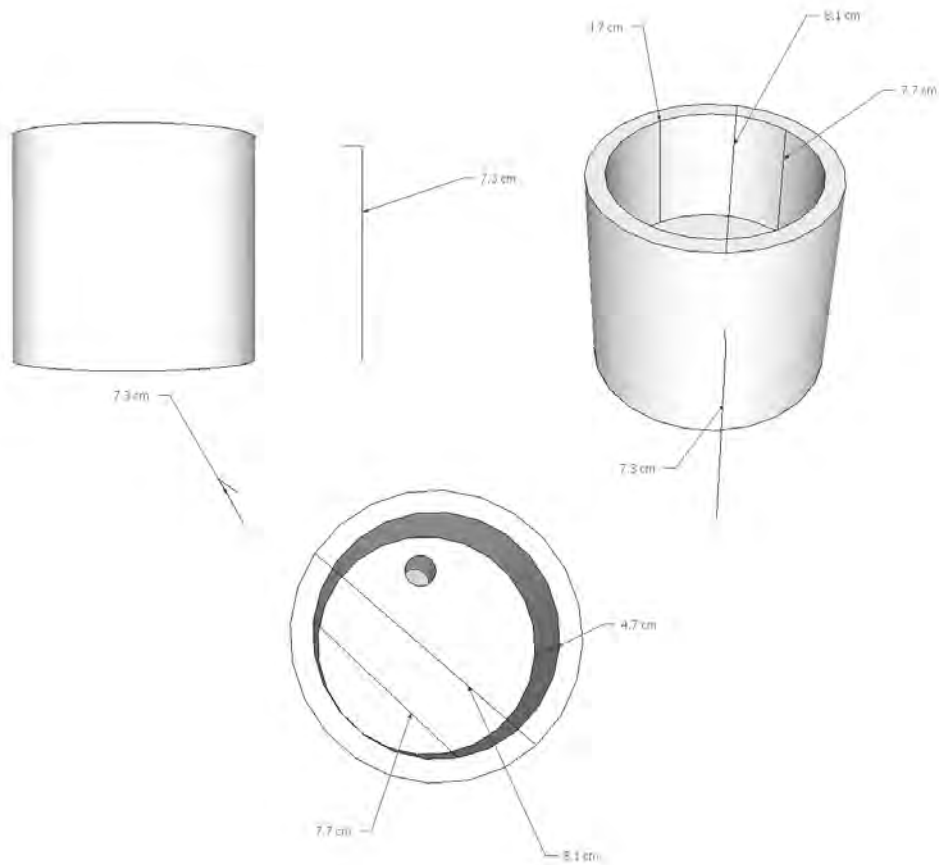


Figure B.1.: The layout over the piston made of delrin.

## C. Structural attenuation measurements

### C.1. Instrumentation

- Windows 7 64-bit computer, Intel core i7 @ 2.60 GHz, 8.00 GB RAM
- Brüel & Kjær 4944A microphone, Volvo identity: GLJ 978:1 91600-JS-SKÅP 2489421
- Brüel & Kjær 4935 array microphone(s), Volvo identity: GLJ 9336 97523-JS 97523
- Brüel & Kjær 4189A microphone, Volvo identity: GLJ 885:1 91600-NVH-SKÅP 02349588
- Brüel & Kjær Holography system, Volvo identity: GLJ 933:3 91600-NVH-HOLO
- Brüel & Kjær Front-End Controller module 7539, Volvo identity: TL1 Lilla
- Brüel & Kjær Front-End Controller module 7537A, Volvo identity: GLJ 933:1/2 91600-NVH-HOLO
- Brüel & Kjær Pistonphone 4228, Volvo identity: GLJ 933:5 91600-NVH-SKÅP
- Brüel & Kjær Sound level calibrator 4230, Volvo identity: KAL 613:1 91600-NVH-SKÅP 91600
- Amplifier: NAD 302, Volvo identity: TUE-1188:1 92470-AUDIO-VAG 92470
- Loudspeaker element: TPC80NV/4
- Loudspeaker element: FRS 8-4ohm
- Engine: 4-cylinder prototype diesel engine, serial no.: 1DDM1A76
- Software: Brüel & Kjær Pulse LabShop, version 17.1.0
- Software: Brüel & Kjær Array Acoustics Post-processing, version 17.1.0.22
- Software: Brüel & Kjær Pulse Reflex, version 17.1.0
- Software: MatLab R2012a/ R2012b

## C.2. Measurement areas

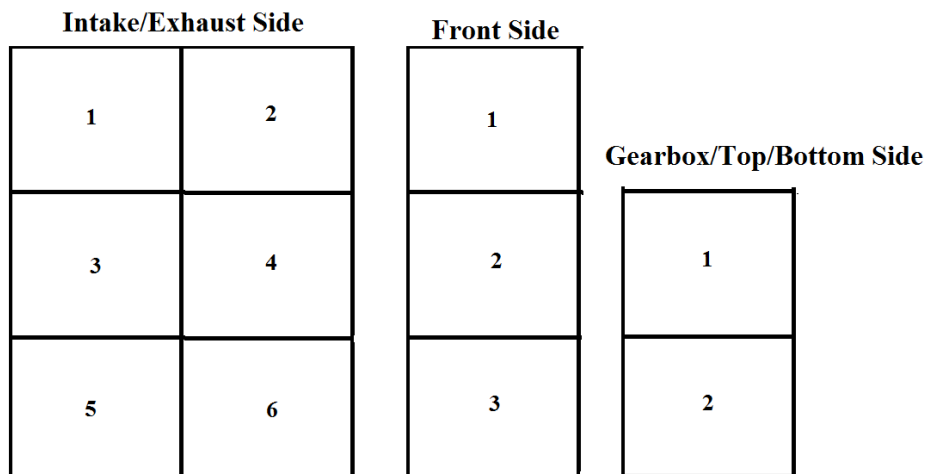


Figure C.1.: The measurement areas that each side of the engine were divided into.

## C.3. Post-Processing

### C.3.1. Setup in Array Acoustic

Acoustic Image Parameters	SONAH	Frequency Analysis	Calculation Plane [m]	Reference Selector	SQ Mapping Parameters
Processing type: <b>Stationary</b>	Spatial Smoothing: <b>Medium</b>	Time Window: <b>As Measured</b>	Distance to calc. Plane: <b>0.03</b>	Reference type: <b>Fixed</b>	Sharpness Calc. Method: <b>Zwicker</b>
Output: <b>Pressure/Intensity</b>	Regularization: <b>Manual</b>	Time start: <b>0s</b>	Minimum X: <b>0</b>	PCD Threshold: <b>30dB</b>	Low Level Compatibility Correction: <b>No</b>
	Regularization Range: <b>20dB</b>	Time Stop: <b>10s</b>	Maximum X: <b>0.33</b>	References: <b>Ref/Aux1(AtcRef#1)</b>	Apply SPL Dynamic Range: <b>No</b>
	Increased Lows freq. Smoothing: <b>On</b>	Synthesis type: <b>ConstantBW</b>	Minimum Y: <b>0</b>	Reference Normalization: <b>Overall</b>	SPL Dynamic Range: <b>7dB</b>
		Freq. range: <b>6.4kHz (Userdefined)</b>	Maximum Y: <b>0.27</b>	Virtual Reference: <b>Off</b>	
		Lower center freq.: <b>400Hz</b>	X direction spacing: <b>0.03</b>	Virt. Ref. X-pos: <b>0m</b>	
		Upper center freq.: <b>4kHz</b>	Y direction spacing: <b>0.03</b>	Virt. Ref. Y-pos: <b>0m</b>	
		Bandwidth: <b>1Hz</b>			
		Number of FFT Lines: <b>6400</b>			
		Line spacing: <b>1Hz</b>			
		Frequency span: <b>6400Hz</b>			

## D. Measurements conducted on the other sides

Only two frequencies for each side has been chosen here to demonstrate that the Lucas near-field function works on the other side as well.

### D.1. Gearbox side

#### D.1.1. Lucas Near-Field function vs. Lucas function

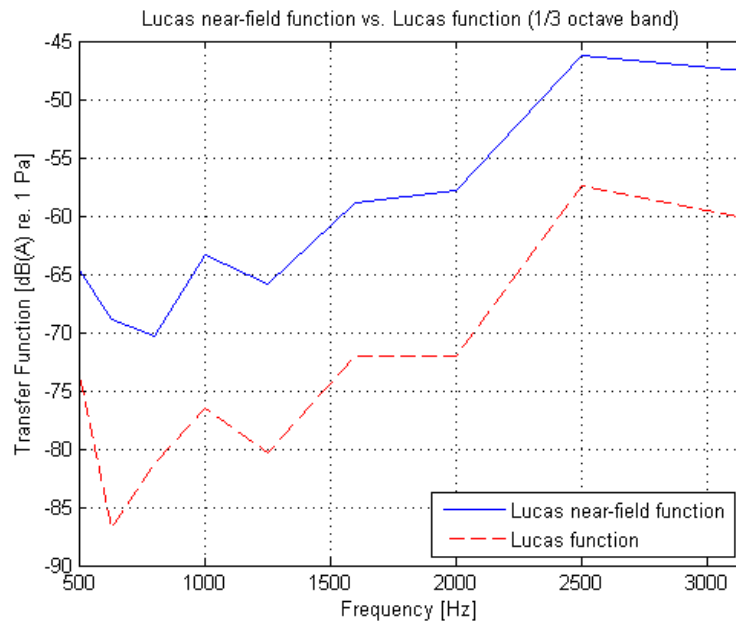


Figure D.1.: The Lucas Near-Field function vs. the Lucas function with "Open" assembly design.

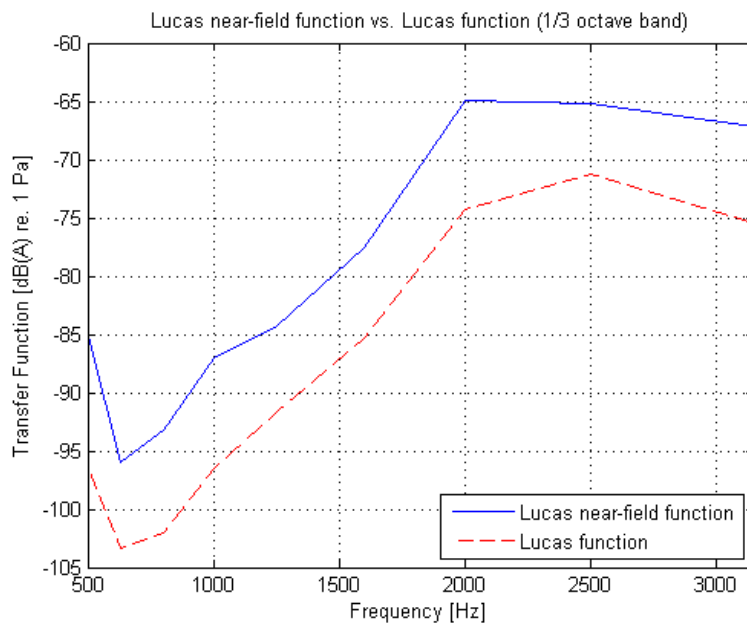


Figure D.2.: The Lucas Near-Field function vs. the Lucas function with "Closed" assembly design.

## D.1.2. Array Acoustic

### "Open" assembly design

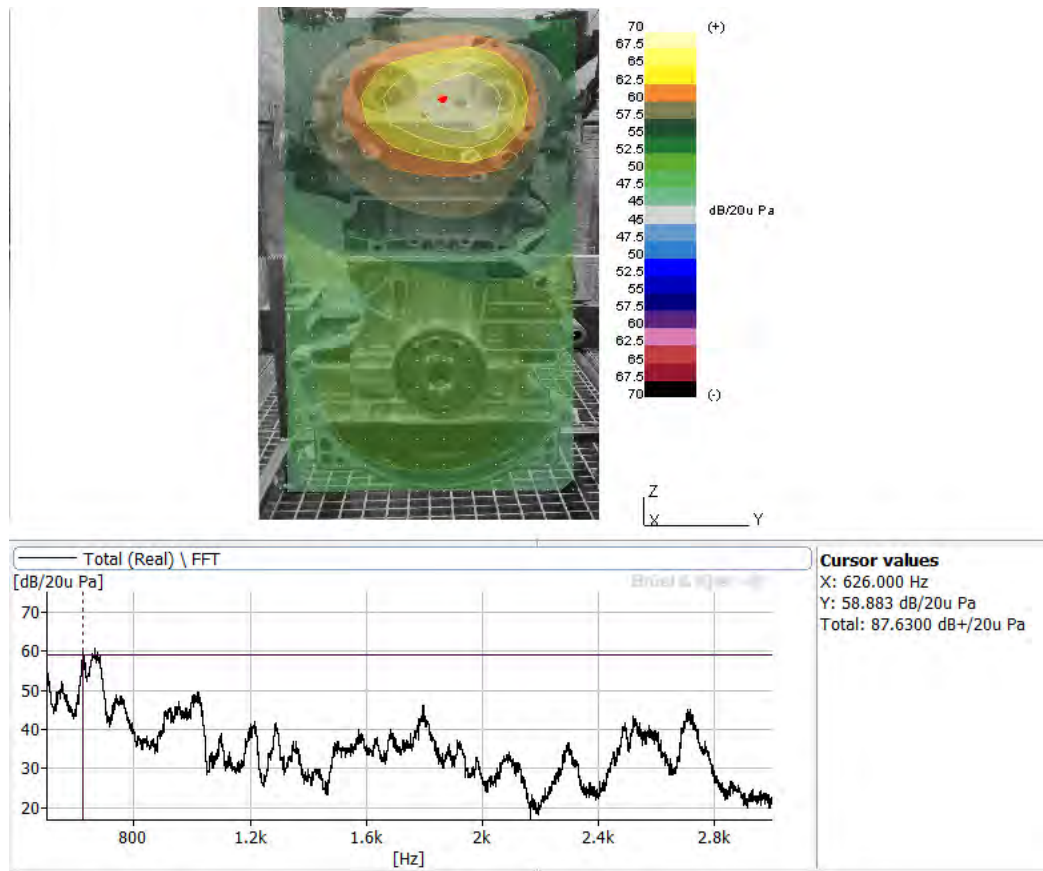


Figure D.3.: The estimated radiated sound pressure level at 626 Hz.

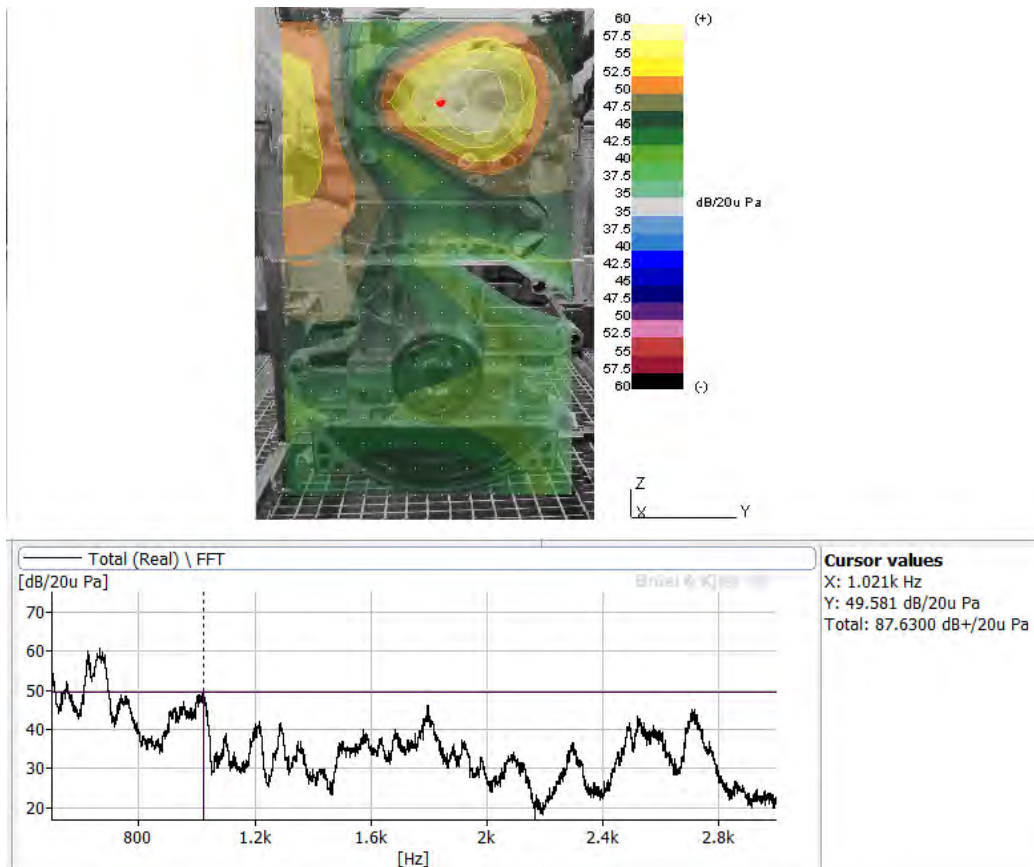


Figure D.4.: The estimated radiated sound pressure level at 1021 Hz.

”Closed” assembly design

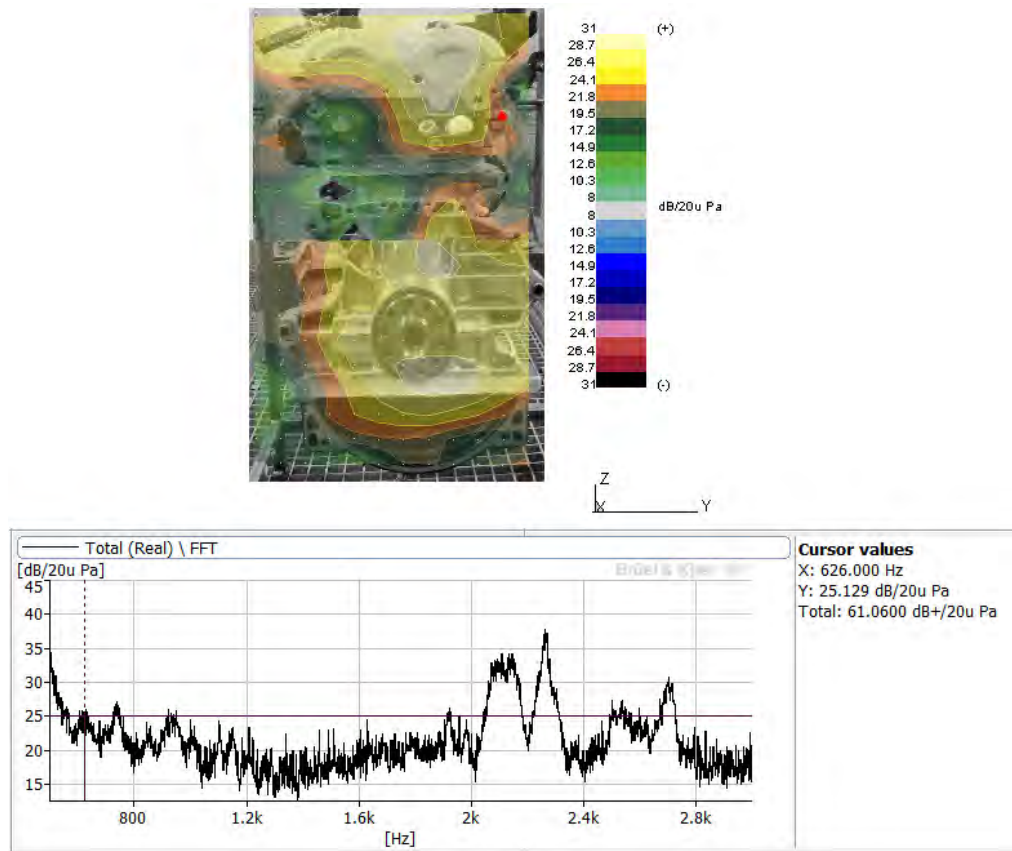


Figure D.5.: The estimated radiated sound pressure level at 626 Hz.

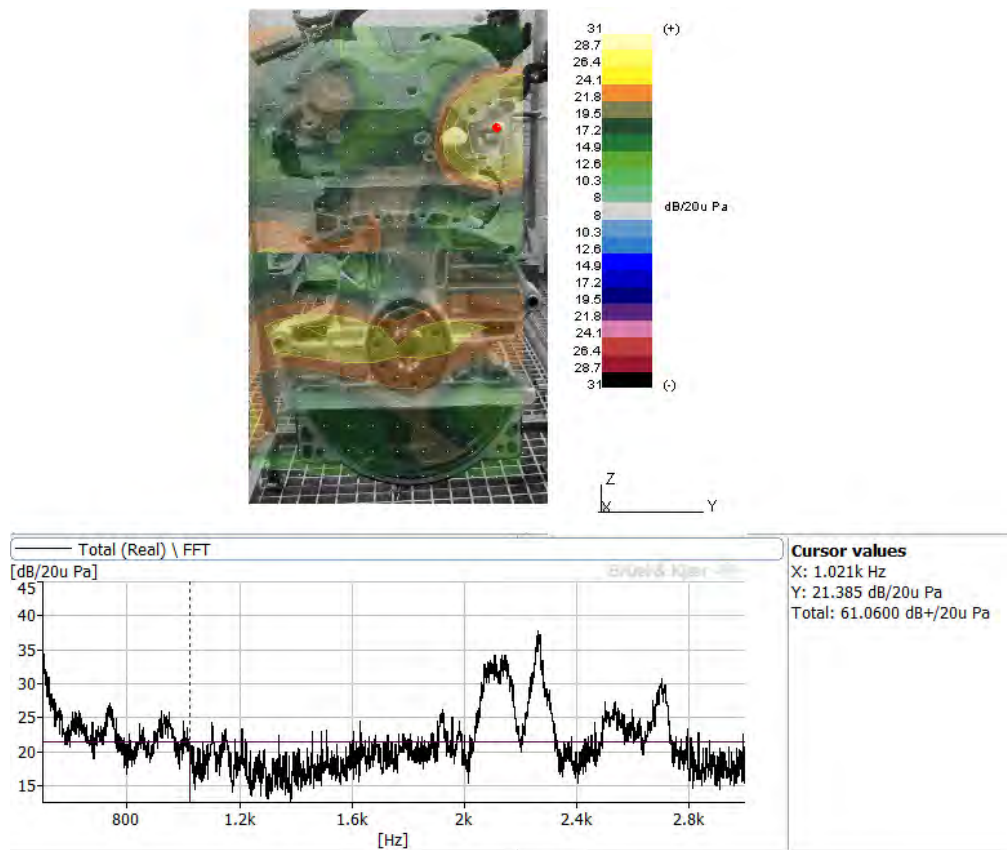


Figure D.6.: The estimated radiated sound pressure level at 1021 Hz.

### D.1.3. Lucas near-field function

”Open” assembly design

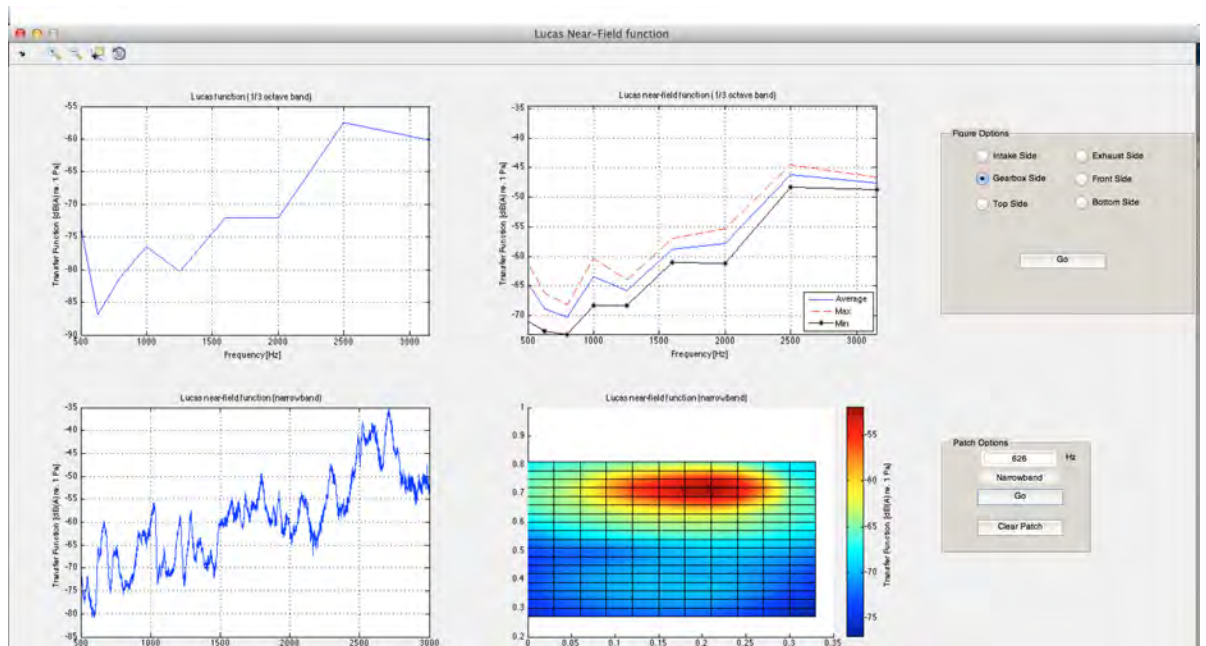


Figure D.7.: The Lucas Near-Field program; the frequency for the transfer function is 626 Hz.

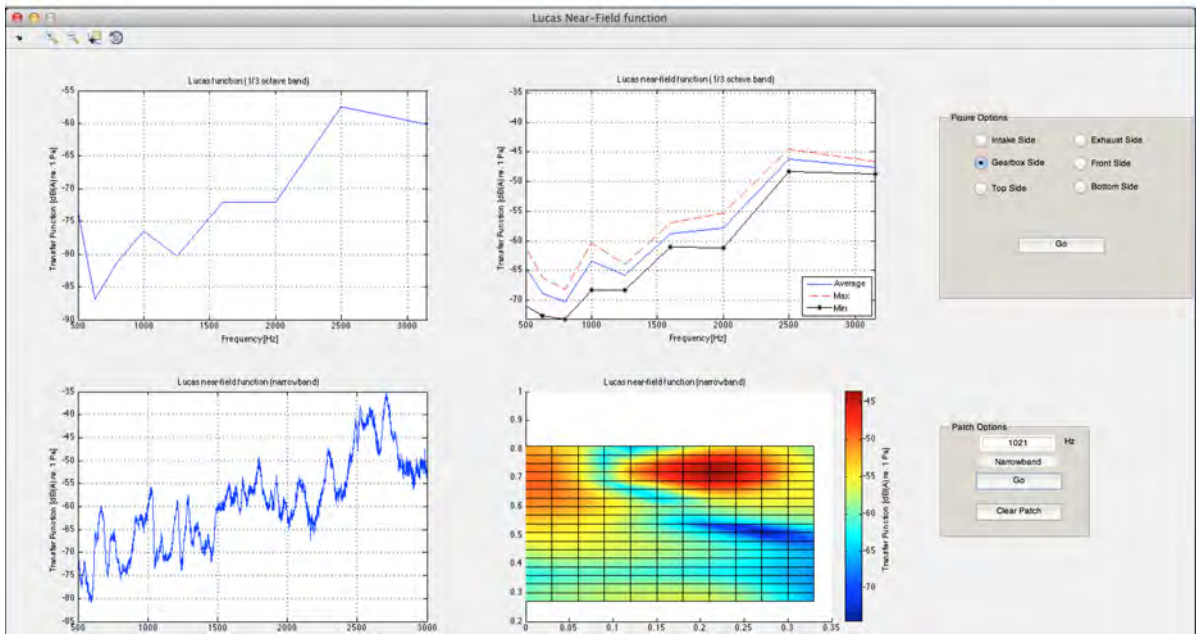


Figure D.8.: The Lucas Near-Field program; the frequency for the transfer function is 1021 Hz.

## ”Closed” assembly design

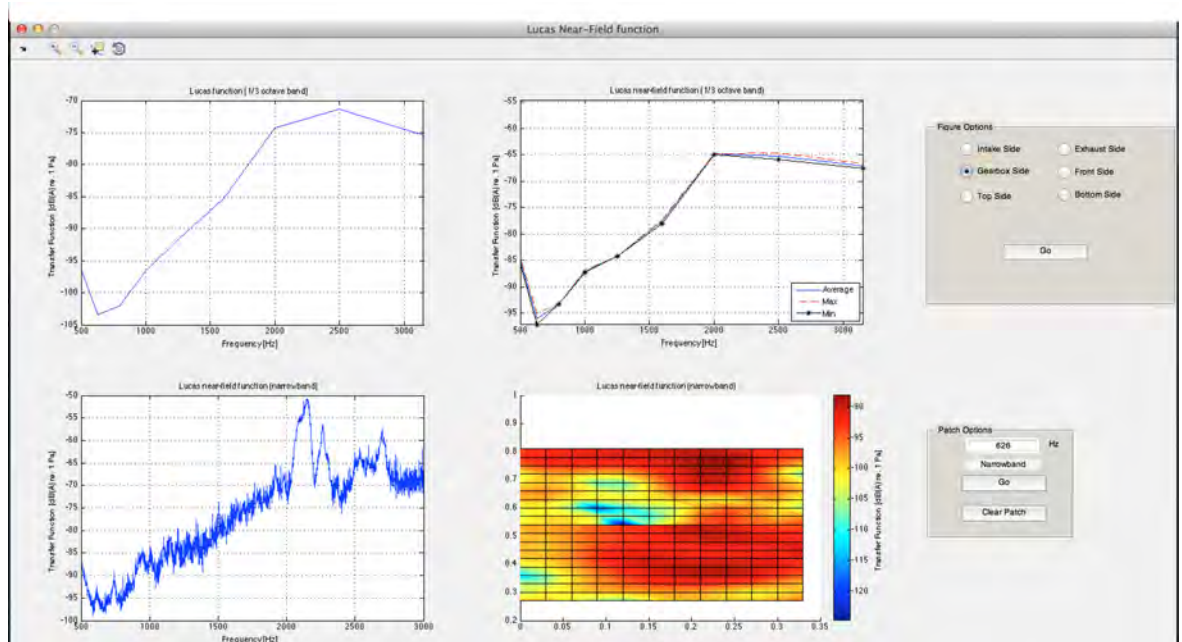


Figure D.9.: The Lucas Near-Field program; the frequency for the transfer function is 626 Hz.

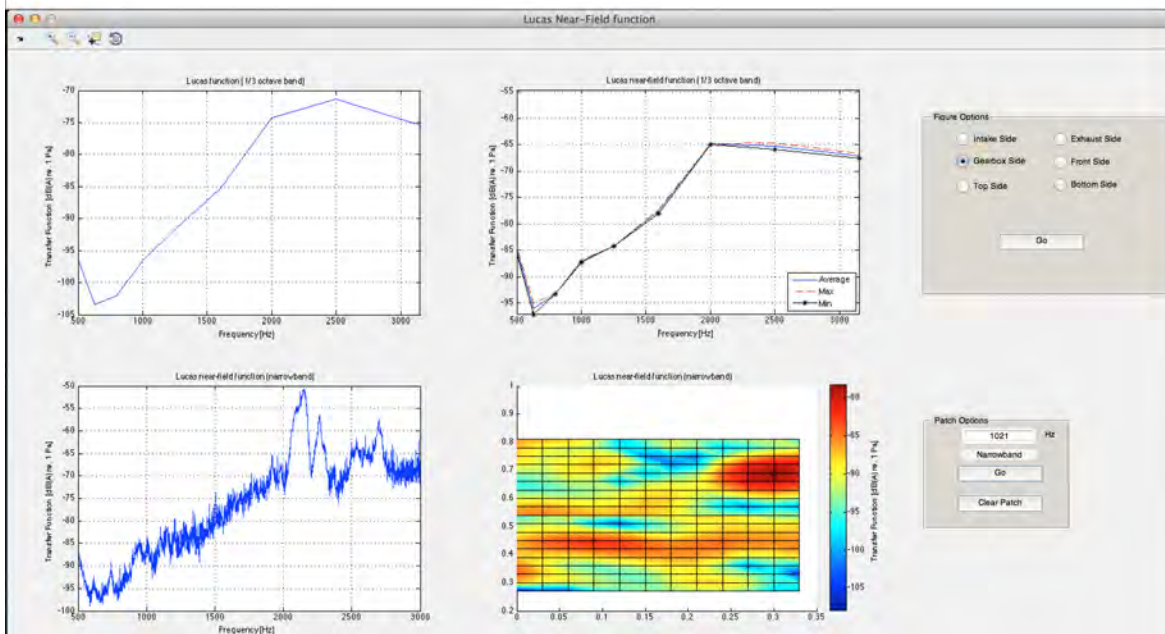


Figure D.10.: The Lucas Near-Field program; the frequency for the transfer function is 1021 Hz.

## D.2. Exhaust side

### D.2.1. Lucas Near-Field function vs. Lucas function

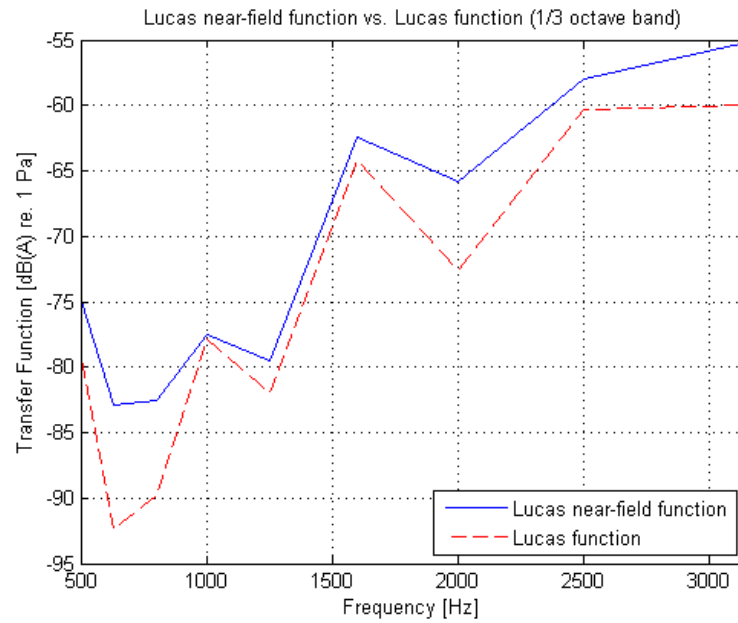


Figure D.11.: The Lucas Near-Field function vs. the Lucas function with "Open" assembly design.

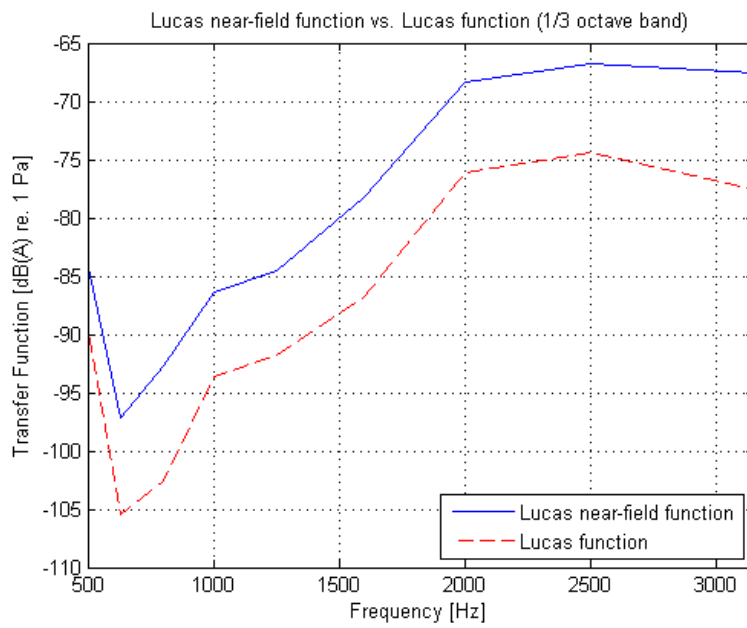


Figure D.12.: The Lucas Near-Field function vs. the Lucas function with "Closed" assembly design.

## D.2.2. Array Acoustic

### "Open" assembly design

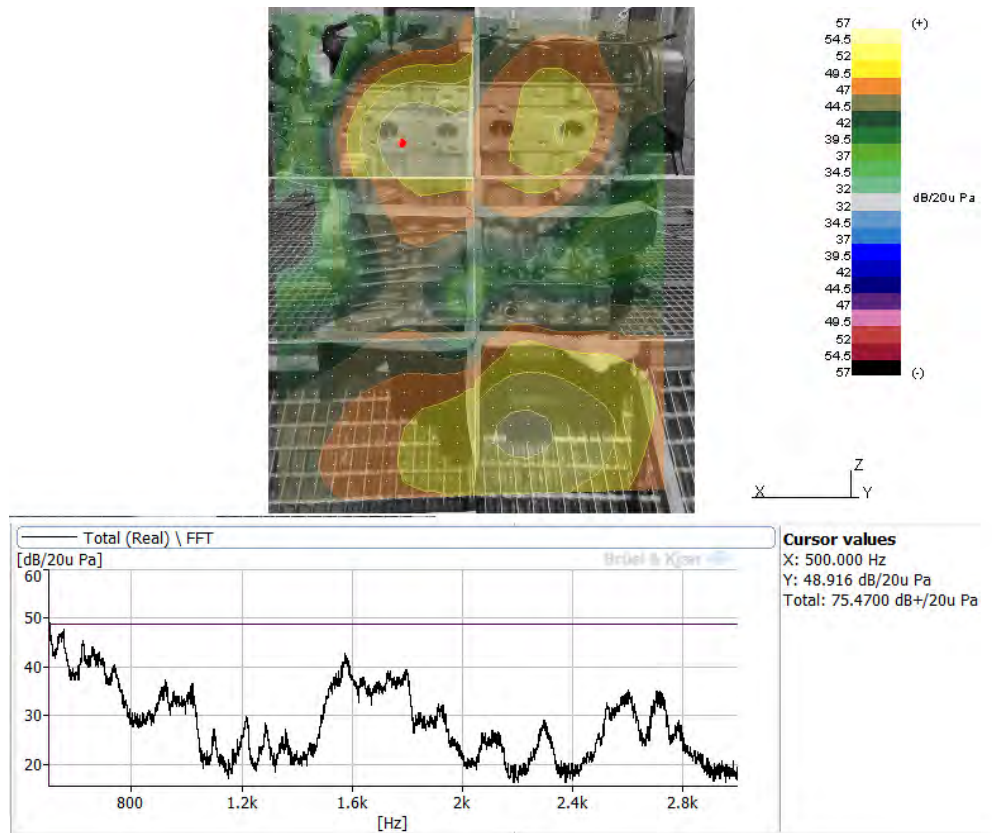


Figure D.13.: The estimated radiated sound pressure level at 500 Hz.

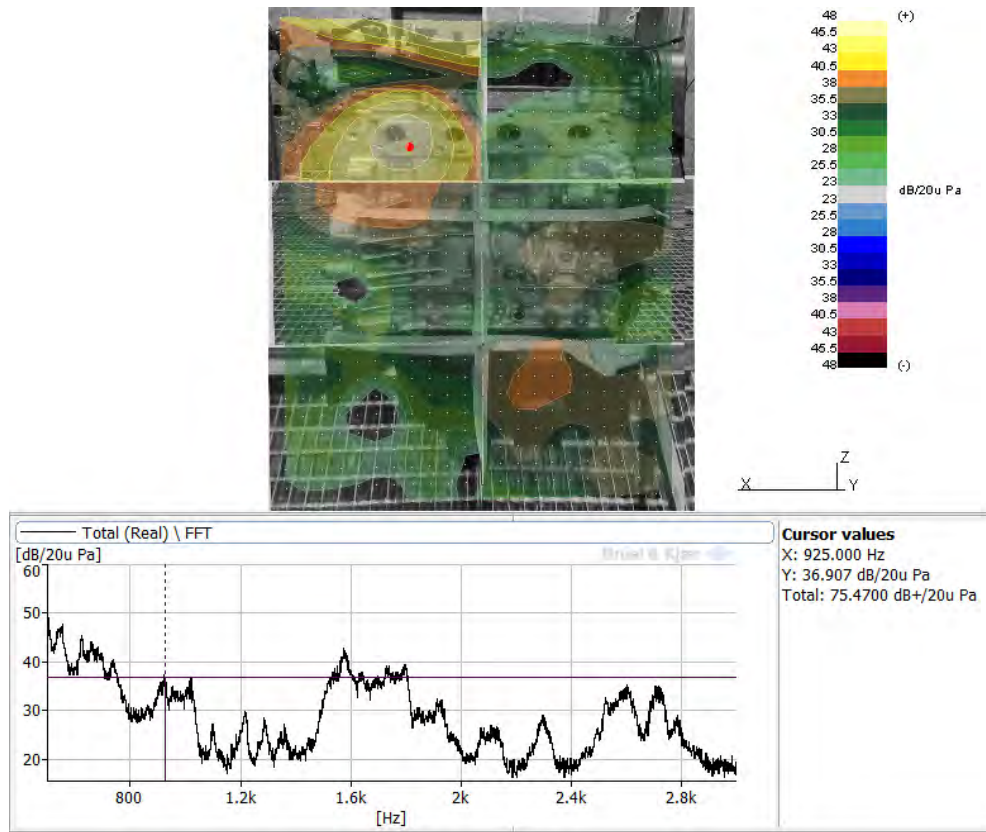


Figure D.14.: The estimated radiated sound pressure level at 925 Hz.

”Closed” assembly design

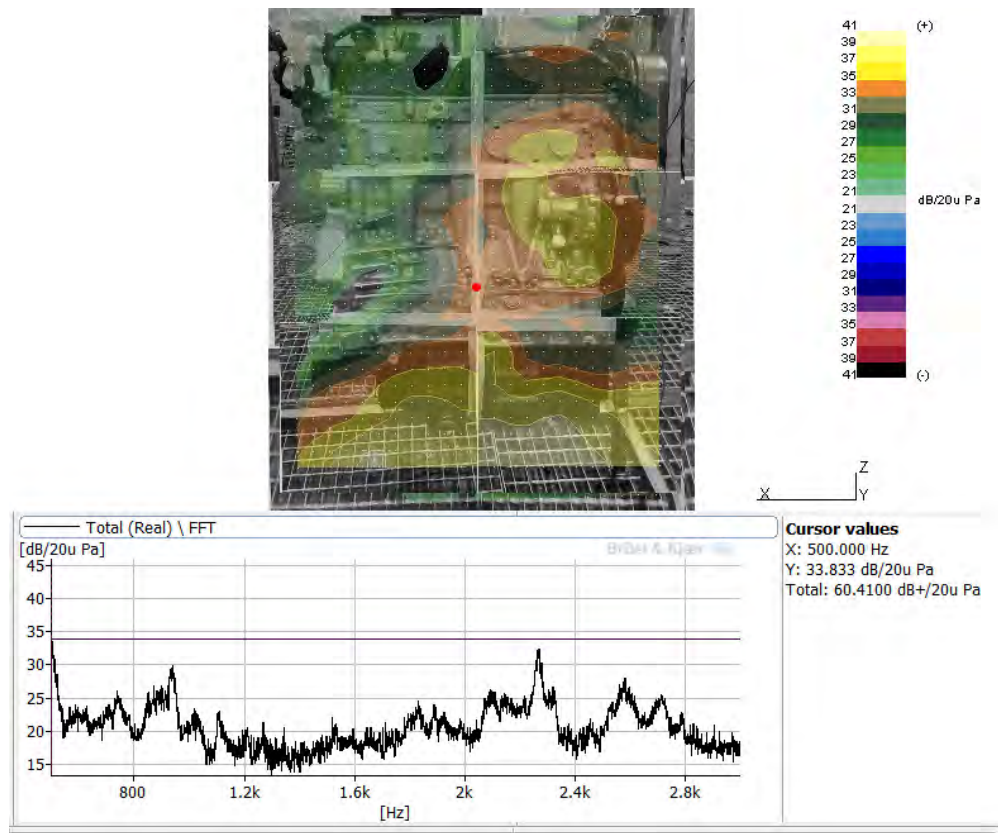


Figure D.15.: The estimated radiated sound pressure level at 500 Hz.

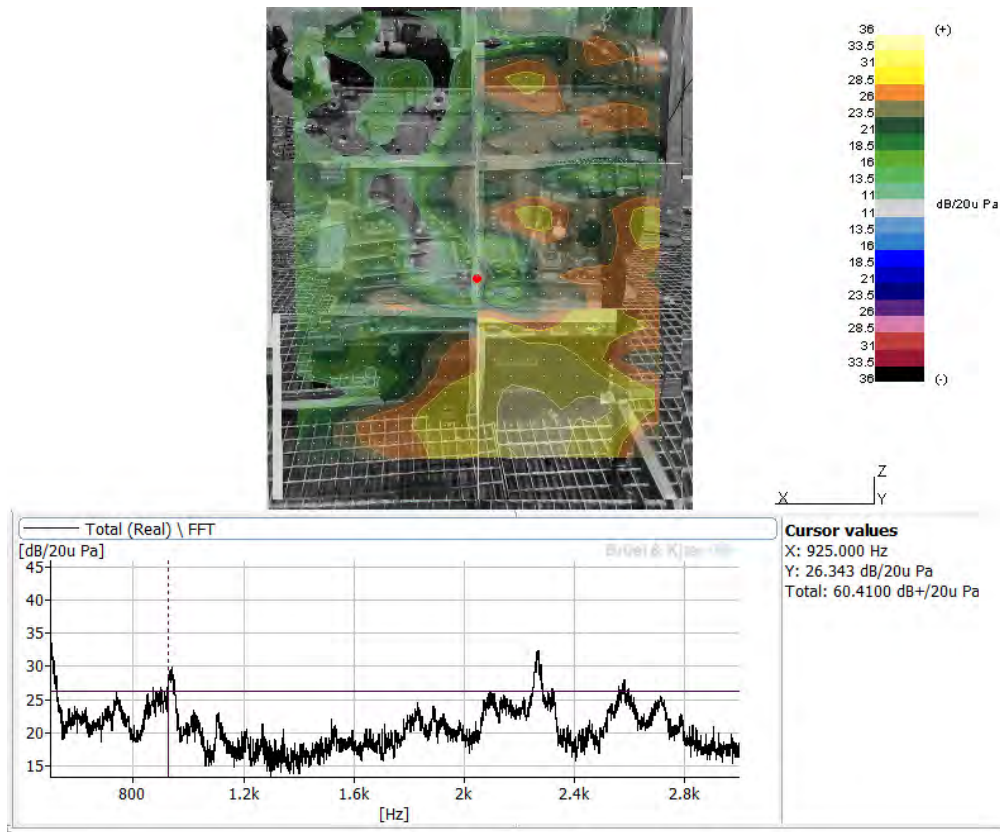


Figure D.16.: The estimated radiated sound pressure level at 925 Hz.

### D.2.3. Lucas Near-Field function

”Open” assembly design

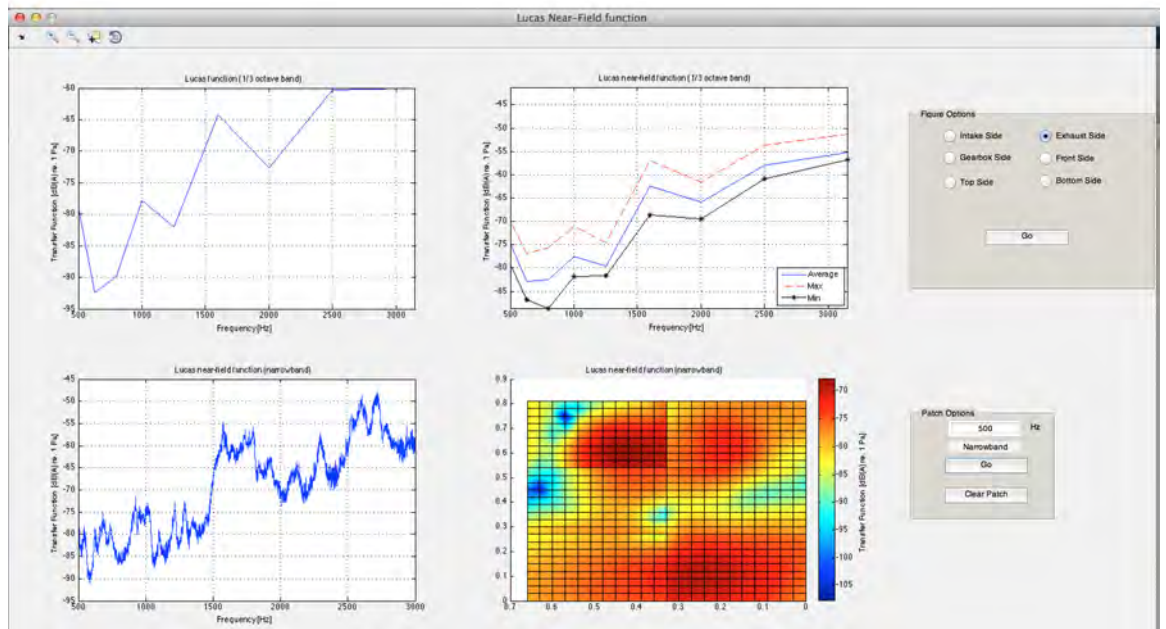


Figure D.17.: The Lucas Near-Field program; the frequency for the transfer function is 500 Hz.

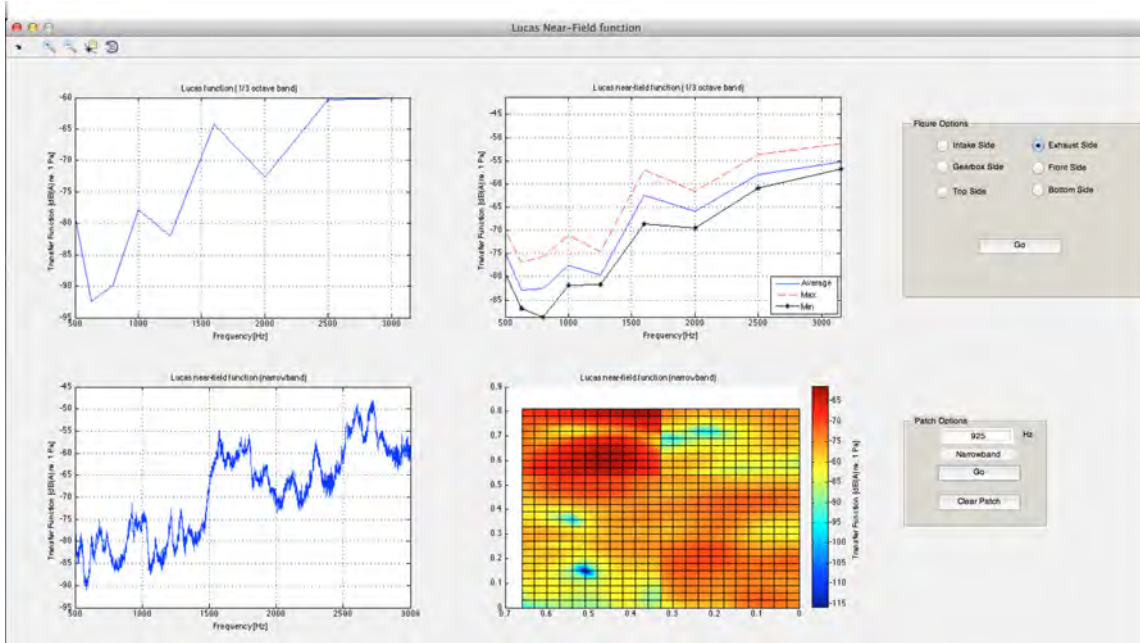


Figure D.18.: The Lucas Near-Field program; the frequency for the transfer function is 925 Hz.

## ”Closed” assembly design

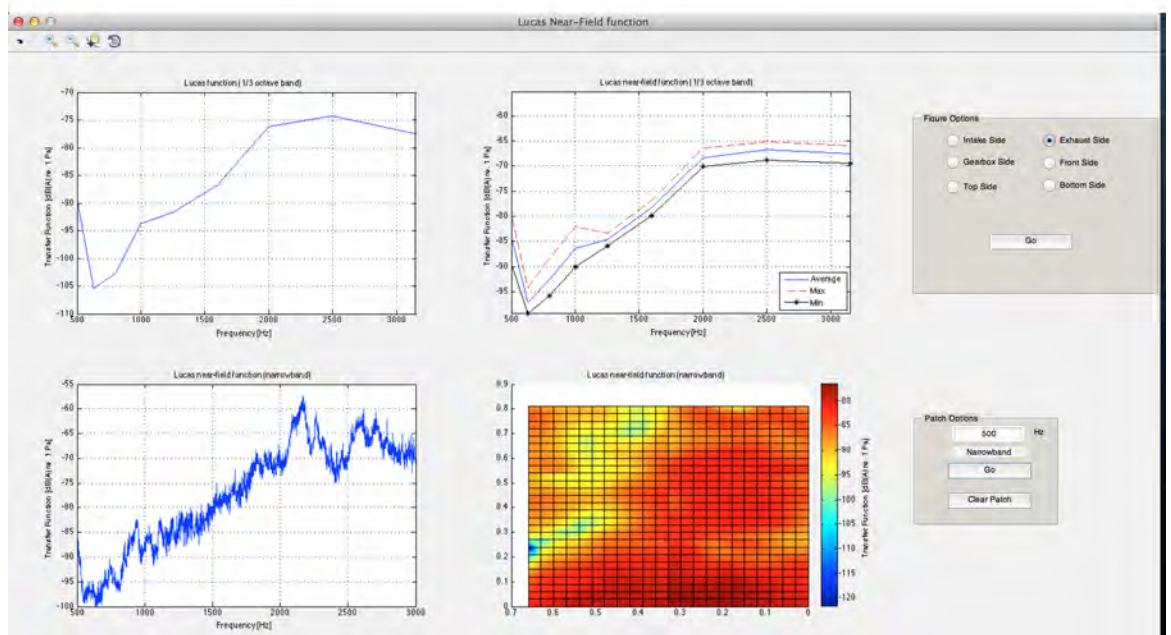


Figure D.19.: The Lucas Near-Field program; the frequency for the transfer function is 500 Hz.

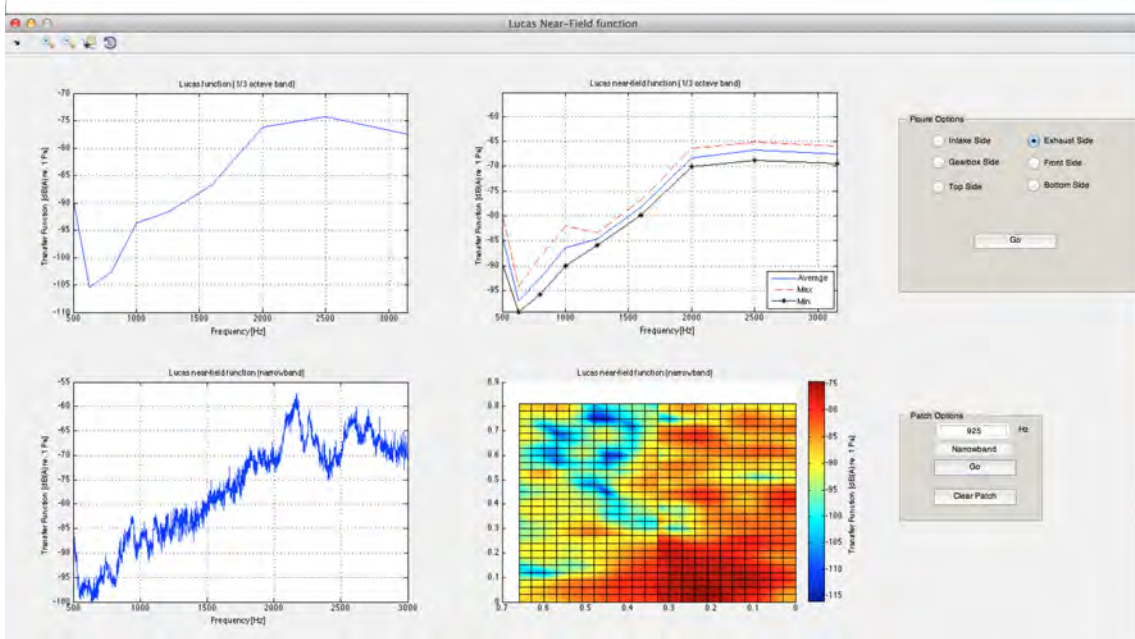


Figure D.20.: The Lucas Near-Field program; the frequency for the transfer function is 925 Hz.

### D.3. Front side

#### D.3.1. Lucas Near-Field function vs. Lucas function

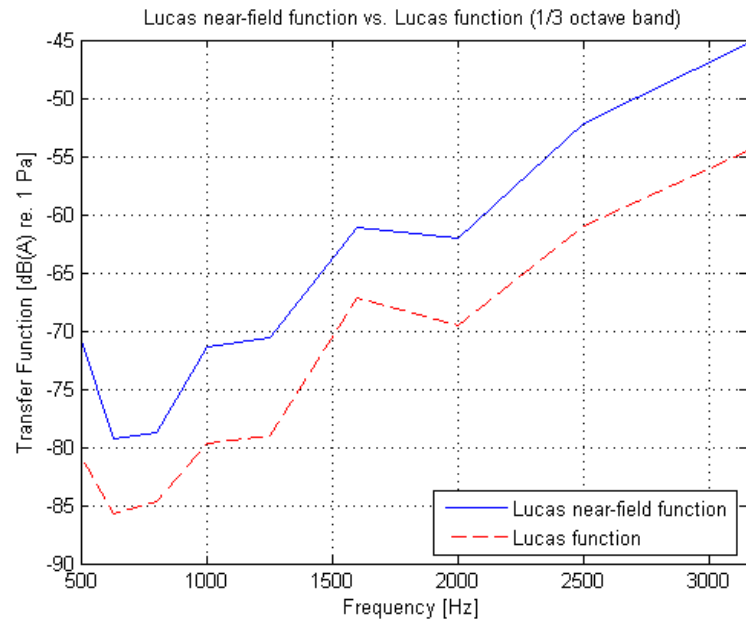


Figure D.21.: The Lucas Near-Field function vs. the Lucas function with "Open" assembly design.

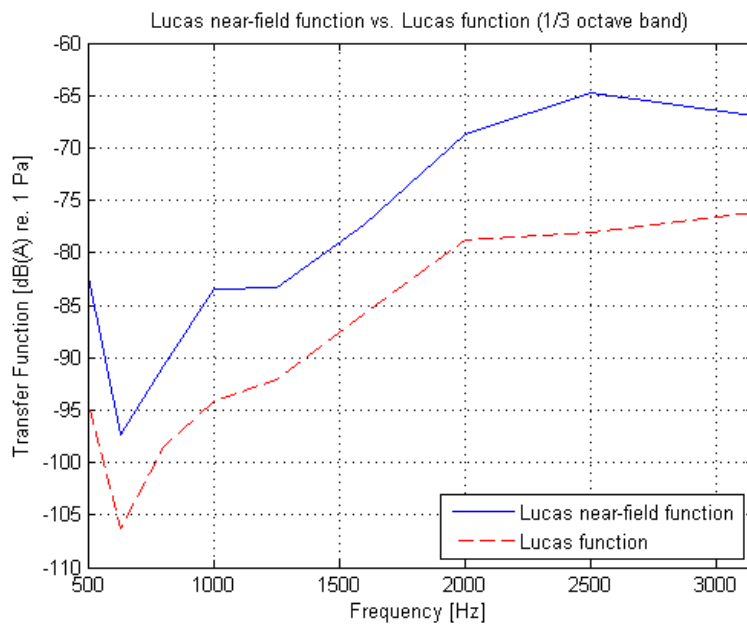


Figure D.22.: The Lucas Near-Field function vs. the Lucas function with "Closed" assembly design.

### D.3.2. Array Acoustic

"Open" assembly design

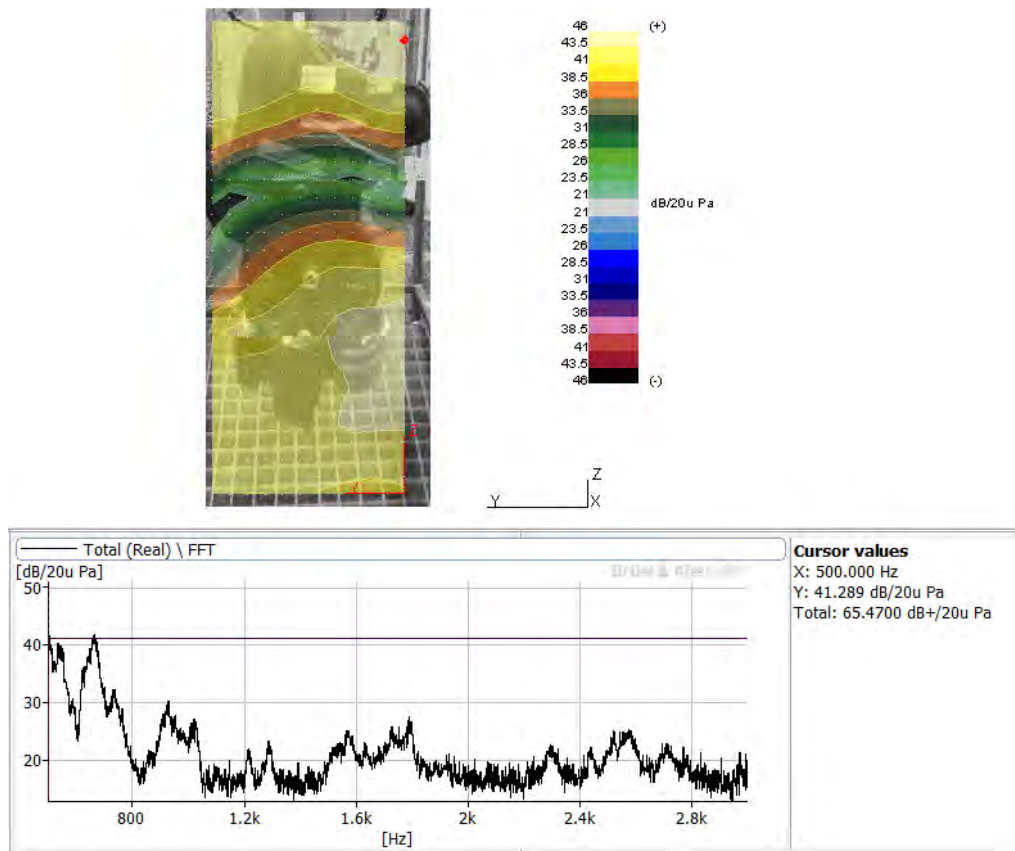


Figure D.23.: The estimated radiated sound pressure level at 500 Hz.

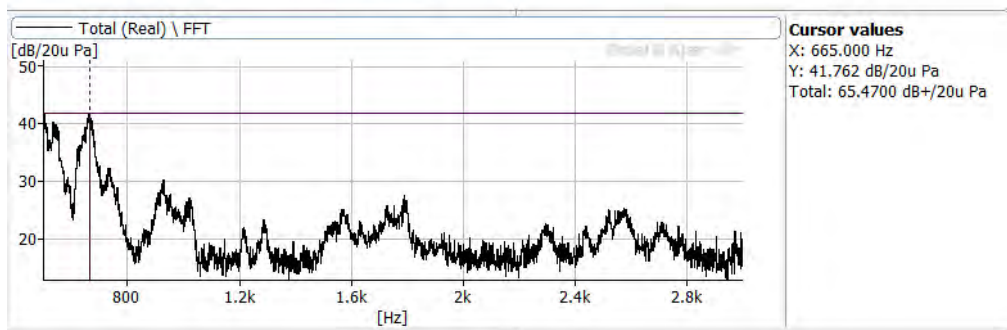
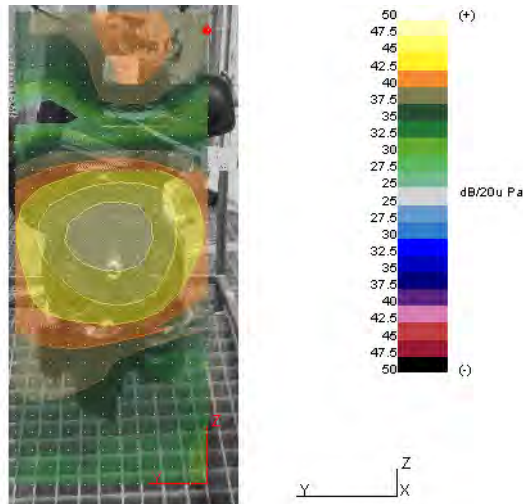


Figure D.24.: The estimated radiated sound pressure level at 665 Hz.

”Closed” assembly design

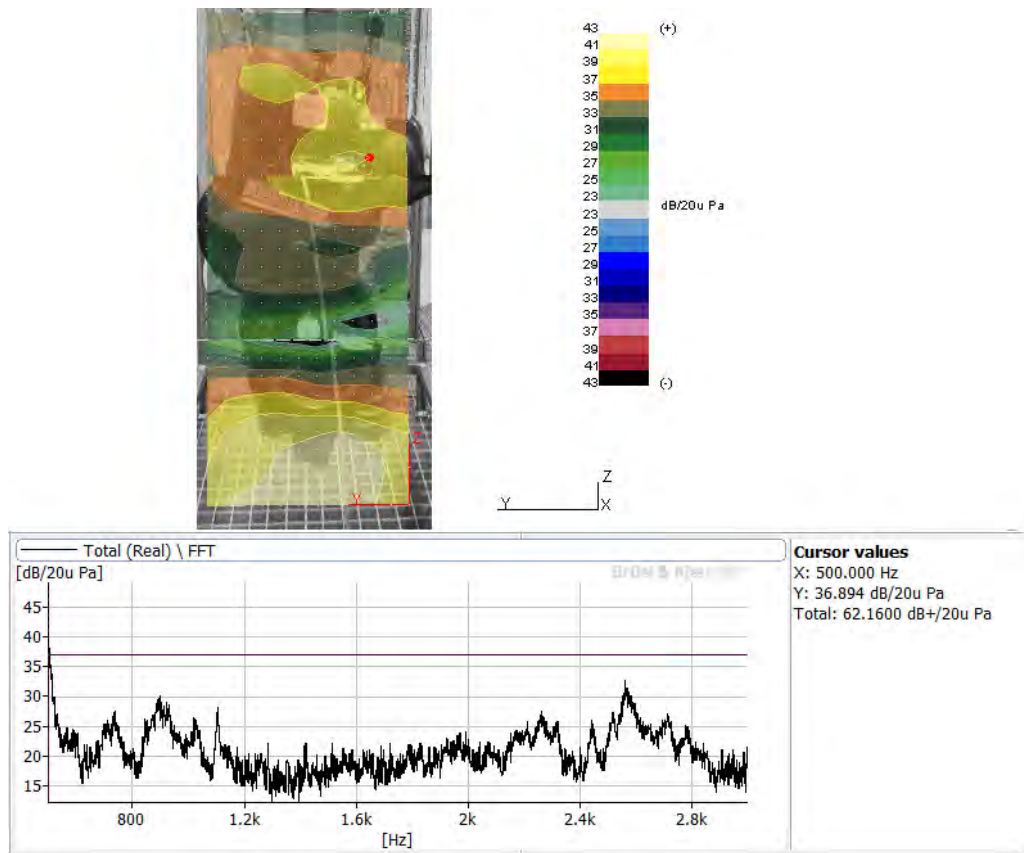


Figure D.25.: The estimated radiated sound pressure level at 500 Hz.

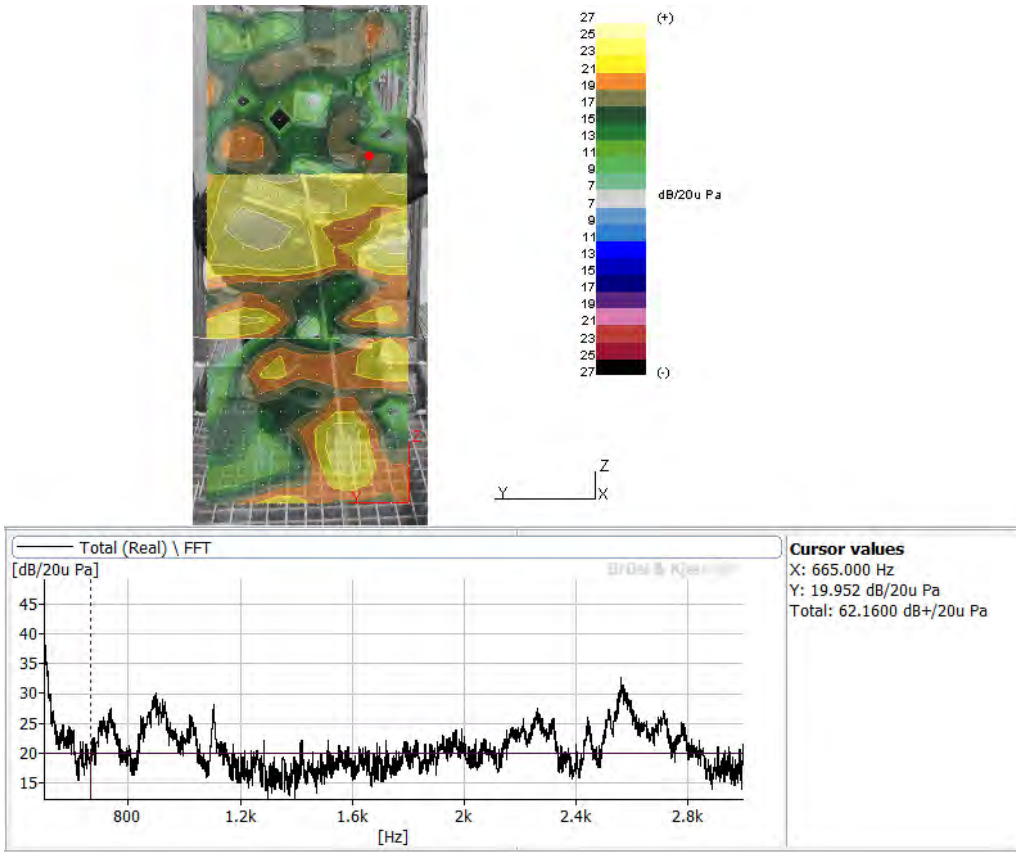


Figure D.26.: The estimated radiated sound pressure level at 925 Hz.

### D.3.3. Lucas Near-Field function

”Open” assembly design

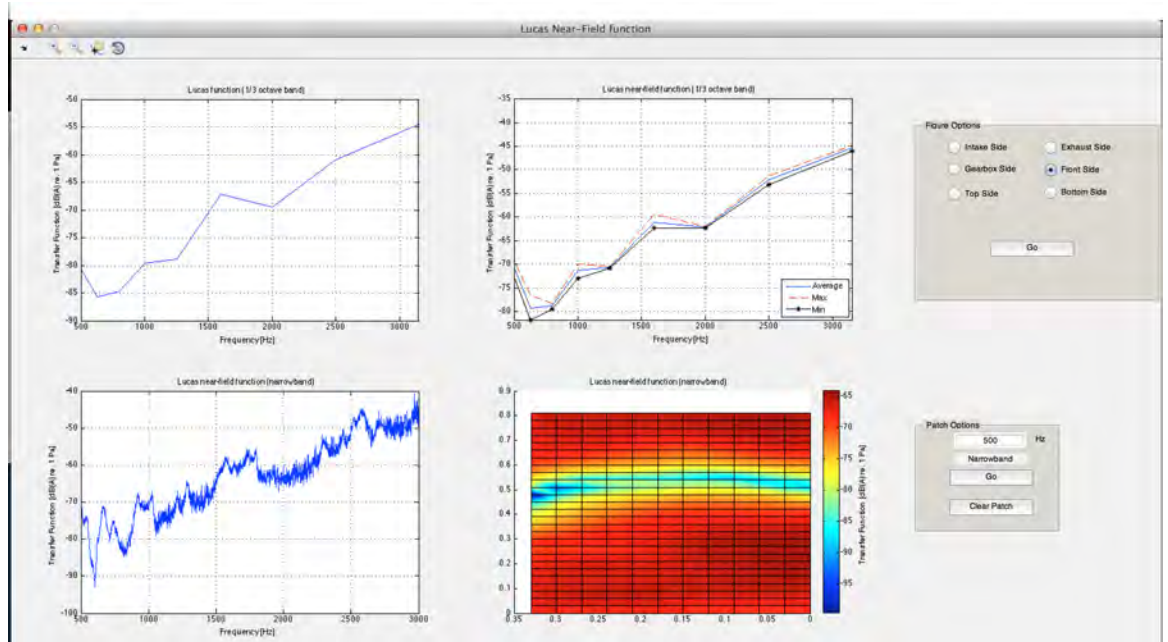


Figure D.27.: The Lucas Near-Field program; the frequency for the transfer function is 500 Hz.

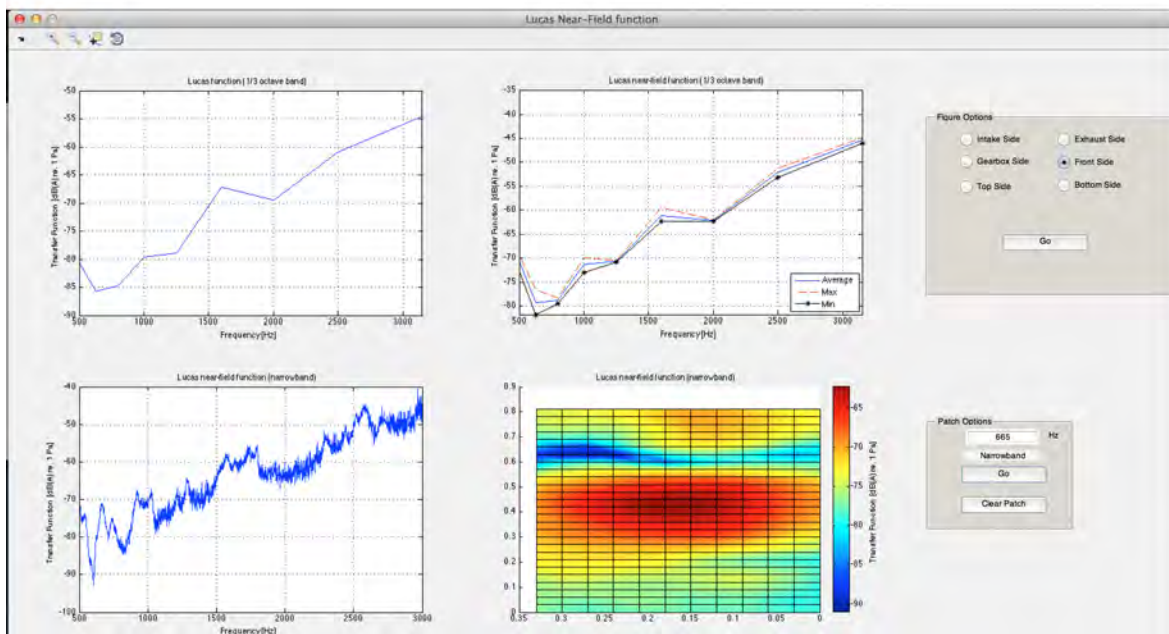


Figure D.28.: The Lucas Near-Field program; the frequency for the transfer function is 665 Hz.

”Closed” assembly design

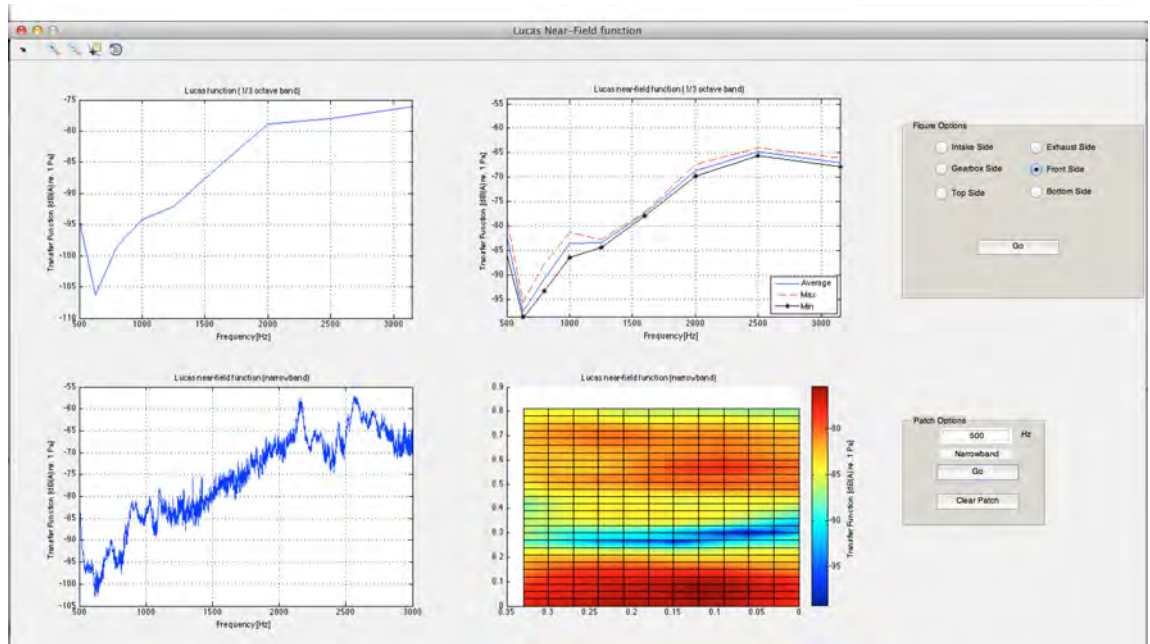


Figure D.29.: The Lucas Near-Field program; the frequency for the transfer function is 500 Hz.

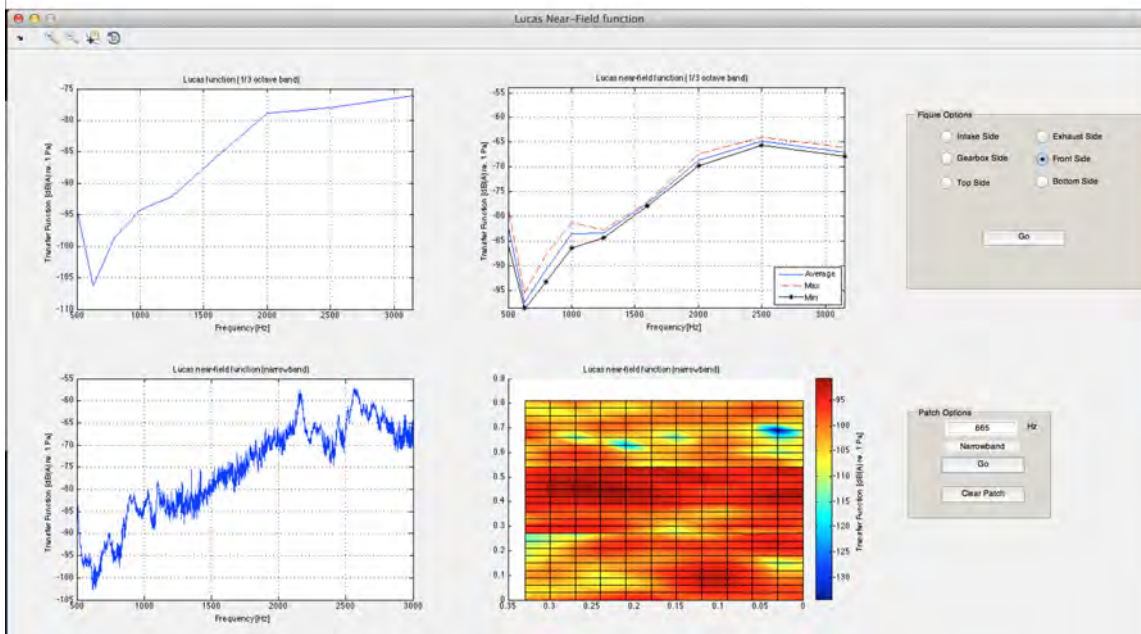


Figure D.30.: The Lucas Near-Field program; the frequency for the transfer function is 665 Hz.

## D.4. Top side

### D.4.1. Lucas Near-Field function vs. Lucas function

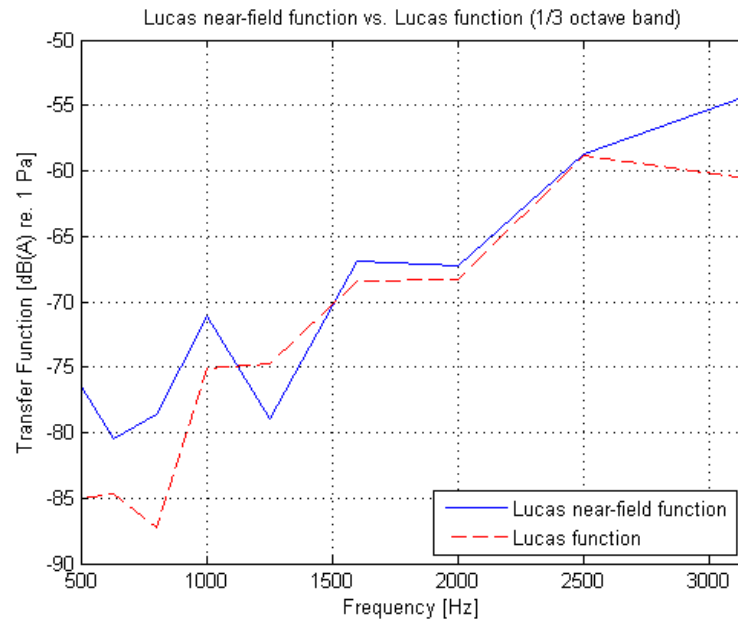


Figure D.31.: The Lucas Near-Field function vs. the Lucas function with "Open" assembly design.

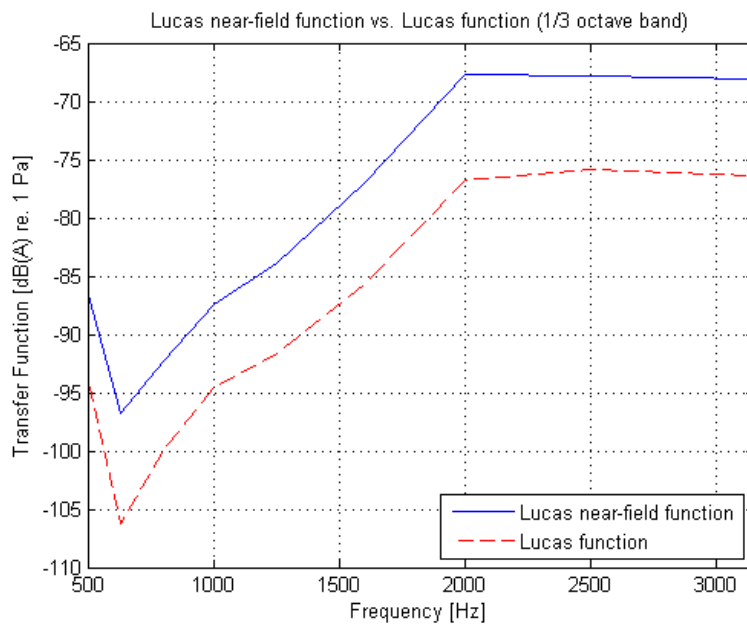


Figure D.32.: The Lucas Near-Field function vs. the Lucas function with "Closed" assembly design.

## D.4.2. Array Acoustic

### "Open" assembly design

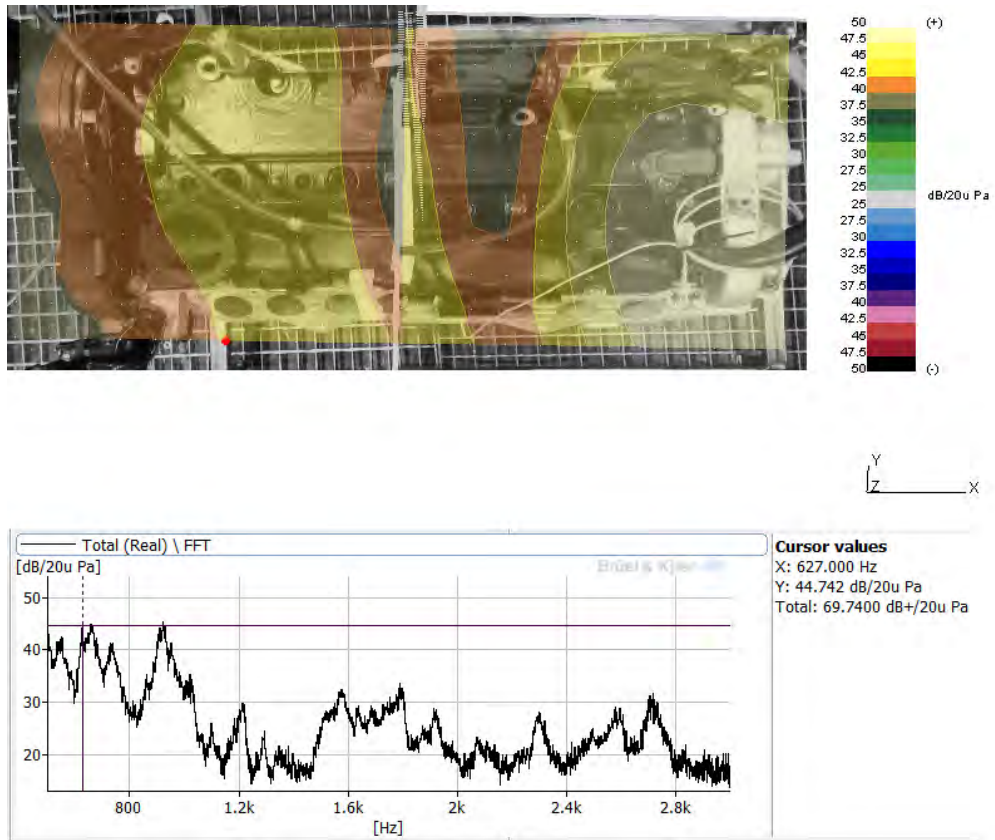


Figure D.33.: The estimated radiated sound pressure level at 627 Hz.

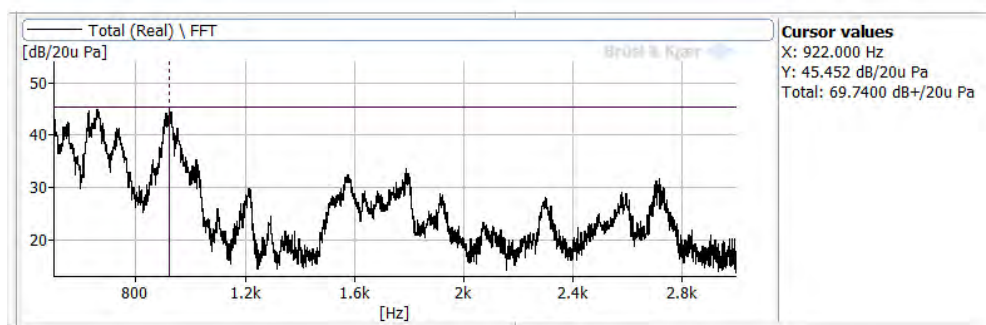
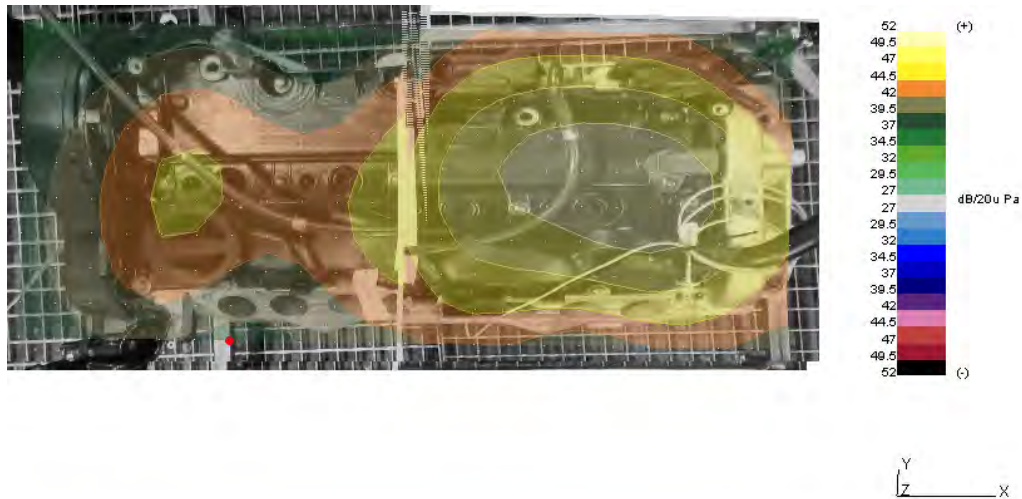


Figure D.34.: The estimated radiated sound pressure level at 922 Hz.

”Closed” assembly design

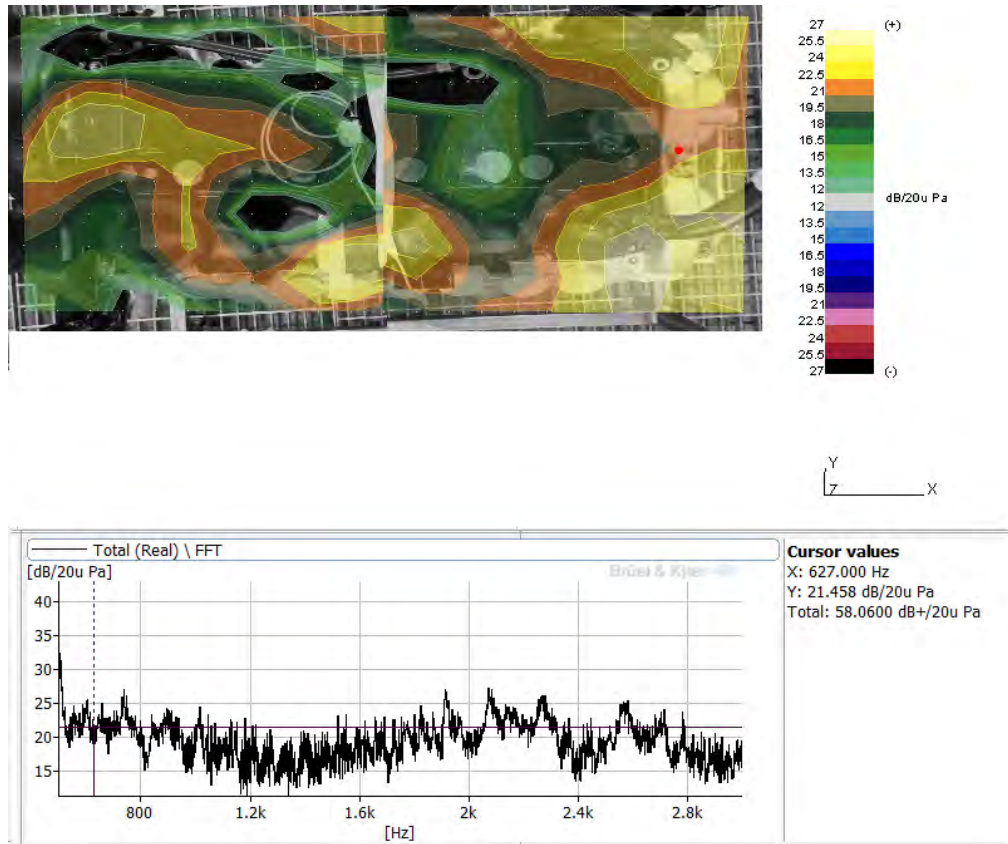


Figure D.35.: The estimated radiated sound pressure level at 627 Hz.

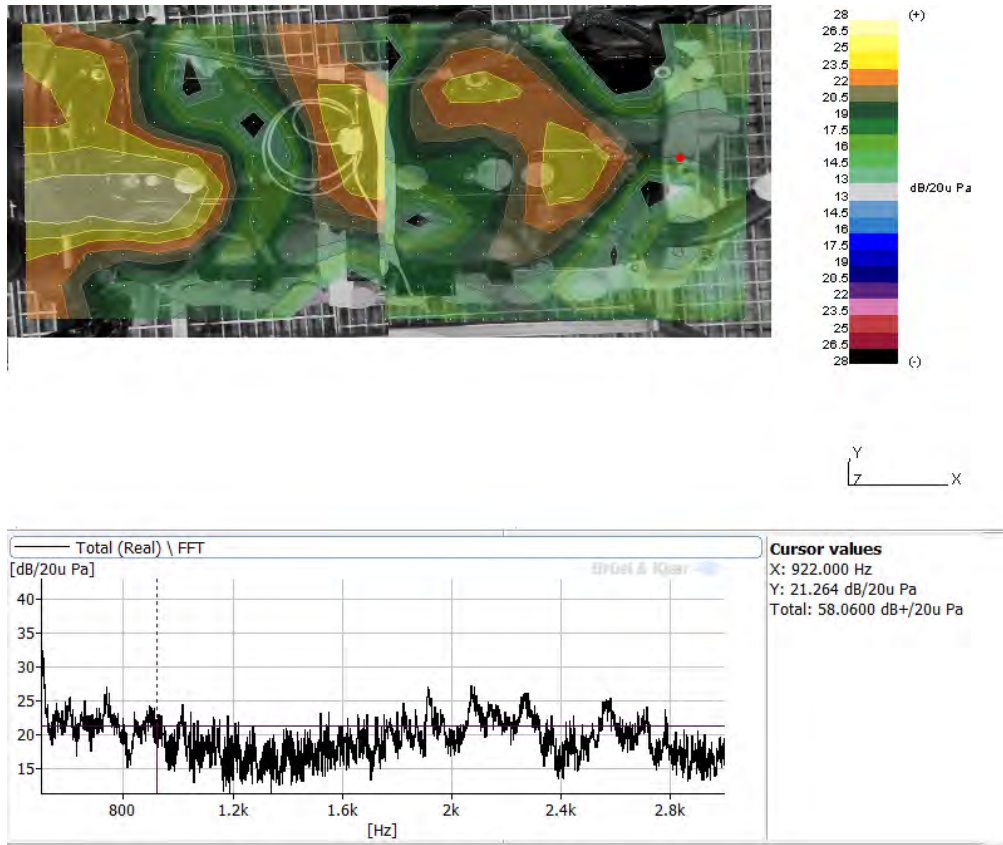


Figure D.36.: The estimated radiated sound pressure level at 922 Hz.

### D.4.3. Lucas Near-Field function

”Open” assembly design

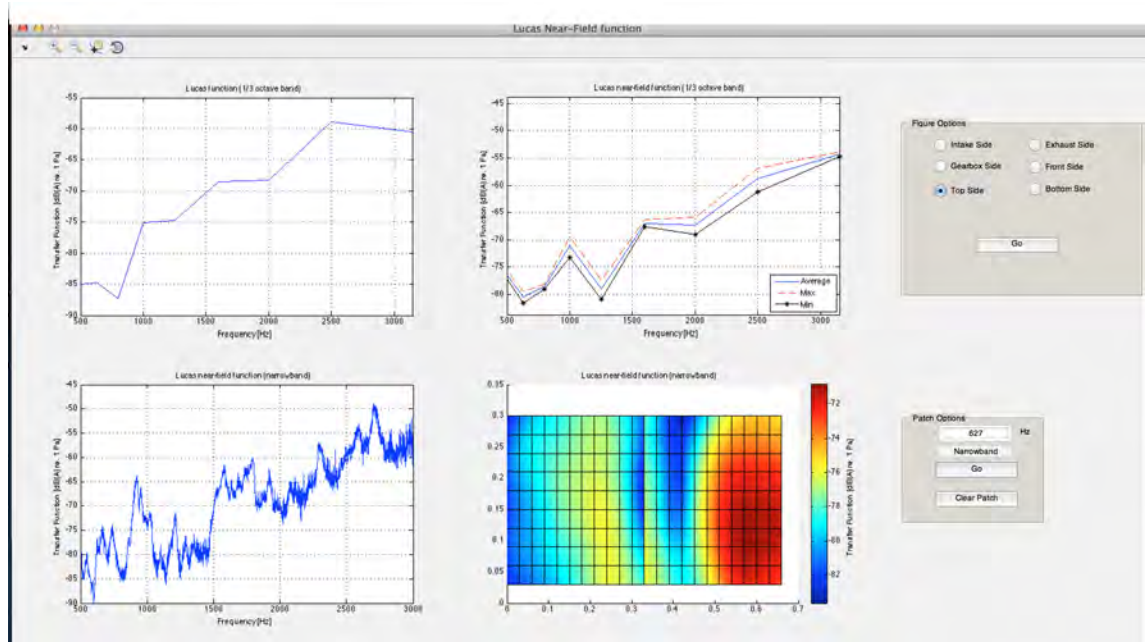


Figure D.37.: The Lucas Near-Field program; the frequency for the transfer function is 627 Hz.

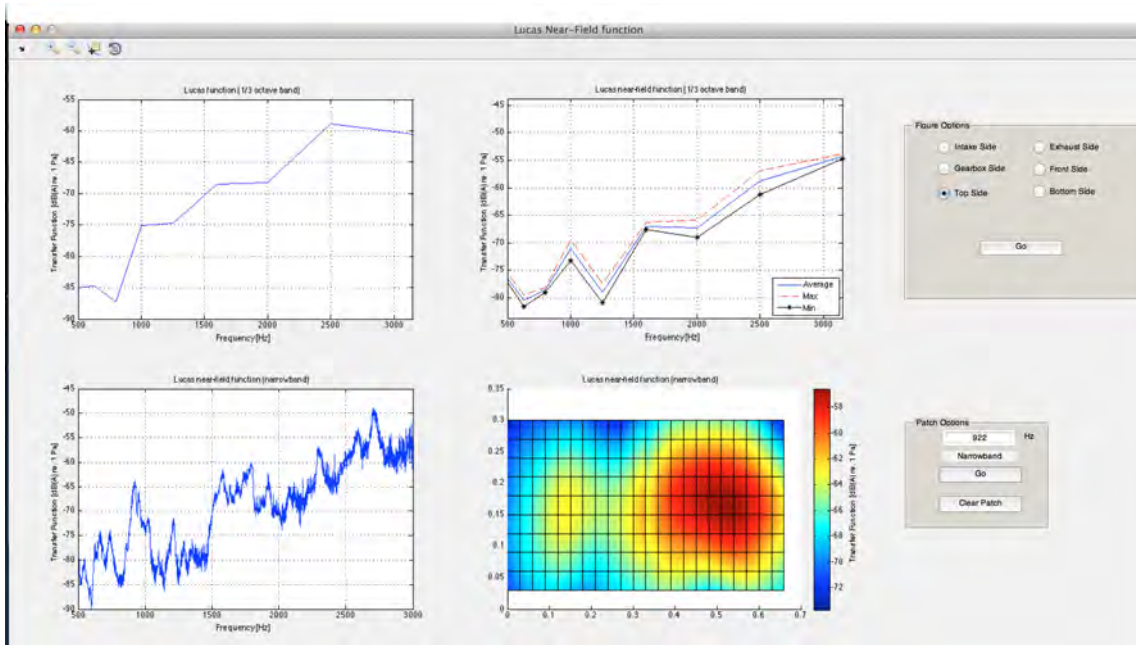


Figure D.38.: The Lucas Near-Field program; the frequency for the transfer function is 922 Hz.

## ”Closed” assembly design

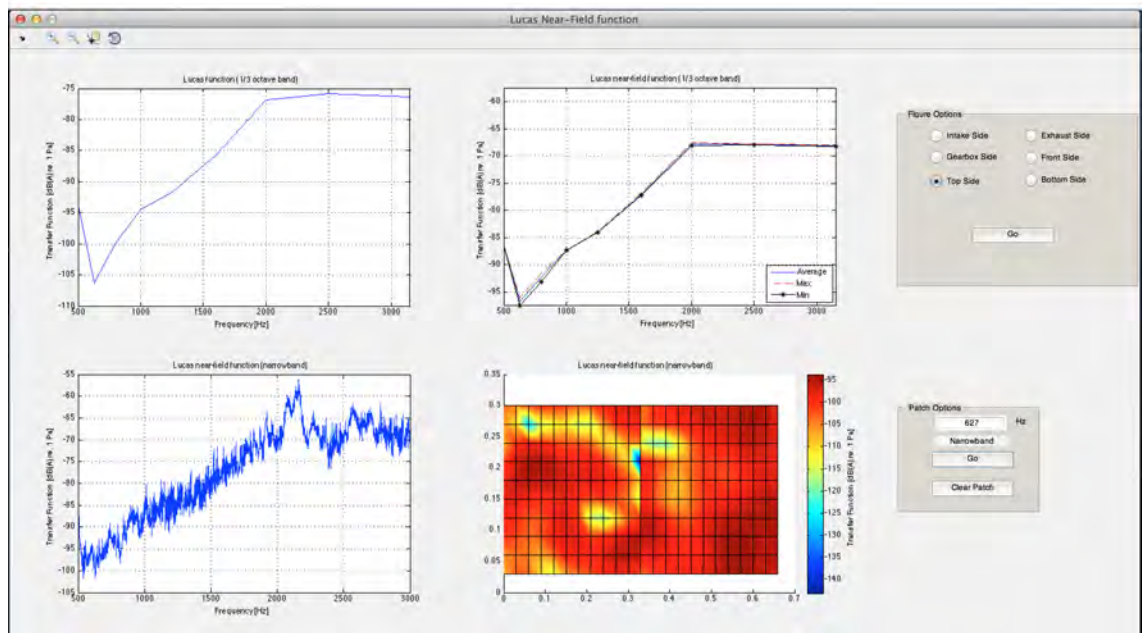


Figure D.39.: The Lucas Near-Field program; the frequency for the transfer function is 627 Hz.

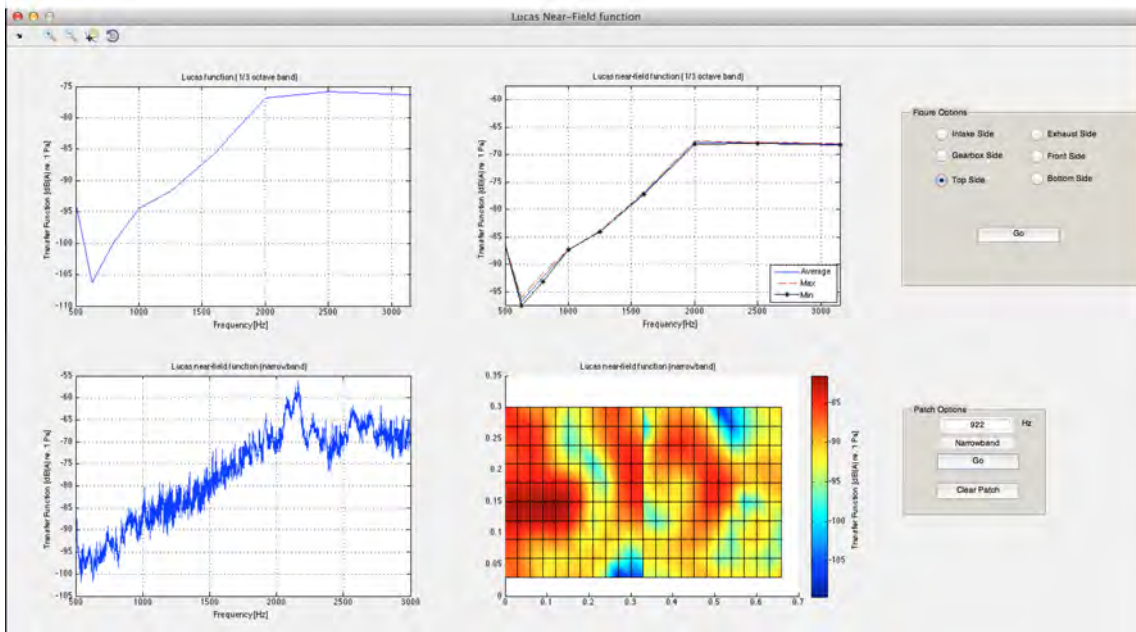


Figure D.40.: The Lucas Near-Field program; the frequency for the transfer function is 922 Hz.

## D.5. Bottom side

There are not any big difference between the two different assembly designs because there was not any openings to close.

### D.5.1. Lucas Near-Field function vs. Lucas function

There are not any comparison between Lucas Near-Field function and Lucas function because it was not possible to place a microphone 1 metre away from the engine.

## D.5.2. Array Acoustic

### "Open" assembly design

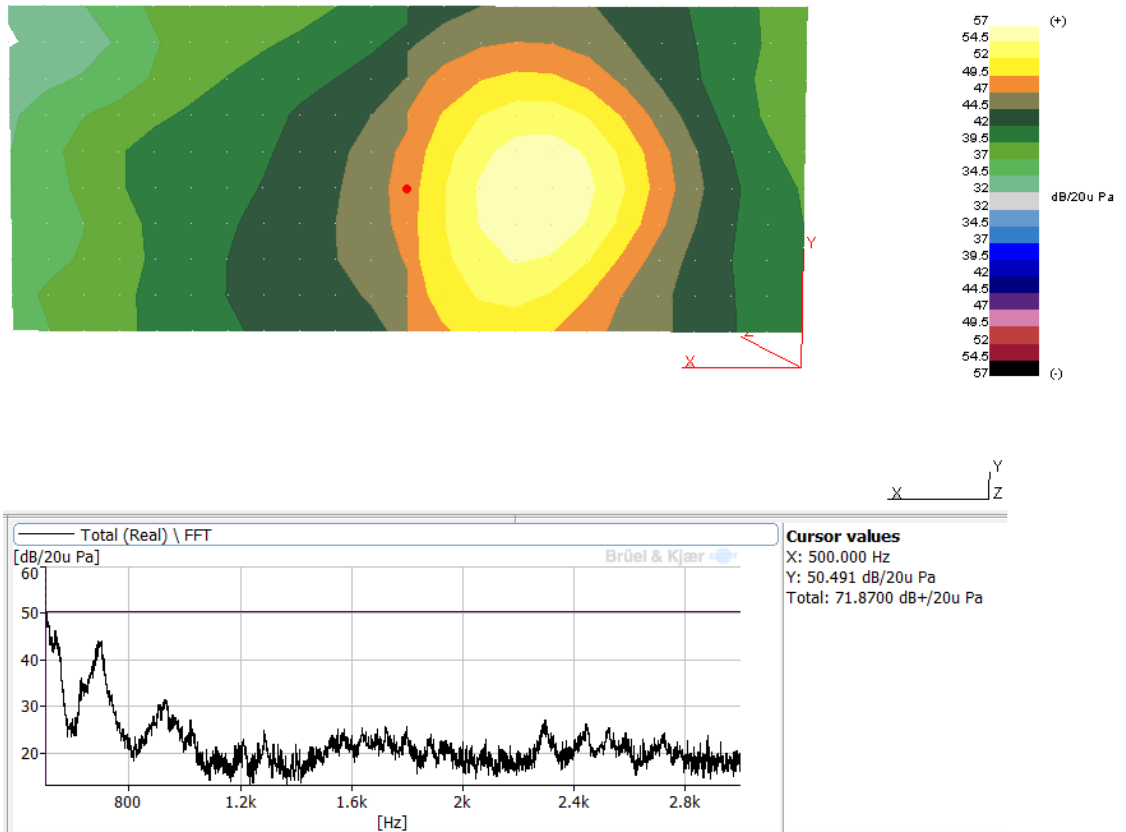


Figure D.41.: The estimated radiated sound pressure level at 500 Hz.

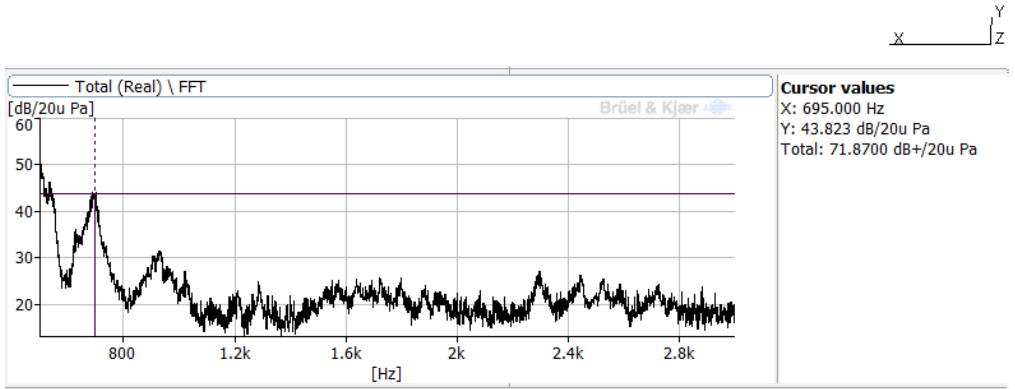
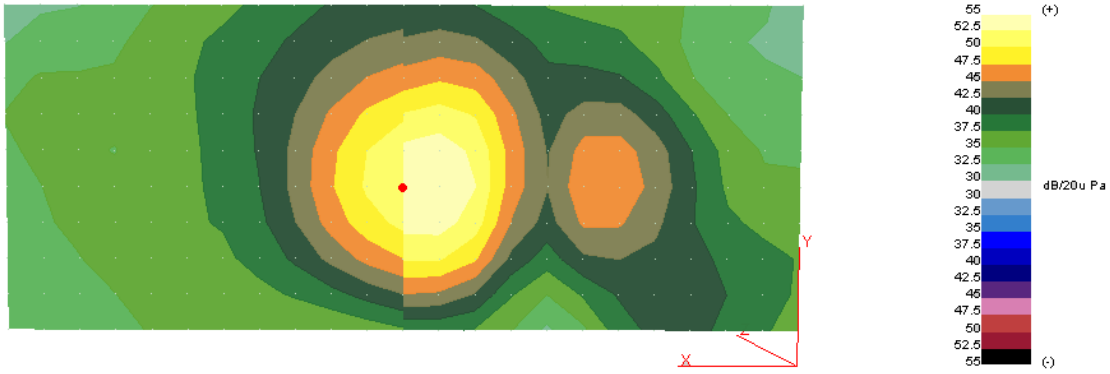


Figure D.42.: The estimated radiated sound pressure level at 695 Hz.

”Closed” assembly design

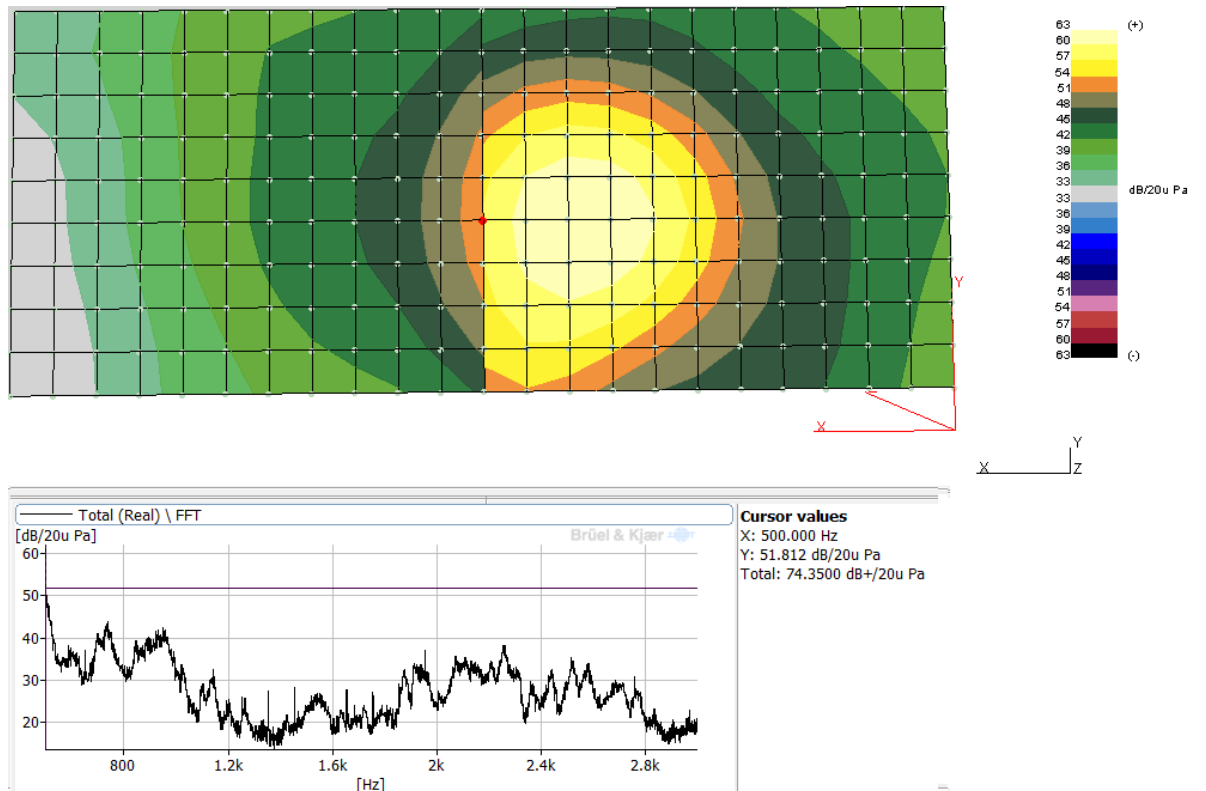


Figure D.43.: The estimated radiated sound pressure level at 500 Hz.

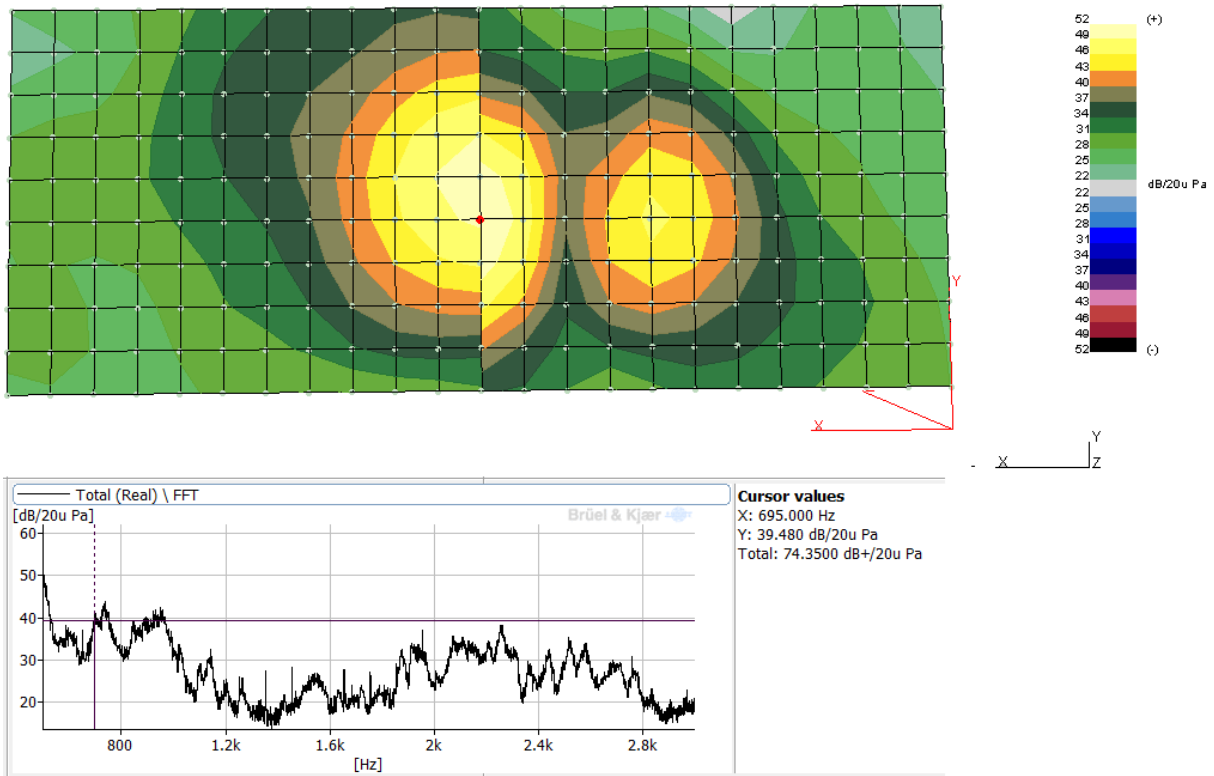


Figure D.44.: The estimated radiated sound pressure level at 695 Hz.

### D.5.3. Lucas Near-Field function

”Open” assembly design

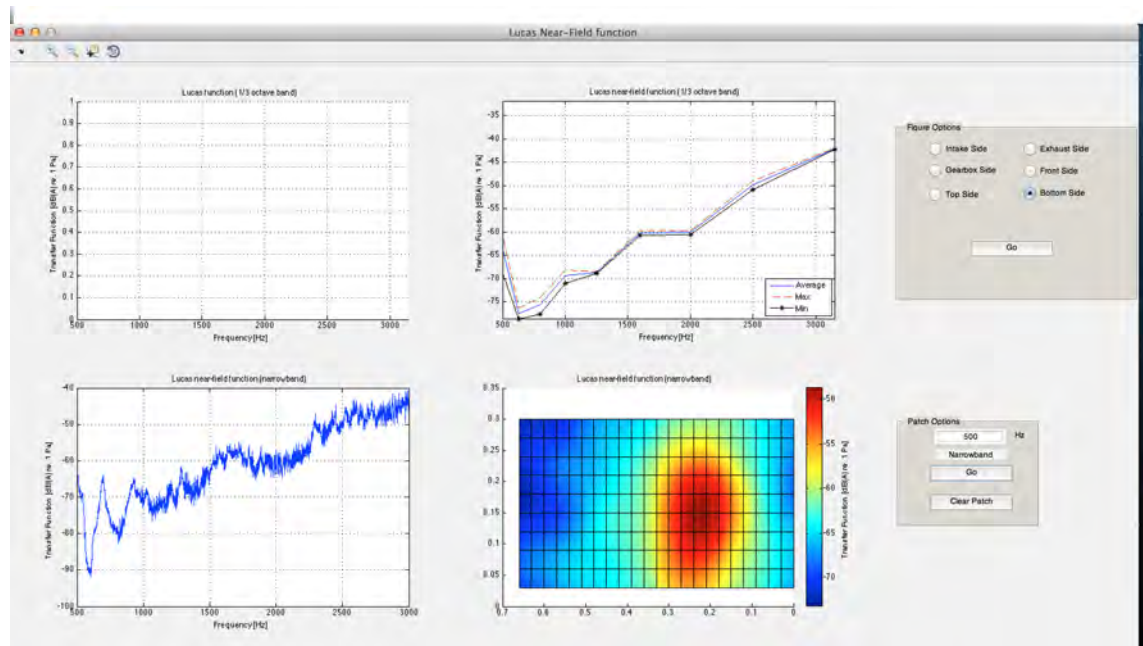


Figure D.45.: The Lucas Near-Field program; the frequency for the transfer function is 500 Hz.

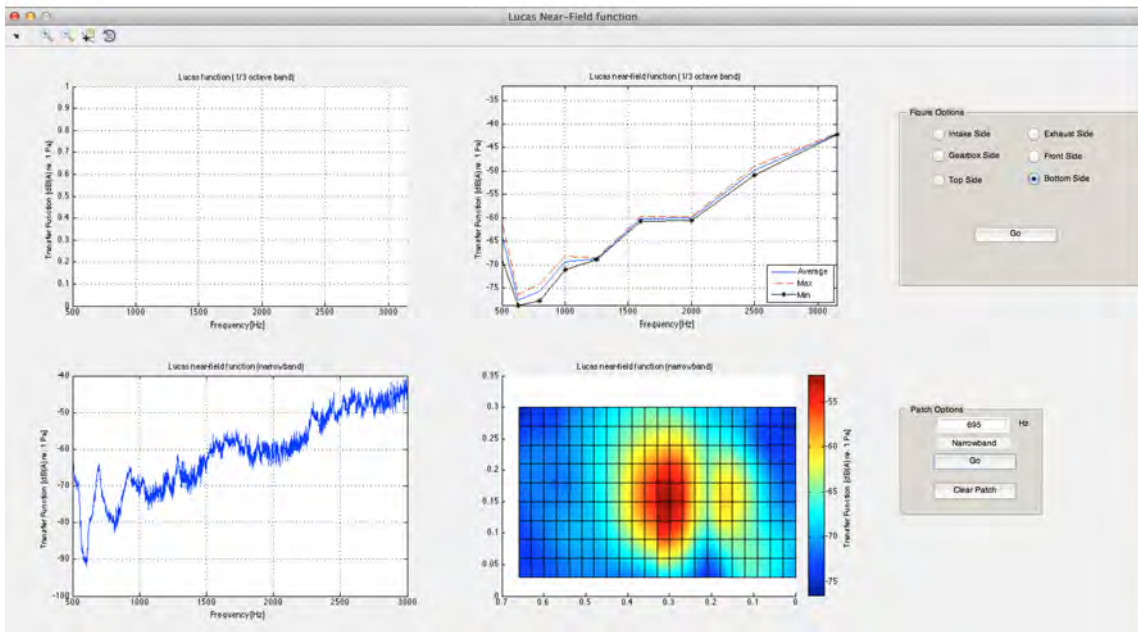


Figure D.46.: The Lucas Near-Field program; the frequency for the transfer function is 695 Hz.

## ”Closed” assembly design

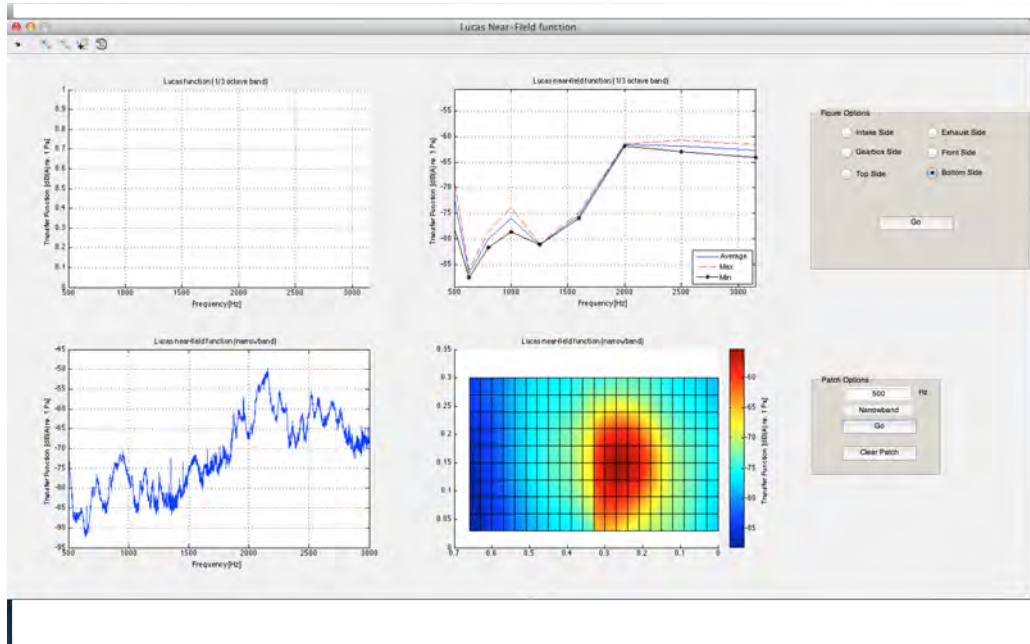


Figure D.47.: The Lucas Near-Field program; the frequency for the transfer function is 500 Hz.

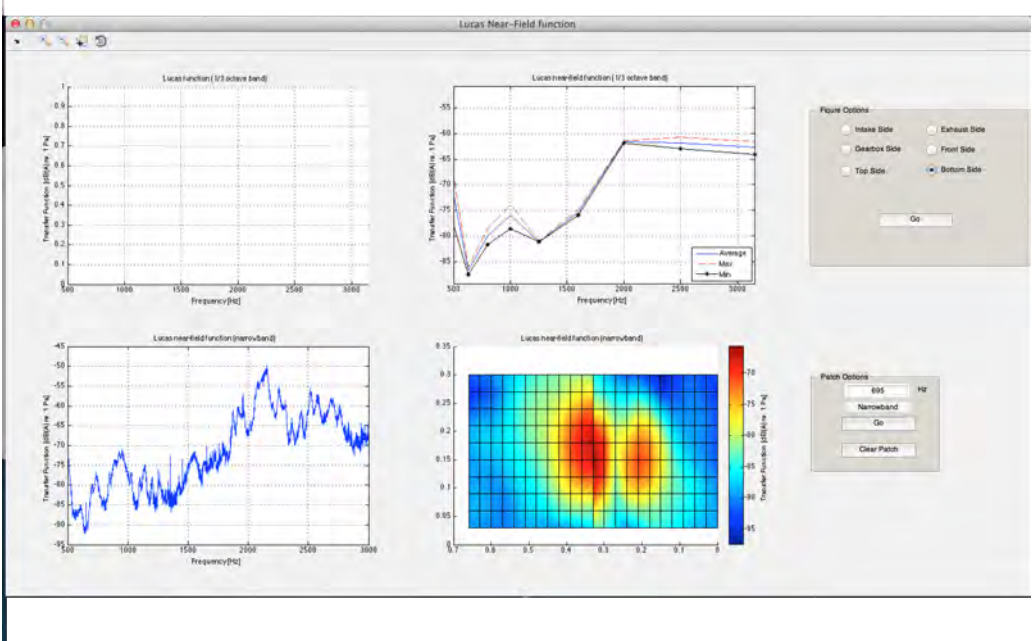


Figure D.48.: The Lucas Near-Field program; the frequency for the transfer function is 695 Hz.